Generation of a transgenic zebrafish with a fluorescent TNF-alpha reporter gene

By

Wade Ambrose

Thesis presented in fulfilment of the requirements for the degree of

Master of Physiological Sciences in the Faculty of

Science Stellenbosch University

Supervisor: Prof. Carine Smith

Co-supervisor: Dr. Anton Du Preez van Staden

December 2022

Declaration

By submitting this thesis electronically, I declare that the entirety of the work contained therein is my own, original work, that I am the sole author thereof (save to the extent explicitly otherwise stated), that reproduction and publication thereof by Stellenbosch University will not infringe any third party rights and that I have not previously in its entirety or in part submitted it for obtaining any qualification.

December 2022

Abstract

Given the high degree of innate immune system conservation between zebrafish and humans, researchers have taken a keen interest in utilising zebrafish to unpack innate immunity related mechanisms. Notably, transgenic zebrafish expressing reporter genes are routinely employed for monitoring the spatio-temporal dynamics of innate immunity related proteins *in vivo*, and thus, are an invaluable tool to the zebrafish research community. While a number of alternative protein detection methods are available, they are subject to inference from tissue samples, often acquired through invasive techniques, which are incapable of accurately monitoring the spatio-temporal dynamics of protein expression *in vivo*. Given our research group's interest in innate immune processes, as well as the advantageous applications of transgenic zebrafish, this study aimed to develop a stable transgenic zebrafish line, expressing a reporter gene under the transcriptional control of the pro-inflammatory cytokine TNF-α.

For this, the transgene construct, pRSF-zTNFα-mCherry – expressing the fluorescent protein mCherry under the transcriptional control of the zebrafish TNF-α1 promoter – was designed and synthesized. Zebrafish embryos were transfected with the transgene construct by microinjection at the single-cell stage. Following microinjection, an acute inflammatory response was induced in transfected zebrafish larvae, coupled with fluorescence microscopy, to access the number of zebrafish in which the transgene was successfully integrated into the genome. Likewise, a genotyping method, using PCR, was developed to assess the rate of successful transgene integration.

The data presented in this study illustrates the successful synthesis of the pRSF-zTNFα-mCherry transgene construct. Transfection of zebrafish larvae with the construct yielded zero zebrafish with detectable mCherry expression, using a stereomicroscope fitted with a fluorescent light source, both before and after the induction of an acute inflammatory response. Genotyping, however, revealed that the transgene was successfully integrated into the genome of the majority of transfected zebrafish, despite the inability to visually illustrate expression of the transgene. The transgene integration rate observed in this study was considerably higher than those previously seen in literature, in which similar transfection techniques were used. Potential reasons for the lack of detectable transgene expression were discussed throughout this study, namely: insufficient equipment sensitivity; insufficient transgene stimulation; integration of a dysfunctional transgene.

While the study at hand was unable to demonstrate a TNF-α response spatio-temporally, many of the methodologies needed for the development of transgenic zebrafish were introduced and explored within the research group for the first time. Likewise, the means of both accessing and improving on future transgenic zebrafish development were investigated. In conclusion, this study lays the foundation for prospective transgenic zebrafish development – a model that will be utilized within the research group moving forward.

Opsomming

Gegewe die hoë mate van aangebore immuunstelselbewaring tussen sebravisse en mense, het navorsers 'n groot belangstelling in die gebruik van sebravisse om aangebore immuniteit-verwante meganismes te ontrafel. Veral transgeniese sebravisse wat verslaggewergene uitdruk, word gereeld aangewend vir die monitering van die ruimtelike-tydelike dinamika van aangebore immuniteit-verwante proteïene *in vivo*, en is dus 'n waardevolle hulpmiddel vir die sebravisnavorsingsgemeenskap. Alhoewel 'n aantal alternatiewe proteïen-metingsmetodes beskikbaar is, is hulle onderhewig aan afleidings van weefselmonsters, wat dikwels deur indringende tegnieke verkry is, en wat dus nie in staat is om die ruimtelike-tydelike dinamika van proteïenuitdrukking *in vivo* akkuraat te reflekteer nie. Gegewe ons navorsingsgroep se belangstelling in aangebore immuunreaksies, sowel as die voordelige toepassings van transgeniese sebravis, het hierdie studie ten doel gehad om 'n stabiele transgeniese sebravislyn te ontwikkel, wat 'n verslaggewergeen uitdruk onder die transkripsiebeheer van die pro-inflammatoriese sitokien TNF-α.

Hiervoor is die transgeenkonstruk, pRSF-zTNFα-mCherry – wat die fluoreserende proteïen mCherry onder die transkripsiebeheer van die sebravis TNF-α1 promotor uitdruk – ontwerp en vervaardig. Sebravis embrio's is getransfekteer met die transgeen konstruk deur mikro-inspuiting op die enkelsel stadium. Na mikro-inspuiting is 'n akute inflammatoriese reaksie in getransfekteerde sebravislarwes geïnduseer. Fluoresensie mikroskopie is ingespan om te bepaal in hoeveel sebravisse die transgeen suksesvol in die genoom geïntegreer is. Net so is 'n genotiperingsmetode, wat gebruik maak van PCR, ontwikkel om alternatiewelik toegang tot die persentasie van suksesvolle transgeen-integrasie te bepaal.

Die data wat in hierdie studie aangebied word, illustreer die suksesvolle sintese van die pRSF-zTNFα-mCherry transgeen konstruk. Transfeksie van sebravislarwes met die konstruk hetgeen sebravis opgelewer met waarneembare mCherry-uitdrukking (sigbaar op ‘n stereomikroskoop met fluoreserende ligbron), beide voor en na die induksie van 'n akute inflammatoriese reaksie, nie. Genotipering het egter aan die lig gebring dat die transgeen suksesvol in die genoom van die meerderheid getransfekteerde sebravisse geïntegreer is, ten spyte van die onvermoë om visueel die uitdrukking van die transgeen in genoemde sebravisse te demonstreer. Die transgeen-integrasietempo wat in hierdie studie waargeneem is, was aansienlik hoër as dié wat voorheen in literatuur gesien is, waarin soortgelyke transfeksietegnieke gebruik is. Potensiële redes vir die gebrek aan waarneembare transgeenuitdrukking is deurgaans in hierdie studie

bespreek, naamlik: onvoldoende toerusting sensitiwiteit; onvoldoende transgeenstimulasie; integrasie van 'n disfunksionele transgeen.

Terwyl die studie wat voorhande nie in staat was om ’n ruimtelike-tydelike TNF-α te demonstreer nie, is baie van die tegnieke wat nodig is vir die ontwikkeling van transgeniese sebravisse vir die eerste keer binne die navorsingsgroep bekendgestel en ondersoek. Net so is die maniere om toegang te verkry tot en te verbeter op toekomstige transgeniese sebravisontwikkeling, ondersoek. Ten slotte, hierdie studie lê die grondslag vir voornemende transgeniese sebravisontwikkeling – 'n model wat in die navorsingsgroep gebruik sal word om vorentoe te beweeg.

Acknowledgements

To Prof Carine Smith, thank you for the guidance, care and support. Without your ambition and methodical supervision, this study would not have been possible. You have been a mentor figure that has not only guided me through my studies, but also supported me through this period of my life, in which I have learned invaluable lessons.

To Du Preez, thank you for opening up your lab to me and affording me both the time and expertize needed to complete this study. Without your assistance this project would not have been possible.

To Kelly, Yigael, and Lesha, thank you for the very necessary technical support and assistance needed throughout this study.

To all the members of the Smith Group, thank you for supporting me throughout this degree, both in and out of the lab. You have taught me the value of teamwork and I will always cherish the friendships I made. I couldn't have asked for a better group of people to work with.

To my family and friends, thank you for your constant love and support. David, I couldn't have struck up a friendship with a more like-minded person. You kept me going when times were tough. Thank you for the adventures both in and out of the lab. To my brother, Dylan, thank you for encouraging me to push myself. Your hard work and dedication has not only helped me through my degree, but also set an example for me to follow. Finally, to my mom, thank you for giving me the kind-hearted love and support that you could only receive from a mother. Your attention to the small details was the key to me accomplishing all that I have throughout this degree.

I would like to acknowledge and thank the National Research Foundation for their financial support throughout this degree.

All figures, where stated, were created with https://biorender.com/ and https://www.snapgene.com/

Table of Contents

List of figures

Figure 3.2: XhoI digestion of pMiniT 2.0 plasmids cloned with various TNF-α1 promoter fragment sizes. Lane 1: ~3300 bp TNF-α1 promoter fragment and ~2500 bp pMiniT 2.0 backbone. Lane 2-3: ~3700 bp TNF-α1 promoter fragment and ~2500 bp pMiniT 2.0 backbone. Band highlighted in black box: ~3700 bp TNF-α1 promoter fragment isolated for second PCR amplification for addition of an I-SceI and PstI recognition sequence at the 5' and 3' ends of the fragment respectively (see Figure 3.6).

Figure 3.3: Illustrative diagram of layout of short fragment sequence data presented in Figures 3.4 and 3.5.

Figure 3.4: 5' to 3' alignment of sequenced TNF-α1 promoter fragment (from Figure 3.2, lane 2) and *Danio rerio* reference genome, GRCz11, using the forward primer 'zTNF Forw' (Table 3.1). The highlighted sequence represents the forward primer used for sequencing and begins at the 5' distal end of the TNF-α1 promoter.

Figure 3.5: 5' to 3' alignment of sequenced TNF-α1 promoter fragment (from Figure 3.2, lane 2) and *Danio rerio* reference genome, GRCz11, using the reverse primer 'zTNF Rev' (Table 3.1). The highlighted sequence represents the reverse primer used for sequencing and starts at the 3' coding region of the TNF-α1 promoter.

Figure 3.6: Lane 2: PCR amplification of the ~3700 bp TNF-α1 promoter fragment from clone 2 seen in Figure 3.2, lane 2. PCR amplifications were performed using the primers 'I-SceI zTNF Forw' and 'PstI zTNF Rev' (see table1).

Figure 3.7: PCR amplification of the fragments to be used as reporter genes for pRSF-zTNFα-mCherry. Lane 1: GFP with the addition of a PstI and XhoI recognition domain on the 5' and 3' terminals respectively. Lane 2: mCherry with the addition of a PstI and XhoI recognition domain on the 5' and 3' terminals respectively. Band highlighted in black box: mCherry fragment chosen for further synthesis of the transgene construct.

Figure 3.8: PCR amplification of three variations of the SV40 Poly (A) tail; the fragment to be used as a termination sequence in pRSF-zTNFα-mCherry. Lane 1: SV40 Poly (A) tail. Lane 2: SV40 Poly (A) tail with the addition of XhoI and I-SceI recognition domains on the 5' and 3' terminals respectively. Lane 3: An elongated SV40 Poly (A) with the addition of XhoI and I-SceI recognition domains on the 5' and 3' terminals respectively. Band highlighted in black box: SV40 Poly (A) tail fragment chosen for further synthesis of the transgene construct.

Figure 3.9: Digestions of pRSF-zTNFα-mCherry plasmid with various restriction enzymes to confirm the presence of the constituent transgene fragments of pRSF-zTNFα-mCherry. Lane 1: digestion of the 2499 bp I-SceI control plasmid, NotI-linearized pGPS2, digested with I-SceI. Lane 2: pRSF-zTNFα-mCherry plasmid from clone 2A digested with I-SceI (Red arrow: transgene insert; blue arrow: plasmid backbone). Lane 3: pRSF-zTNFα-mCherry plasmid from clone 2B digested with I-SceI. Lane 4: pRSF-zTNFα-mCherry plasmid from clone 2A digested with PstI and NotI. Lane 5: pRSF-zTNFα-mCherry plasmid from clone 2B digested with PstI and NotI. Lane 6: pRSF-zTNFα-mCherry plasmid from clone 2A digested with XhoI. Lane 7: pRSF-zTNFα-mCherry plasmid from clone 2B digested with XhoI.

Figure 3.10: Map of the pRSF-zTNFα-mCherry plasmid annotated with the enzyme digestion sites, I-SceI, PstI, NotI, and XhoI, all of which were used to determine the presence of the constituent fragments of the transgene insert. Create with SnapGene.com.

Figure 3.11: Plasmid map of pRSF-zTNFα-mCherry including annotated final transgene construct, as well as the location of primers used to generate the consensus sequence for sequencing of the pRSF-zTNFα-mCherry transgene insert. Create with SnapGene.com.

Figure 3.12: Single-cell zebrafish embryo at 0.2 hours post fertilization. At this stage the single-cell may be difficult to see, and so correct orientation of the egg is critical prior to microinjection. Here the single-cell can be seen at the bottom right pole of the yolk. The yolk and cell may be prone to rotating before the microinjection tip is able to penetrate either. For ease of microinjection, it is recommended that the cell is orientated on the opposite side of the yolk from where the microinjection tip penetrates the chorion. In a single, swift, and precise motion, the tip is pushed through the yolk, near the cell, and into the single-cell.

Figure 3.13: Graph representing the daily percentage of live zebrafish following microinjection at the single-cell stage with various dyes. Zebrafish microinjected with 0.0167% methylene blue were spawned from the same batch as those that were not injected in control group 1. Likewise, zebrafish that were microinjected with 0.05% phenol red were spawned from the same batch as those that were not injected in control group 2, as well as those that were sham injected by mechanical insertion of the microinjection tip with no solution injected.

Figure 3.14: Digestion of pRSF-zTNFα-mCherry plasmid DNA with I-SceI enzyme for 1 hour at 37°C. Ladder: λ PstI; lane 1: Control digestion in the presence of 0% methylene blue; Lane 2: Digestion in the presence of 0.0167% methylene blue; Lane 3: Digestion in the presence of 0.025% methylene blue. Highlighted red box: plasmid backbone and transgene insert dropout from successful digestion of pRSF-zTNFα-mCherry with I-SceI. Red arrow: Undigested pRSF-zTNFα-mCherry plasmid.

Figure 3.15: Illustration of caudal fin amputation of 9 dpf transfected zebrafish. For amputations, a transverse cut was made across the caudal fin, just short of the notochord, entirely removing the distal section of the caudal fin. Created with BioRender.com.

Figure 3.16: Plasmid map of pRSF-zTNFα-mCherry including annotated final transgene construct, as well as primers sets for TNF-α1, mCherry, and SV40 Poly (A) fragments, used to genotype transfected zebrafish. Create with SnapGene.com.

Figure 3.17: PCR amplification of TNF-α1, mCherry, SV40 Poly (A), and VHL from transfected zebrafish DNA. DNA isolated from each fish (1, 2, and 12A), using the HotSHOT method, was PCR amplified using undiluted and 1/10th dilutions of the DNA respectively. A plasmid control (pRSF-zTNFα-mCherry) was PCR amplified for 3 primer sets (TNF-α, mCherry, and SV40 Poly (A)), while on the far right of each primer set (TNF-α, mCherry, and SV40 Poly (A), and VHL) a negative control was amplified.

Figure 3.18: Representation of optimized PCR amplification of SV40 Poly (A) (row 1) and VHL (row 2) for genotyping of transfected zebrafish. Row 1: SV40 Poly (A) PCR amplification from non-transfected control fish; transfected fish (1-9) with 1/10th dilutions of DNA obtained from the HotSHOT method; negative PCR control; pRSF-zTNFα-mCherry as a positive plasmid control. Row 2: PCR amplification of VHL from non-transfected control fish; transfected fish (1-9) with 1/10th dilutions of DNA obtained from the HotSHOT method; negative PCR control; pRSF-zTNFα-mCherry as a positive plasmid control.

Figure 3.19: PCR analysis of the percentage of positive and negative transgenic zebrafish for SV40 Poly (A) given the outcome of control primers. Presence of the SV40 Poly (A) fragment from the pRSF-zTNFα-mCherry transgene was used to confirm whether or not the pRSF-zTNFα-mCherry transgene was successfully integrated into the genome of transfected zebrafish. For each sample tested, the presence of both control genes, VHL and TNF-α1 was considered, and the outcomes grouped accordingly. Total samples = 66 of 66

Figure 3.20: PCR analysis of the percentage of positive and negative transgenic zebrafish for mCherry given the outcome of control primers. Presence of the mCherry fragment from the pRSF-zTNFα-mCherry transgene was used to confirm whether or not the pRSF-zTNFα-mCherry transgene was successfully integrated into the genome of transfected zebrafish. For each sample tested, the presence of both control genes, VHL and TNF-α1 was considered, and the outcomes grouped accordingly. Total samples = 43 of 66

Figure 3.21: Simple flow diagram for clarity on how the transgene integration rates were determined from the data seen in Figure 3.19 and Figure 3.20.

List of tables

Table 3.9: List of primers used for genotyping transfected zebrafish larvae. VHL primers were used to amplify a 412 bp fragment of the control gene VHL, an endogenous zebrafish gene. TNF-α1 plasmid primers were used to amplify a 349 bp fragment of the zebrafish TNF-α1 promoter, a gene both endogenous to zebrafish, as well as the pRSF-zTNFα-mCherry transgene. mCherry and SV40 Poly (A) primers were used to amplify a 299 bp fragments found only on the pRSF-zTNFα-mCherry transgene. All fragments, with sizes between 299 bps and 412 bps, were amplified on the same PCR run.

Table 3.10: List of reagents added to each PCR reaction: 5X Q5® Reaction Buffer, 5X Q5® High GC Enhancer, forward and reverse primers, dNTP mix (10 µM), and Q5® High-Fidelity Polymerase (2000 units/ml) were all supplied by New England Biolabs (NEB, South Africa).

Table 3.11: Thermocycler parameters used for simultaneous amplification of four primer sets: VHL; TNF-α1; SV40 Poly (A); and mCherry. See Table 3.9 for primer sequences.

List of abbreviations

+6 AA	First six amino acids
ATP	Adenosine triphosphate
bp/kbp	Base pair/kilobase pair
$CaCl_2$	Calcium chloride
CAF	Central Analytical Facilities
CCL20	Chemokine (C-C motif) ligand 20
CD14	Cluster of differentiation 14
Cdipt	CDP-diacylglycerol--inositol 3-phosphatidyltransferase
CRISPR	Clustered regularly interspaced short palindromic repeats
crRNA	Clustered regularly interspaced short palindromic repeats RNA
dNTP	Deoxynucleotide triphosphates
Dpf	Days post fertilization
DPI	Days post injection
DSB	Double-strand breaks
E. coli	*Escherichia coli*
EDTA	Ethylenediamine tetraacetic acid
ER	Endoplasmic reticulum
Erg-1	Early growth response protein 1
gDNA	Genomic DNA
GFP/ eGFP	Green fluorescent protein/ enhanced Green fluorescent protein
HDR	Homology directed repair
HEG	Homing-endonuclease gene
HK	Head kidney
HPI	Hours post injury
hTNF-α	Human Tumour Necrosis Factor alpha
IBD	Inflammatory bowel disease
IL-17	Interleukin-17
IL-1β	Interleukin-1 beta
IL-6	Interleukin-6
IL-8	Interleukin-8

ITR	Inverted terminal repeat
KCl	Potassium chloride
LPS	Lipopolysaccharides
MB	Methylene blue
MD-2	Myeloid differentiation factor 2
Mg^{2+}	Magnesium ion
$MgSO_4$	Magnesium sulfate
MHC III	Major histocompatibility complex III
MMP-9	Matrix metalloproteinase 9
Mpeg1	Macrophage expressed gene 1
Mpx	Myeloid-specific peroxidase
MYD88	Myeloid differentiation primary response 88
NaOH	Sodium hydroxide
NEB	New England Biolabs
NFAT	Nuclear Factor of Activated T-Cells
NF-kB	Nuclear factor-kappa B
NHEJ	Non-homologous end joining
PBS	Phosphate Buffered Saline
PCR/qPCR	Polymerase chain reaction/ Quantitative real-time Polymerase chain reaction
redox	Oxidation-reduction reaction
ROS	Reactive oxygen species
Rpm	Revolutions per minute
SAVC	South African Veterinary Council
SDS	Sodium dodecyl sulfate
sgRNA	Single-guide RNA
SP1	Specificity protein 1
SV40 Poly (A)	Simian virus 40 Polyadenylation
TACE	Tumor necrosis factor-alpha converting enzyme
TALEN	Transcription activator-like effector nuclease
TLR4	Toll-like receptor 4
Tm	Primer melting temperature
TNBS	Trinitrobenzene sulfonic acid
TNF-α	Tumour Necrosis Factor alpha
tracrRNA	Trans-activating CRISPR RNA

Tris-HCl	Tris(hydroxymethyl)aminomethane hydrochloride
uhrf1	Ubiquitin-like with PHD and RING finger domains 1
USE	Upstream Sequence Element
VHL	Von Hippel-Lindau Tumor Suppressor
WGD	Whole-genome duplication
WPI	World Precision Instruments
WT	Wild type
ZFIN	Zebrafish Information Network
ZFN	Zinc-finger nucleases
zTNF-α	Zebrafish Tumour Necrosis Factor alpha

Chapter 1

Introduction

The use of *Danio rerio* (zebrafish) for experimental research is a rapidly developing field of science. A growing body of researchers have taken to using the zebrafish to study a number of biological models [1]. While many of these models are traditionally investigated using mammals such as rodents, the switch to zebrafish presents itself with many advantages [2]: Firstly, zebrafish remain transparent for several days during early developmental stages, allowing for easy visualization of internal tissues and organs, which are otherwise difficult to see in most mammals. Additionally, zebrafish have incredibly high fecundity, spawning offspring as often as once every one to two weeks, with clutch sizes anywhere from 200 to 300 eggs. This high turnover of zebrafish offspring allows for regular large-scale experimental screening assays. Coupled with the rate of breeding, zebrafish are capable of reaching sexual maturity at the age of three months, allowing for greater logistic feasibility of generational studies. Finally, a major attraction of the zebrafish model in the context of our research is the high levels of innate immune system conservation between zebrafish and humans [3,4]. In the chapters to follow, aspects of this innate immune system conservation will be explored, with particular interest given to inflammatory processes and related pathophysiologies. Given the many advantages outlined above, the zebrafish is increasingly used for a number of models investigating toxicology, drug discovery, developmental biology, behavioural studies, molecular genetics and notably, inflammation related studies [5–7]. One significantly advantageous application of zebrafish is the monitoring of *in vivo* protein dynamics through the use of stable transgenic zebrafish lines. The utility of stable transgenic zebrafish lines expressing reporter genes is an invaluable tool used to understand the spatio-temporal dynamics of protein expression and has become a standard practice in many zebrafish labs. While a number of alternative methods of protein detection are available, they are all subject to inference from tissue samples, often acquired through invasive techniques, and are all incapable of accurately monitoring the spatio-temporal dynamics of protein expression *in vivo*. This latter shortfall is particularly prevalent when studying proteins that display localized and/or transient expression – one such group of proteins being pro-inflammatory cytokines. As seen in the chapters to follow, there are significant similarities between the human and zebrafish innate immune systems. Therefore, the development of a stable transgenic zebrafish line would add a highly beneficial research tool with which to study aspects of chronic inflammatory disease *in vivo* and longitudinally in the same organism. This study explored the feasibility of developing and maintaining a stable

transgenic zebrafish line expressing reporter proteins under the same transcriptional control mechanisms as inflammatory related proteins, specifically zebrafish TNF-α. A number of careful considerations were applicable at all stages of this project, from the design of the transgene to be integrated into the zebrafish genome, to the practical execution and validation of success of the experiment. In the following chapter, a comprehensive review of the most relevant literature consulted is provided.

Chapter 2

Literature review

2.1 Zebrafish inflammatory models

One of the many uses of zebrafish is as a tool for studying inflammatory related processes. Not only do zebrafish share high levels of innate immune system conservation with humans, they also only develop a mature adaptive immune system at 3 to 4 weeks, allowing for isolated studies of the innate immune system before then. As such, a large number of inflammatory models have been developed using zebrafish larvae. Broadly, these models can be separated into pathogenic and non-pathogenic inflammatory models. While pathogenic inflammatory models are extensive and versatile, our research group mostly utilizes non-pathogenic inflammatory models, with the exception of exposure to lipopolysaccharide (LPS) endotoxins. The chapter to follow will briefly outline and summarize a few of these models, including intestinal inflammation, LPS-induced inflammation, and wound-induced inflammation. Likewise, with each model explored, particular attention will be given to the inflammatory phenotypes resulting from induction of the model.

First introduced by two research groups in 2010 (Oehlers et al. [8] and Fleming et al. [9]), exposure of zebrafish larvae to trinitrobenzene sulfonic acid (TNBS) is used to induce an intestinal inflammation model with phenotypic changes resembling mammalian inflammatory bowel disease (IBD). This model is now routinely used in our research group and is emerging as a standard for studying intestinal inflammation in zebrafish. While the exact mechanisms of pathogenesis leading to an inflammatory response in zebrafish larvae as a result of TNBS exposure have not been fully elucidated, it has been suggested that TNBS may act as a haptenizing agent directly disrupting mucin production and epithelial cell homeostasis. This may, in turn, disrupt local microbiota interactions with host epithelial cells resulting in an intestinal inflammatory response [10]. Morpholino knock down of Myeloid differentiation primary response 88 (MYD88), a major adaptor molecule for TLR signalling, resulted in resilience to TNBS challenge, reinforcing the importance of local microbiota to TNBS induced intestinal inflammation [10]. However, it is worth noting, as will be discussed later, that the extent to which zebrafish TLR4 recognizes LPS and propagates an inflammatory signalling cascade in a MYD88-dependant manner, is largely debated within the zebrafish community. In this model, observed gut morphologies included enlarged gut lumen as well as the disappearance of

intestinal crypts and villi [9]. Likewise, leukocyte infiltration and marked upregulation of the pro-inflammatory markers TNF-α, IL-1β, IL-8, MMP-9, and CCL20 have been observed as a response to TNBS exposure [8–10]. Of specific relevance to the thesis topic, the importance of TNF-α as a cytokine central to the perpetuation of IBD-like inflammation has been demonstrated in zebrafish larvae. For example, Marjoram et al., (2015), showed that loss-of-function mutations in *ubiquitin-like protein containing PHD and RING finger domains 1* (*uhrf1*) results in hallmark IBD phenotypes. It has been suggested that mutations of *uhrf1*, an epigenetic regulator, results in considerable hypomethylation of the TNF-α promoter and upregulation of the cytokine. Not only does TNF-α over expression precede the IBD-like phenotypes in the model presented by Marjoram et al., (2015), but morpholino knock down of TNF-α in these mutant fish was capable of rescuing the IBD-like phenotype.

As seen above, mutagenesis is another means of inducing inflammations in zebrafish. This method largely relies on loss-of-function phenotypes as a results of gene disruption. An example of this is mutations in the *CDP-diacylglycerol—inositol 3-phosphatidyltransferase* (*cdipt)* gene [11,12]. *Cdipt* mutants result is dysregulation of phosphatidylinositol (PI) synthesis leading to chronic endoplasmic reticulum (ER) stress [12]. While this may cause a number of pathological phenotypes, one of particular interest is the persistence of a phenotype in the gastro-intestinal tract resembling IBD. An eventual consequence of ER stress in the intestinal epithelial cells of *cdipt* mutants is the presence of an inflammatory response. This includes infiltration of macrophages and neutrophils; goblet cell apoptosis; impaired proliferation; and upregulation of pro-inflammatory cytokines (IL-6, IL-8 and IL-17) [13].

Puried endotoxins, such as LPS, are regularly used to induce an acute inflammatory response and is typically achieved by immersion of zebrafish larvae in media containing LPS or by injection of LPS into the larval yolk sac. Zebrafish exposure to LPS has been shown to induce many of the inflammatory signs typically seen in mammals, notably extravascular leukocyte migration, increased ROS production, and upregulation of pro-inflammatory cytokines such as TNF-α, IL-1β, and IL-6 [14,15]. Following LPS challenge, a wide variety of zebrafish tissues including the brain, gills, heart, liver, spleen, head kidney, intestine, muscle and skin were shown to upregulate the pro-inflammatory cytokine TNF-α [16]. Similarly, in line with human innate immunity, zebrafish leukocytes upregulate TNF-α secretion in response to bacterial challenge. For example, zebrafish macrophages have been shown to undergo polarization and migration, coupled with robust TNF-α upregulation, as result of infection from the gram-negative bacteria *E. coli* [17].

Another commonly used zebrafish model of inflammation is caudal fin amputation, where inflammation is induced by transection of either the distal or proximal caudal fin, just short of the notochord, using a sterile scalpel. Amputations initially result in an acute, local inflammatory response in which leukocytes infiltrate the wounded area. In larval amputation models, early neutrophil infiltration is followed by M1 macrophage infiltration - which has been shown to peak at about 6 hours post injury and is accompanied by upregulation of pro-inflammatory cytokines such as TNF-α, IL-1β and IL-6 [18–20]. During resolution of this inflammatory response, neutrophils are either depleted by apoptosis or migrate away from wounded area [21], while M1 macrophages transition to M2 macrophages in which TNF-α is significantly downregulated. Interestingly, while TNF-α downregulation is a sign of inflammation resolution, it has been suggested that the cytokine is critical in blastema formation during the process of tissue regeneration that succeeds inflammation [18]. This regenerative capacity of zebrafish following tailfin amputations is routinely used as a model for investigating the mechanism of tissue regeneration.

Interestingly, over the past decade, and likely due to the completion of the sequencing of the zebrafish genome in 2013 [22], a large proportion of studies investigating zebrafish inflammation have made use of transgenic zebrafish lines, including many of the models and studies discussed above. Macrophage migration and polarization is routinely investigated using transgenic zebrafish expressing a fluorescent protein under the control of the Macrophage-expressed gene 1 (Mpeg1) promoter [23]. Neutrophils are similarly visualized using the myeloperoxidase (mpx) promoter [20]. Likewise, the expression profile of many cytokines, chemokines, and other inflammatory markers are regularly investigated using transgenic zebrafish, including TNF-α, IL-1β and NF-kB [17,24–26]. The abundance of zebrafish transgenic lines stretches well beyond immuno-related protein expression. So much so that the Zebrafish information network (ZFIN) has curated publications on over 6466 transgenic zebrafish constructs [27]. Given the variety of transgenic zebrafish available, researchers frequently make use of cross-breeding between transgenic lines to develop double-transgenic zebrafish lines. For example, Nguyen-Chi et al., (2015), [17] developed a transgenic line, Tg(mpeg1:mCherryF/tnfa:eGFP-F), for the co-visualization of both TNF-α and macrophage specific Mpeg1 expression.

The advantageous potential of transgenic zebrafish lines is clearly evident from their abundant use in research. As such, it is in the interest of our research group to develop transgenic zebrafish capable of expressing fluorescent proteins as real-time indicators of expression of

mediators of inflammation. While inflammatory profiles and phenotypes vary across differing models, as seen above, there are central pro-inflammatory markers that appear to be common to most models. One of these markers is the pro-inflammatory cytokine TNF-α; a cytokine with a central role in intestinal inflammation, LPS-induced inflammation, and wound-induced inflammation (as well as the tissue regeneration process). Given our research groups interest in these models, the sections to follow will discuss the mechanisms of TNF-α regulation in zebrafish, followed by methodological considerations in developing a transgenic line of fluorescent TNF-α reporter zebrafish.

2.2 Zebrafish TNF-α

Zebrafish TNF-α propagates an inflammatory cascade. This pleotropic cytokine is expressed in response to a number of damage and pathogenic related stimuli, as is classically seen in mammals. Likewise, signalling following zebrafish TNF-α receptor binding, results in either apoptosis, necroptosis, or cell survival. In all, as discussed below, zebrafish TNF-α appears to share a number of structurally and functionally conserved features with its mammalian counterpart. It is worth noting that many mechanisms of zebrafish TNF-α function are yet to be unpacked, and so, in some respects, researchers have made inferences from studies on closely related teleost fish based on assumptions of conservation. The most pertinent information on zebrafish TNF-α structure, regulation and expression will be presented in the following section.

In terms of homology to human cytokines, unlike the single TNF-α gene present in humans (hTNF-α), zebrafish appear to have two homologues of the TNF-α gene (zTNF-α), namely zTNF-α1 and zTNF-α2 [16]. It has been suggested that the presence of two TNF-α homologues, a phenomenon also reported for a number of other zebrafish cytokines, arose as a result of a whole-genome duplication (WGD) event in early teleost lineages. Generally, following genome duplication events, most duplicated genomic material tends to become non-functional through accumulation of mutations. Alternatively, duplicated genomic material may remain functional via neo-functionalization, or sub-functionalization, the latter of which involves both genes fulfilling the role of the of the original gene [28]. Following the WGD of teleost fish, approximately 15 – 25% of duplicated genomic material was retained through neo-functionalization and sub-functionalization [28]. Structural and functional analysis suggests that both zTNF-α homologues

congruently work in a sub-functional manner to fulfil a similar immune role to that seen with hTNF-α.

2.2.1 Structure

Structural analysis of zTNF-α1 and zTNF-α2 reveals that both cytokines share 55% amino acid similarity (37.9 % amino acid identity). Meanwhile, hTNF-α1 and zTNF-α1 share 29.3% amino acid identity [29]. Structurally, both zebrafish homologues share conserved functional domains with hTNF-α, most notably, (a) a well-defined transmembrane domain, (b) TNF-α converting enzyme (TACE) cleavage sites and (c) a number of signature TNF motifs [16]. Interestingly, despite the general conservation of TNF-α TACE domains among teleosts, in zTNF-α2 a TACE domain was identified further upstream, closer to the C-terminal than those commonly illustrated in other teleosts. It has been proposed that this may increase the ability of TACE to cleave the transmembrane molecule. As a result both proteins may function sub-functionally, where zTNF-α1 operates more as a transmembrane protein than zTNF-α2, while the later may function more as a soluble protein [30]. Finally, much like hTNF-α, zTNF-α1 functions as a homotrimer. Interestingly, four amino acids shown to be essential to receptor-ligand binding of mouse TNF-α to hTNF-receptor 1, appear to be conserved in zTNF-α1. This, coupled with further 3D modeling and in silico analysis, suggests that zTNF-α1 may have the potential to bind to hTNF-R1 [29]. Although zTNF-α1 and zTNF-α2 are located on different chromosomes - chromosome 19 and 15 respectively - both are surrounded by numerous homologues of genes typically associated with the mammalian major histocompatibility complex III (MHC III) [16,31], again suggesting a conserved, shared immuno-regulatory role of zTNF-α1 and zTNF-α2.

2.2.2 Regulation and expression

Much like in humans, the zebrafish innate immune system has the ability to respond to a variety of pathogenic and non-pathogenic associated stimuli. A number of these stimuli have been highlighted in chapter 2, including tail fin wounds, TNBS immersion, and LPS exposures. Interestingly, however, very few papers investigating zebrafish TNF-α in a physiological context draw attention to the presence of zTNF-α2. As such, most studies investigating zebrafish “TNF-α” are specifically investigating zTNF-α1.

Kinoshita et al., (2014), compared the expression profile of zTNF-α1 and zTNF-α2 in the context of LPS exposure [16]. Firstly, this study observed that the basal levels of zTNF-α1 and zTNF-α2 expression were comparatively similar across a number of adult zebrafish organs including the brain, gills, heart, liver, spleen, head kidney, intestine, muscle and skin. The same study measured levels of zTNF-α1 and zTNF-α2 expression in head kidney cells isolated from zebrafish exposed to LPS. Here zTNF-α1 was upregulated between 1 and 24 hours post injection (HPI) while zTNF-α2 was upregulated between 4 and 24 HPI. Both cytokines showed similar levels of upregulation between 8 and 24 HPI with both peaking at 24 HPI. Interestingly, zTNF-α1 showed considerably higher levels of upregulation than zTNF-α2 between 1 and 4 HPI. This study suggests that zTNF-α1 may act as an acute and longer lasting response cytokine while zTNF-α2 is a delayed response cytokine. Although the relationship between zTNF-α1 and zTNF-α2 expression is mostly conserved across zebrafish tissues, the dynamics of TNF-α1 and TNF-α2 appears to differ among teleost fish. In rainbow trout HK macrophages stimulated with LPS, TNF-α1 showed delayed peaks in expression compared to TNF-α2 [30].

Interestingly, in terms of innate immune system recognition of LPS, there appears to be a difference between mammalian species and zebrafish. In mammals, an inflammatory response to LPS is traditionally mediated via the TLR4 receptor. While zebrafish possess two homologues of the mammalian TLR4, they do not possess the necessary chaperone proteins needed to bind LPS to TLR4, namely MD-2 and CD14 [32]. As such, research has shown that the zebrafish response to LPS may occur in a TLR4/MYD88-independant manner, but to what extent is still debated as the details and significance of this alternative mechanism remains to be fully elucidated (see Figure 2.1) [32,33]. It has been proposed that while some mechanisms of pathogen recognition are divergent between mammals and teleosts, the downstream signalling cascades following said recognition appear to be somewhat more conserved [7].

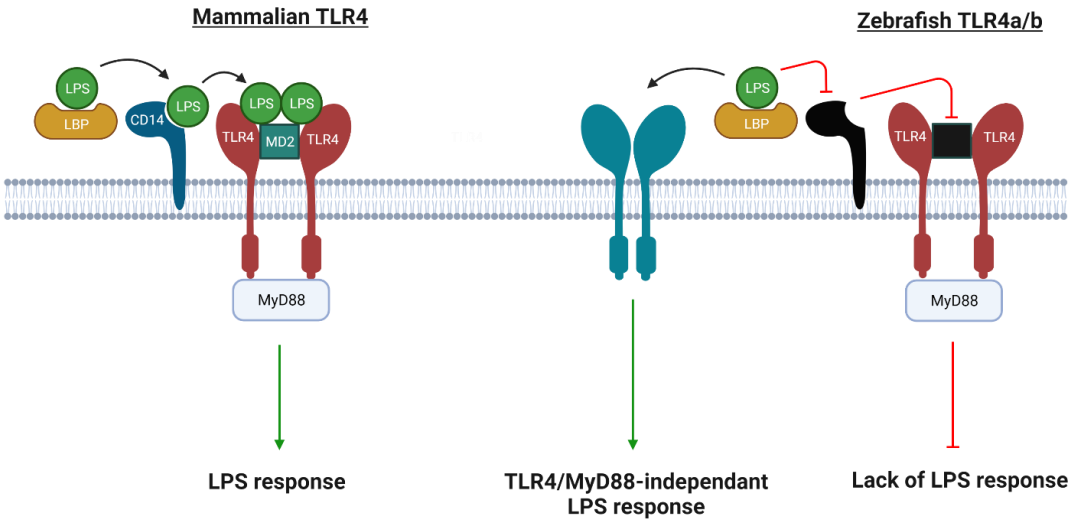

Figure 2.1: Comparison of mammalian and zebrafish responses to LPS via TLR4/MYD88 signalling. Created with BioRender.com.

Unfortunately, very little investigation has looked into the regulatory mechanisms of zTNF-α at the transcriptional level. Annotations of the zTNF-α1 and zTNF-α2 promoters are basic and do not describe much more than the transcription and translation start sites. As such, mapping of transcription factor binding sites on the zTNF-α1 and zTNF-α2 promoters is incredibly scarce. It is worth noting that a number of homologues of human TNF-α transcription factors have been identified in zebrafish. Some of these include NF-κB, NFAT, SP1 and Erg-1 [34–37]. Although these inflammatory-related transcription factors have been described in zebrafish, experimental validation assessing the expression profile of zTNF-α1 and zTNF-α2 in direct response to these transcription factors, as well as in silico mapping of the zTNF-α1 and zTNF-α2 promoters for transcription factor binding sites is needed to properly elucidate their role in zTNF-α expression. In terms of epigenetic regulation, Marjoram et al., (2015), showed that in the context of inflammatory bowel disease, hypomethylation of the zTNF-α1 promoter in gut epithelial cells resulted in increased expression of zTNF-α1 [38]. While very little investigation has been done in this regard, similar regulatory mechanisms have been elucidated in human leukocytes [39]. Much like transcriptional regulation, very little research has investigated post-transcriptional regulation of zebrafish TNF-α. An observation worth noting was made by Marjoram et al., (2015): the relative levels of zTNF-α1 protein expression (quantified using a fluorescent reporter gene) were higher than qPCR-quantified mRNA levels of zTNF-α1. The authors suggested that this may be due to unknown post-transcriptional regulatory mechanisms.

A number of the major post-translational modifications observed in mammalian TNF-α appear to be conserved in zebrafish TNF-α (see Figure 2.2). Both zebrafish TNF-α homologues appear to have a well conserved transmembrane domain suggesting migration of the proteins to the cell membrane where they are functionally active [30]. Similarly, zTNF-α1 has been shown to arrange in a homotrimer at cell membrane much like mammalian TNF-α [29]. Finally both zTNF-α1 and zTNF-α2 possess an extracellular TACE cleavage domain [30]. Like their mammalian counterparts both TNF-α proteins are functionally active as either membrane bound proteins or soluble proteins following TACE cleavage.

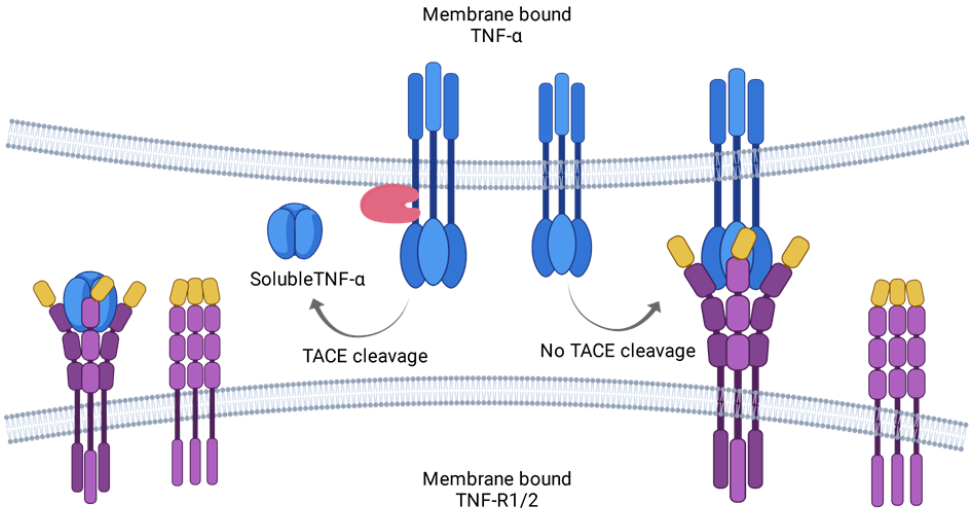

Figure 2.2: Post-translational formation of the TNF-α homotrimer at the cell surface. Here TNF-α is either functionally active as a membrane bound protein or a soluble protein following TACE cleavage. Created with BioRender.com.

While both cytokines appear to fulfil similar physiological roles, due to the lack of comparative literature, it is unclear to what extent they operate in a sub-functional manner. It is evident, however, that both zebrafish TNF-α's are pleotropic cytokines central to inflammation, much like their mammalian counterpart. As such it is in the interest of our research group to develop a reporter gene under the control of TNF-α transcriptional mechanisms to measure as a proxy for inflammation. The vast majority of literature exploring zebrafish TNF-α is focused on zTNF-α1. As a result most inflammatory models investigated in zebrafish with intended future applicability in mammalian systems has drawn on data from zTNF-α1 more than zTNF-α2. Likewise, the

finer structure of the zTNF-α1 protein as well as the few known transcriptional and post-transcriptional regulatory mechanisms has been described considerably more in zTNF-α1 than zTNF-α2. The work presented in this thesis intended to use the TNF-α reporter gene to further our understanding of inflammation in zebrafish. For these reasons we decided to develop a reporter gene that reflects production of zTNF-α1 rather than zTNF-α2. The next section will discuss the various considerations to take into account when developing the zTNF-α1 reporter gene.

2.3 Transgenic zebrafish development

Given the many advantages of zebrafish research and the necessity to monitor TNF-α in a number of inflammatory models, the study at hand intended to develop a transgenic line of zebrafish expressing a reporter gene under the same transcriptional regulatory mechanisms as the zebrafish pro-inflammatory cytokine zTNF-α1. Many avenues of transgenic reporter gene design are possible, and so thorough investigation was performed when considering each aspect. The following section will cover each of these consideration and the rationale behind each method of choice. For this a number of factors related to the process of transgenesis need to be discussed. This will included: The history and contemporary views on various methods; competing approaches for methods; and biological explanations of each method. While there are many ways to perform transgenic work in zebrafish, emphasis will be placed on the on the more standard practices in the zebrafish community.

2.3.1 Transient and stable reporter gene assays

2.3.1.1 Transient reporter gene assays

Transient expression of a transgene involves the temporary expression of a transgenic construct. Classically, this is performed by inserting a transgene-carrying vector into the extrachromosomal space of the host cell, where it will not integrate into the host genomic DNA but will use endogenous transcriptional mechanisms to produce transgene mRNA. Due to the lack of genomic integration, the transgene will remain in the extrachromosomal space where it

will not replicate. As such the transient vector will be expelled from the host cells line due to lack of replication and metabolic burden on the host cells [40]. This process is hastened if the vector does not carry a selectable marker that infers a selection pressure advantage to the host cells. Due to the nature of transient transgenic assays, expression of the transgene will only last for several hours to several days before the transgene is lost from the host cells (see Figure 2.3).

While transient transgene expression has a few limitations, it is routinely used in a number of study types, particularly *in vitro* studies. For example, in studies where cells are transfected with mRNA to be rapidly expressed, integration into the genome is not necessary [41]. This ease of transient transgene assays is particularly attractive in cell culture studies where tran

sgene delivery is easy and relatively efficient. However, a major shortfall of transient assays is the need to re-transfect samples before every assay. This may become laborious and expensive.

In zebrafish-based research, transient assays are typically reserved for cell culture-based studies where it is a common practice. As such, protocols for transient transfection of zebrafish cell lines are not difficult to come by [42,43].

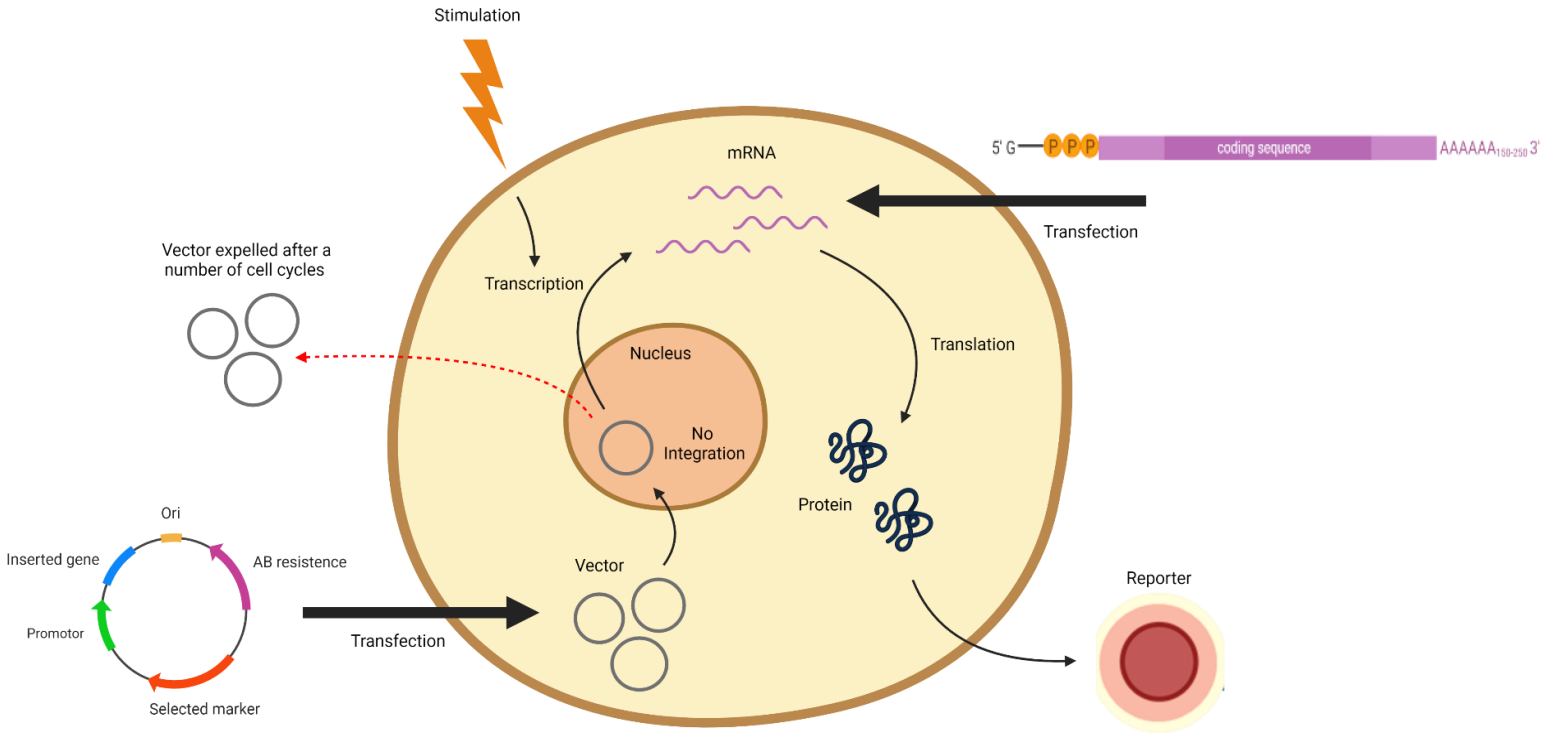

Figure 2.3 Representation of the process of transient reporter gene expression. Here a transgene vector is delivered into the cell where it does not integrate into the host genome but is capable of transcribing reporter gene mRNA which in turn is translated into the desired reporter protein. Due to lack of integration, the transient vector or mRNA will be eventually expelled from the host cell. Created with BioRender.com.

2.3.1.2 Stable reporter gene assays

Unlike transient transgene gene expression, stable transgene expression relies on the integration of the transgene into the host cell's genomic DNA. Successfully integrated transgenes will remain in the host genome from generation to generation, unlike transient transgenes. While the initial efforts of developing a transgenic line are laborious and time consuming, the long term benefit of generational transgene propagation, without the need to re-transfect cells for every assay performed, make stable transgenic lines an attractive pursuit.

The first stable transgenic zebrafish line was developed by Stuart et al., (1988), and since then the use of stable transgenic zebrafish lines have been adopted for a multitude of study types. Particularly, the use of stable transgenic lines expressing reporter genes to understand the dynamics of protein expression has become an invaluable tool and standard practice in zebrafish-based research. As previously discussed, one notably interesting application of transgenic zebrafish lines is the ability to cross transgenic lines. For example, Nguyen-Chi et al. utilized a double transgenic line to track the expression of zTNF-α1 in macrophages. More specifically, the line possessed a fluorescent mCherry reporter under the transcriptional control of the ubiquitously expressed macrophage specific protein, mpeg1, as well as a fluorescent eGFP reporter under the transcriptional control of the zTNF-α1 promoter Tg(mpeg1:mCherry-F/tnfa: eGFP-F) [18].

As the aim of this study is to visualise protein dynamics *in vivo*, we opted to develop a stable zebrafish transgenic line expressing a reporter gene under the control of zTNF-α1 transcriptional mechanisms.

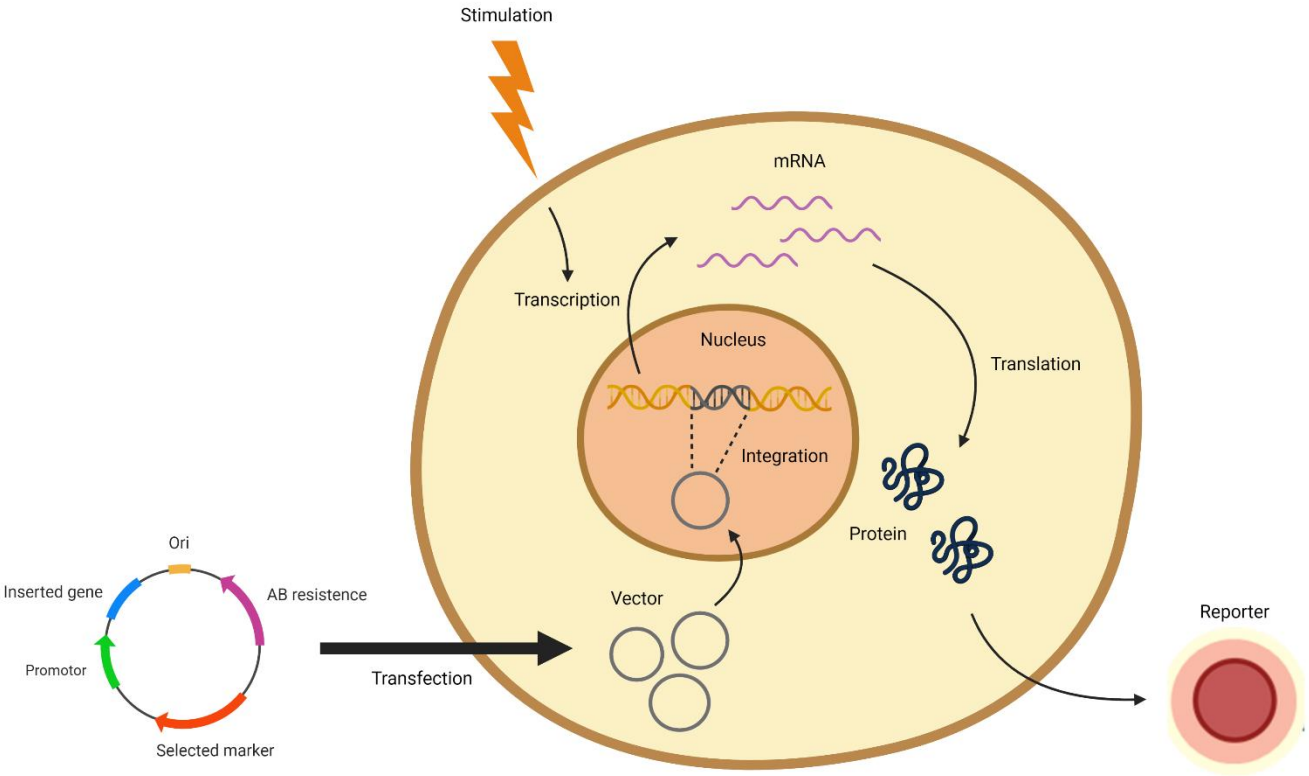

Figure 2.4: Representation of stable reporter gene assays. Here a transgene vector is delivered into the cell where it is integrated into the host genome. The integrated transgene is capable of transcribing reporter gene mRNA which in turn is translated into the desired reporter protein. Given the integration into the host genome, the transgene will remain in the host from generation to generation. Created with BioRender.com.

2.3.2 Transgene design

Careful design of the transgenic construct used to transfect zebrafish is pivotal in the successful development of a transgenic zebrafish line. Traditionally, transgenic constructs for monitoring the spatio-temporal dynamics of a gene of interest are designed as follows: A reporter gene, often coding for a light emitting protein (which will be discussed later), is immediately preceded

by an inducible regulatory element. While this may include enhancer elements, it is most commonly a gene promoter – the primary element responsible for gene transcriptional regulation [44]. Next, a Poly (A) tail is usually added to the construct, downstream of the reporter gene. This element is necessary for transgene mRNA stabilization and promotion of translation [44,45]. Finally, the elements needed to integrate the transgene construct into the host genome are included within the vicinity of the transgene construct, usually on the peripheries of the construct (this will be discussed in a later section). These factors need to be considered when designing a transgene construct and will be discussed below. In summary, these include the gene of interest to be monitored, the reporter gene used to monitor the dynamics of said gene, and the method of integration of the transgenic construct into the host genome.

2.3.2.1 Gene of interest

With interest in the dynamics of zTNF-α1 in zebrafish inflammation, the current study intended to develop an inducible zTNF-α1 reporter transgenic line under the transcriptional control of the zTNF-α1 promoter. Unfortunately, very little research has reported on the zTNF-α1 promoter. Annotations of the promoter region are basic and do not describe much more than the transcription and translation start sites. As described in a previous chapter, a number of orthologues of hTNF-α transcription factors have been identified in zebrafish; however, their role in zTNF-α1 transcriptional regulation is yet to be elucidated. In humans the TNF-α gene has a proximal promoter of approximately 180 base pairs (bps) upstream of the transcription start site, while the distal promoter is approximately 872 bps [46,47]. On average, gene promoters are about 1000 bps [48], and so without knowledge of potential transcription factor binding sites upstream of the zTNF-α1 gene, it is reasonable to assume that the promoter may be within a few hundred to a few thousand bps upstream of the transcription start site. With that in mind it may be worth consulting studies that have developed zebrafish zTNF-α1 transgenic lines.

Only two notable studies have managed to design zTNF-α1 promoter driven, reporter gene, transgenic zebrafish lines. In 2015 Nguyen-Chi et al. developed a zebrafish transgenic line expressing eGFP under the transcriptional control of the zTNF-α1 promoter, Tg(tnfa:eGFP-F) [17]. Transcription of the cassette in question was under the control of the 3.8 kbp promoter fragment preceding the zTNF-α1 gene. This transgene was inducible following stimulation from

both *E. coli* infection as well as tail fin injury. Around the same time Marjoram et al. developed a transgenic zebrafish line, TgBAC(tnfa:GFP), in much the same way as the line described above [24]. One notable difference is the use of a 50 kbp promoter fragment. This transgene was inducible following stimulation form the commonly used inflammatory stimulant, *Mycobacterium marinum*. Interestingly this transgenic line was capable of detecting basal expression of zTNF-α1 in the eye, brain, dorsal root ganglion neurons, and the posterior gut epithelium.

Given the likely excess of using a promoter much longer than a few thousand bps, and following the example of previously validated transgenic lines, for this study we have opted to isolate and use a zTNF-α1 promoter region of about 3.7 kbps.

2.3.2.2 Reporter gene

Reporter genes have been widely used for a number of study types, both *in vitro* and *in vivo*. Of particular interest to this study is the common practice of placing a reporter gene downstream of an inducible promoter; the promoter of a gene of interest; to monitor the dynamics of said gene. Many types of reporter gene systems have been utilized in zebrafish transgenic related studies. Given the optical transparency of zebrafish, especially at early developmental stages, the most noteworthy among these include light emitting reporter genes, such as fluorescent and luciferase reporter genes. When deciding which of these reporter gene systems are the best suited for a particular study, a number of factors should be considered including: wavelength (colour); signal strength; reporter gene stability; and cofactor dependency [49]. Given the ubiquitous use of fluorescent and luciferase reporter genes in zebrafish studies, a number of these consideration will be discussed for each of the two reporter gene types.

2.3.2.2.1 Luciferase

Luciferase is a bioluminescent protein derived from the firefly (*Photinus pyralis).* The luciferase bioluminescent reaction is catalysed by luciferin, ATP, Mg^{2+}, and O_2. In some studies, the need for these additional substrates to catalyse the luciferase reaction may be a limiting factor. While this is often less of an issue with cell lysates, administration of these cofactors for *in vivo* reactions has traditionally proven difficult, although for zebrafish whole embryo luciferase assays, some protocols simply add luciferin to embryo water [50]. A major advantage of bioluminescence is the ability to quantify light emission using a luminometer, and thus quantify levels of protein expression via a luciferase reporter gene. While this is a major upside to

luciferase assays, it is coupled to the inability of the luminometer to determine spatial dynamics of luciferase light emission. Finally, two additional advantages of luciferase assays include incredibly high sensitivity, with low background noise [51,52]. The luciferase reporter gene assay is an attractive assay with a number of advantages and disadvantages, and as such the zebrafish community have taken to using the reporter gene in a number of study types, *in vitro* and *in vivo* alike [50,53].

2.3.2.2.2 Fluorescent proteins

Like luciferase, fluorescent proteins are light emitting proteins routinely used as reporter genes. These proteins contain chromophores that emit light when excited by light. Excitation and emission wavelengths vary between chromophores, giving rise to a number of different colour-emitting fluorescent proteins. The most commonly used fluorescent protein among reporter genes is the jellyfish (*Aequorea victoria)*-derived green fluorescent protein (GFP). Transgenic zebrafish lines routinely employ the use of GFP reporter genes [17,18,54]. While GFP is often used in zebrafish reporter gene research, one partial drawback is lost signal due to background noise caused by zebrafish tissue auto-fluorescence [55]. A useful alternative to GFP is the *Discosoma*-derived red fluorescent protein DsRed. A particularly useful derivative of DsRed is monomeric mCherry, which has been shown to emit brighter signals and mature quicker than most fluorescent proteins [56,57]. In general, once mature, fluorescent proteins tend to have a considerably longer half-life than the luciferase protein. Furthermore, the usefulness of fluorescent proteins in reporter gene assays is a double edged sword: on one hand, sub-cellular quantification of fluorescent protein expression is possible using flow cytometry, while another major advantage of fluorescent proteins is the ease of monitoring spatio-temporal dynamics with fluorescence microscopy. With these useful properties in mind we chose to employ mCherry as our fluorophore of choice.

2.3.3 Integration methods

Following the delivery of a transgenic cassette into developing embryos, a number of methods are employed to facilitate integration of that transgenic material into the genome. These methods can be broadly categorised as ‘targeted integration methods’ or ‘random integration methods’. Simply, targeted integration involves inserting a transgene into a known, predetermined location of the genome, while the genomic location of randomly integrated

transgenic material is not predetermined and less specific. Both methods typically rely on the induction of double-strand breaks (DSB) from a catalytic enzyme and subsequent DNA repair. Following a DSB cells may utilise one of two major mechanisms to repair DNA damage. Firstly, homology directed repair (HDR) utilises a DNA template with sequences homologues to the DSB ends. Homologous recombination is followed by elongation, after which ligation repairs the cleaved DNA. DNA damage may be repaired through HDR with the help of a sister chromatid as a template, or alternatively, researchers may introduce an exogenous DNA template to introduce new genomic material at the DSB site [58]. Alternatively, non-Homology end joining (NHEJ) is a faster repair mechanism than HDR and typically commences in the absence of templates for homology directed repair. In NHEJ, cleaved ends are directly ligated. Often this is facilitated by direct ligation between short, single stranded overhangs that are homologues to a complementary single strand overhang. Depending on the extent of homology between these overhangs, repair via NHEJ may result in mutations that could change or impair gene function. Like HDR, NHEJ may be utilised by researchers to mutate or knock-out targeted genomic regions, or knock-in exogenous genomic material through the introduction of exogenous DNA with compatible overhangs [58].

While eukaryotic cells are capable of employing any of the repair mechanisms discussed above, researchers often force a particular mode of DSB repair when utilising a specific transgene integration method. Each method was carefully considered and the advantages and disadvantages of each will be discussed below.

2.3.3.1 Targeted integration

Targeted transgene integration is a rapidly developing method that is commonly used in genetic engineering. Here proteins recognise a specific, predetermined DNA sequence and recruit catalytic enzymes to that region. The catalytic enzymes induce a DSB in a specific region at or near a recognition sequence in the genome. Following a DSB the cell utilises one of the DNA repair mechanisms described above. DSB repair may result in mutation or knock-out (and thus functional loss of a gene), or - with the aid of a donor vector - may be used to incorporate exogenous DNA into the host genome.

While a number of targeted gene editing tools are available, the three that are most commonly used in zebrafish genome editing are zinc-finger nucleases (ZFN), transcription activator-like

effector nuclease (TALEN), and clustered regularly interspaced short palindromic repeats (CRISPR)/Cas9 [44]. See Figure 2.5 for a summary of these targeted gene editing tools.

ZFNs were among the early methods of targeted genome editing. This chimeric endonuclease consists of a zinc-finger domain that recognises a specific DNA motif, fused to a catalytic FokI nuclease which induces a double-strand break in the target DNA. To induce a DSB at least two monomeric FokI nucleases are required. In the absence of a HDR template, NHEJ may repair DNA at the expense of possibly inducing a mutation. This may cause mutagenesis and thus functional loss of a target gene – a technique that has been used for the development of loss-of-function zebrafish lines [59].

TALENS are among the newer techniques of genome editing. TALENS consist of two functional domains: DNA binding TaI effector proteins and FokI nuclease for DNA DSB. Much like ZFNs, at least two FokI nucleases are required for DSB induction. Conversely to ZFNs, however, TALENS induce DSBs with high specificity and greater efficiency than ZFNs, making them an attractive alternative to ZFNs [60].

The CRISPR/Cas9 system is the fastest developing genome editing tool amongst those described here. This is largely due to a number of advantages that CRISPR/Cas9 possesses over its predecessors, including ease of use and relatively low cost of acquiring sgRNA, as well as the ability to use multiple sgRNAs in a single reaction, allowing for simultaneous editing of multiple genomic regions [44]. Briefly, CRISPR/Cas9 consists of CRISPR RNA (crRNA) and trans-activating crRNA (tracrRNA), which, when chimerically fused, form the DNA recognition domain of this system, known as the single-guide RNA (sgRNA). Guided to a specific DNA recognition sequence by sgRNA, the Cas protein catalytically cleaves DNA at a specific site [60]. The CRISPR/Cas9 systems is capable of serving a multitude of genome editing purposes in zebrafish research, with the toolbox ever expanding. Chief amongst those include targeted mutagenesis, targeted knock-out and targeted knock-in applications [61].

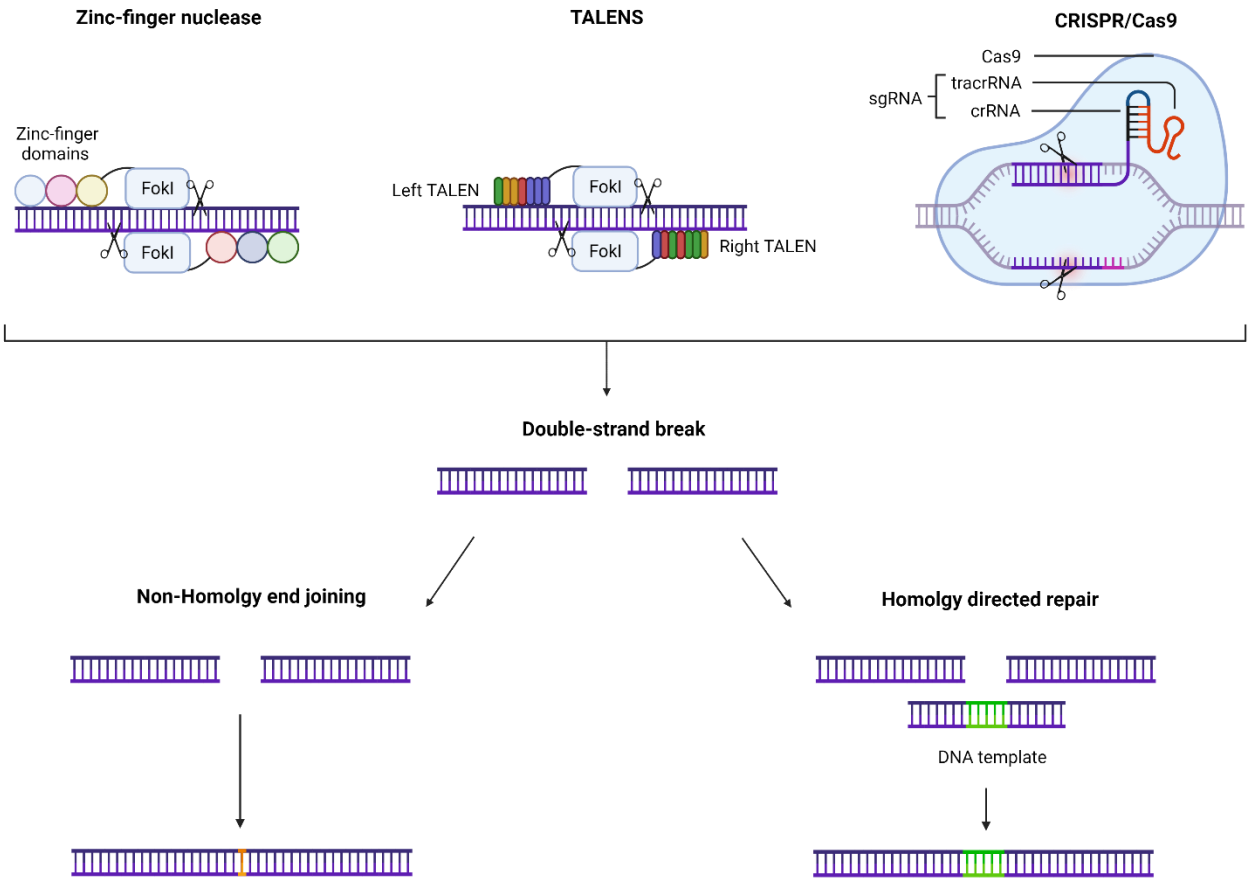

Figure 2.5: Comparison of targeted transgene integration methods, as well as pathways utilized by said methods to repair double-strand breaks. Created with BioRender.com.

2.3.3.2 Random integration

While the targeted gene editing tools described above are rapidly developing, and evermore frequently used for genome editing, particularly in mutagenesis and knock-out models, there are still some difficulties in using them for transgene knock-in. As a result, many researchers choose to integrate genetic material via a random integration method. The two most commonly used contemporary methods employed by the zebrafish community are the transposon Tol2 system, and the Homing-endonuclease I-SceI system [62].

Random integration may theoretically be prone to a number of unwanted effects such as variability in transgene integration site and copy number, transgene silencing and disruption, or ectopic expression of endogenous genes [63]. With experimental design and optimization, each of these potential problems can be mitigated. To properly understand the rationale behind the use of the Tol2 and I-SceI systems, and why they are so commonly used in zebrafish transgenesis, a thorough understanding of how they work is necessary, and so each method will be explored below.

2.3.3.2.1 Transposons

In nature, transposable elements are genetic elements that are able to change their location within a genome. Broadly, there are two classes of transposons: Class I transposons that translocate via RNA intermediates, and class II transposons that translocate directly as DNA elements [64]. The former utilises reverse transcription while the later catalytically excises the transposable DNA element followed by reinsertion of the transposable element; a mechanism often termed 'cut and paste'. Catalytic excision is performed by the transposase enzyme [65]. For excision, the transposases enzyme recognises DNA sequences flanking the transposon, termed inverted terminal repeats (ITRs) [65]. Mechanisms for reintegration of excised transposable elements appear to be less well understood, and highly versatile. As such, transposable elements have been found to reintegrate into a wide variety of genomic regions, coding and non-coding alike [64,66]. In both classes of transposons there are autonomous and non-autonomous transposable elements. Autonomous transposable elements are elements that code for the transposase enzyme, while non-autonomous transposable elements do not code for the transposase and are reliant of the activity of a transposase that has been expressed from outside of the transposable element. While both class I and class II transposable elements are useful to the larger molecular biology community, it is class II transposons that have been largely adapted by the zebrafish transgenic community, most notably the Tol2 transposon.

First described in 1996 by Koga et al., Tol2 is one of first transposable elements observed in vertebrates [67]. This transposon is autonomous in its native host the Medaka fish (*Oryzias latipes*) – a close relative to the zebrafish – where the Tol2 enzyme is coded for between flanking Tol2 ITRs. Manipulation of the peripheral ITRs has allowed researchers to develop DNA cassettes flanked by said domains, without the presence of the coding region for the Tol2 enzyme. These are still capable of being catalytically excised by the Tol2 enzyme, and coupled with isolated exogenous Tol2 enzyme mRNA, are the basis for a system in which DNA manipulation may be performed without the concerns of Tol2 enzyme interference from the host

[68]. A major advantage of utilising Tol2 enzyme mRNA for transgene cassette integration is that the mRNA will only act transiently. Interestingly, Tol2 systems have been shown to be active in all vertebrates tested so far [68]. Thus, due to the lack of the endogenous Tol2 transposase enzyme in the zebrafish genome, and universality of Tol2 based systems, researchers have taken advantage of this system for manipulation of the zebrafish genome. This system was first utilised in 2000 by Kawakami et al. to develop germline transgenic zebrafish [69], and has since been widely adapted for zebrafish transgenesis [44]. Naturally, a growing body of collective evidence has begun to highlight the advantages and disadvantages of Tol2 based systems.

Due to relatively low specificity of the Tol2 enzyme during integration, efficiency of integration is high. Akihiro Urasaki et al. observed that approximately 60% of zebrafish embryos injected with a number of minimal Tol2 constructs managed to pass on the transgene through the germline [70]. Earlier research using a longer version of the same construct produced germline transmission rates of approximately 50% [71]. While a number of factors may explain the high integration efficiency observed above, one primary reason is due to the low target site specificity employed by the Tol2 enzymes for integration. It is suggested that Tol2 has a higher affinity for AT-rich DNA with weak palindromic consensus sequences [72]. Likewise, it appears that the Tol2 enzyme is not reliant on cellular cofactors for integration into the zebrafish genome, lending to the high integration efficiency [72]. Given the high integration efficiency, Tol2 cassettes are capable of integrating into multiple zebrafish loci. Akihiro Urasaki et al., (2006), observed that for three Tol2 constructs the average number of insertions per injected zebrafish was 6.9, 6.9, and 5.5, across 16 different insertion sites [70], while an earlier study using a larger version of these constructs observed an average of 5.6 insertions per zebrafish injected [71]. In fact, researchers were able to identify 338 sites of Tol2 cassette integration within the zebrafish genome, 39% of which were in known or predicted zebrafish genes, mostly introns [72]. This may present as a disadvantage for zebrafish transgenics and could require considerable screening to ensure that an integrated transgene does not significantly interfere with coding regions. Finally, a major advantage of the Tol2 based system is that at any given integration locus, only a single transgene insert is created - alternative enzymatic based methods are known to create concatemer repeats, which may result in gene silencing.

2.3.3.2.2 Homing-endonucleases

Homing-endonuclease genes (HEGs), like transposable elements, are selfish, mobile genetic elements in nature. These nucleases, often referred to as meganucleases due to their relatively

large recognition motifs [73], are coded for by open reading frames found within self-splicing inteins and group I and II introns [74] . The ability to self-splice allows these intervening sequences to remove themselves from the host mRNA or protein and ligate the remaining exons or exteins domains with minimal interference to host coding domains [75]. This process is autocatalytic and does not require traditional spliceosome machinery or endogenous cofactors [75]. The HEG itself is responsible for the inter and intra genomic mobile transfer of these intervening sequences. While vertical transfer is possible, HEGs largely perpetuate through horizontal transfer between alleles. To do this, HEGs recognise specific motifs and induce catalytic double-strand breaks between exons of the homologous allele, often lacking the HEG and self-splicing domains. Endogenous double-strand break repair, mediated through homologous-recombination between the HEG positive and negative allele, allows transfer of the entire intervening sequence. This process is known as 'homing' [76]. While researchers are still unsure about the exact evolutionary advantage inferred to the host from these 'selfish' mobile elements, it has been suggested that they are largely responsible for introduction of new genetic material into host organisms. Similarly, the ability of these intervening sequences to self-splice is considered to be a form of evolutionary mutualism, were intervening sequences may propagate within a genome without causing deleterious effects to protein coding domains.

Insight into the phenomenon of HEG-mediated mobility began in the early 1970s, when researchers described a mobile genetic element in a group I intron of the large rRNA mitochondrial gene of the yeast *Saccharomyces cerevisiae*. The genetic marker, initially termed ω, was shown to be transferable during crosses between ω^+ and ω^- strains [74]. Later observations noted double-strand breaks induced in the ω^- allele by a protein encoded within the ω^+ allele, followed by homologous recombination between both alleles. [74]. This protein was the first homing-endonuclease to be described and is now termed I-SceI by modern nomenclature: intron encoded endonucleases precede with an I- and intein encoded endonucleases preceded with a PI- [73].

I-SceI was quickly adopted by the transgenic community. Soon, I-SceI meganuclease-mediated transgenesis was similarly adopted by the zebrafish and larger teleost community. Prior to I-SceI, among a number of methods, early teleost transgenic work was commonly performed by simple cytoplasmic injection of transgene containing plasmids into fish embryos. While this method did work, it was relatively inefficient due to low transgene integration rates. Consequently, unintegrated extrachromosomal DNA often displayed transient expression during early embryogenesis [77]. In the early 2000's Thermes et al. used a similar plasmid-based

system, with the addition I-SceI recognition sequences flanking the transgene construct. This plasmid, with the I-SceI enzyme, was co-injected into medaka embryos and largely resulted in increased transgene integration and germline transmission [77]. As a result, the use of I-SceI has been successfully used in the transgenesis of zebrafish, a close phylogenetic relative to the medaka fish [78].

To understand I-SceI-mediated transgenesis, it is worth looking into the structural and functional characteristics of the I-SceI enzyme. The I-SceI endonuclease recognises the 18 bp sequence TAGGGATAACAGGGTAAT [78]. Due to the large size of the 18 bp I-SceI recognition sequence, the enzyme's recognition domain should only theoretically occur every $7x10^{10}$ bp. Such a site has not been identified in the zebrafish genome yet [79]. This phenomenon leads to an interesting mechanism of transgene integration that is still not well understood: the enzyme cleaves and liberates the transgene from its plasmid but does not cleave the host genome. This minimizes the deleterious effects occasionally associated with genome shearing seen in restriction enzyme transgenesis [77]. I-SceI acts as a monomeric enzyme that induces an asymmetrical double-strand break at the target sequence. The enzyme remains associated to the larger half of the recognition sequence following cleavage. This may reduce both the degradation of liberated linear transgene strands and the formation of long concatemers [77,78]. As such, transgenesis using I-SceI based mechanisms often results in single-loci integrations with few tandem repeats per integration site. Thermes et al., (2002), reported integrations events with 1-8 tandem copies. While teleost studies reporting on the statistics of transgene germline transmission using I-SceI based mechanisms are scarce, there are a number worth looking into. Using a simple construct, Thermes and colleagues reported a germline transmission of ≈ 50% in Medaka, where I-SceI negative controls were considerably lower [77]. With a similarly simple construct injected into zebrafish embryos, Harrold et al., (2016), were able to obtain a transgene integration rate of 0% - 61% depending on the degree of initial transgenes expression in injected F0 founder fish [80]. Lastly, Soroldoni et al., (2009), showed that microinjection of the I-SceI construct at various cell count stages results in variable germline transmission rates due to mosaic germline integration. For example, in this study, a F0 founder that was injected at the 4-cell stage produced 10% transgenic offspring, at the 2-cell stage produced 20% transgenic offspring, and at the 1-cell stage produced 45% transgenic offspring [79]. The use of the I-SceI integration method presents with a number of advantages and is routinely used in zebrafish transgenic line development. Furthermore, simple protocols for the use of I-SceI are available [78,79]. Given the ease and establishment of the I-SceI

integration method, as well as having the expertise in our lab needed to utilise it, we will be adopting this as our means of transgene integration.

2.4 Transgene construct summary

As seen in the review above, there are a multitude of considerations in designing a reporter gene construct when developing a stable transgenic zebrafish line. With each aspect discussed in thorough detail, the final construct was designed as seen Figure 2.6 and carried on a plasmid vector:

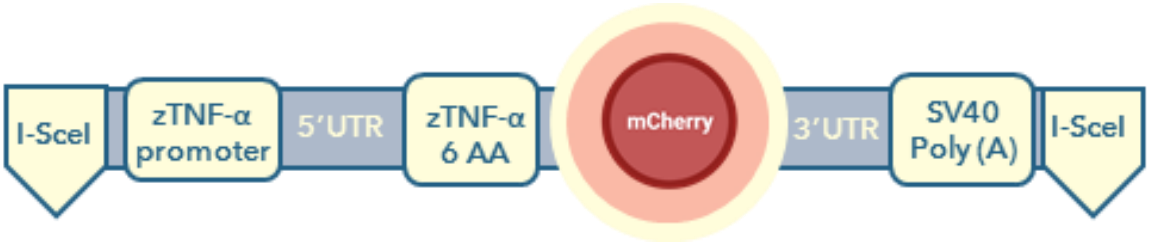

Figure 2.6: Schematic diagram of the transgene construct from 5' to 3': Plasmid DNA; I-SceI meganuclease recognition site; zTNF-α1 promoter region including an additional 18 nucleotides coding for the first six amino acids of the zTNF-α1 protein; mCherry; SV40 poly (A) terminator region; I-SceI meganuclease recognition site; plasmid DNA.

2.5 Transgene delivery

For uptake of the transgene and integration into the zebrafish genome, a suitable vector delivery protocol will need to be employed. While the widely accepted convention is to use microinjection, occasionally, a number of alternative methods are used, such as electroporation of whole embryos and electroporation of sperm culture followed by *in vitro* fertilization [81,82]. Given the ubiquity of the microinjection method as well as equipment availability in our lab, we chose to use this method for transgene delivery in this study.

Chapter 3

Experimental work

Given the method development nature of this study, the results obtained from each experiment performed determined the means of approaching the subsequent experiment. As a result, the chapter to follow will subdivide each major experiment into methods, results, and discussion, followed by the next experiment.

3.1 Part I: Transgene synthesis and cloning

For the synthesis of the transgene construct, several genomic fragments were isolated, amplified, and ligated to develop the final transgene construct pRSF-zTNFα-mCherry. These fragments include the zebrafish TNF-α1 promoter including the first six amino acids of TNF-α1 (+6 AA), the fluorescent reporter gene mCherry, and the SV40 Poly (A) tail sequence. Several variations of each fragment were isolated and amplified prior to accessing and choosing the best suited fragment for synthesis of the final transgene construct. The methods and results to follow will discuss the isolation and cloning of each of these fragments with special attention given to the fragments used in the final transgene construct.

3.1.1 Methods

3.1.1.1 TNF-α1 promotor isolation

Genomic DNA (gDNA) was isolated from wild type (WT) *Danio rerio* (zebrafish) using Qiagen's DNeasy Blood & Tissue Kit (QIAGEN, South Africa), according to manufactures instructions. From isolated gDNA the zebrafish TNF-α1 promoter including the first six TNF-α1 amino acids (+6 AA) were amplified as a single ~3700 bp fragment using a 2-step PCR. For the first PCR reaction the primers 'zTNF Forw' and 'zTNF Rev' (Table 3.1) were used to amplify the genomic TNF-α1 promoter (+6 AA).

Likewise, alternative TNF-α1 promotor fragments were isolated and amplified from gDNA. An ~3300 bp TNF-α1 promoter (+6 AA) fragment was amplified using the primers 'zTNF alt 1 Forw' and 'zTNF Rev' (Table 3.2). Similarly, an ~3700 bp TNF-α1 promoter (+6 AA) fragment was amplified using the primers 'zTNF alt 2 Forw' and 'zTNF Rev' (Table 3.2).

For analysis and downstream applications, the TNF-α1 promoter fragments were individually blunt-end cloned into the intermediate vectors, pMiniT 2.0, using the NEB® PCR Cloning Kit (NEB, South Africa), according to the manufacturer's instructions. The newly cloned pMiniT 2.0 vectors were then transformed into competent *Escherichia coli* cells by heat shock transformation (90 µl competent *E.coli* cells, 10 µl cloned ligation mixture). Transformed cells were then plated (3.7 g/100 ml LB nutrient broth powder, 1.2% agar, and 100 µg/ml ampicillin) and incubated at 37°C overnight. Plated colonies were picked and tested by colony PCR for the presence of the TNF-α1 promoter fragments using the primers 'zTNF Forw' and 'zTNF Rev' (Table 3.1), 'zTNF alt 1 Forw' and 'zTNF Rev' (Table 3.2), and 'zTNF alt 2 Forw' and 'zTNF Rev' (Table 3.2) respectively.

Positive colonies were repicked and inoculated in LB nutrient broth (3.7 g/100 ml LB nutrient broth powder and 100 µg/ml ampicillin) overnight at 37°C under constant aeration. The pMiniT 2.0 plasmids were then isolated from inoculated colonies by miniprep, using Monarch® Plasmid Miniprep Kit (NEB, South Africa), according to the manufacturer's instructions. The isolated pMiniT 2.0 plasmids were digested with XhoI at 37°C for 15 min and run through gel electrophoresis to confirm the presence of the correct fragment sizes. Furthermore, all plasmids were sent for sequencing at the Central Analytical Facilities (CAF), University of Stellenbosch, South Africa, to confirm successful isolation and cloning of the TNF-α1 promoter fragments. Sequence data was produced using the forward and reverse primers initially used to isolate and amplify each TNF-α1 promoter fragment. Sequence data was then aligned to the *Danio rerio* reference genome, GRCz11 from NCBI, using EMBOSS Needle Pairwise Sequence Alignment.

Following confirmation of successful cloning of the TNF-α1 promoter fragments, the primary TNF-α1 promoter fragment (amplified using the primers 'zTNF Forw' and 'zTNF Rev' – Table 3.1), was chosen and again PCR amplified from the pMiniT 2.0 vector using the primers 'zTNF Forw' and 'zTNF Rev'. The DNA product from this reaction was purified using Monarch® PCR & DNA Cleanup Kit (NEB, South Africa), according to manufactures instructions. Purified DNA product was used in the second step of the 2-step PCR. For the second PCR the primers 'I-SceI zTNF Forw' and 'PstI zTNF Rev' (Table 3.1) were used to add an I-SceI and PstI recognition domain to the 5' and 3' ends of the TNF-α1 promotor fragment, respectively.

3.1.1.2 mCherry isolation

For the mCherry fragment, pNZCherry was gifted from Dr. Winschau van Zyl, Dept. Microbiology, Stellenbosch University, from which mCherry was amplified. The primers 'PstI mCherry Forw' and 'XhoI mCherry Rev' (Table 3.1) were used to amplify mCherry with PstI and XhoI recognition domains on the 5' and 3' ends of the fragment respectively.

3.1.1.3 GFP isolation

As an alternative to the mCherry fluorescent protein, GFP was isolated and amplified. For the GFP fragment, pRSFGFP was gifted from Dr. AD van Staden, Dept. Microbiology, Stellenbosch University, from which GFP was amplified. The primers 'PstI GFP Forw' and 'XhoI GFP Rev' (Table 3.2) were used to amplify GFP with PstI and XhoI recognition domains on the 5' and 3' ends of the fragment respectively.

3.1.1.4 SV40 Poly (A) tail isolation

Finally, the SV40 Poly (A) tail was amplified from the LC3-GFP plasmid, a gift from Prof. Ben Loos, Dept. Physiology, Stellenbosch University. Much like the TNF-α1 fragment, the SV40 Poly (A) tail was amplified using a 2-step PCR reaction. For the first PCR reaction the primers 'XhoI SV40 Poly (A) Long Forw' and 'SV40 Poly (A) Rev' were used (Table 3.1). This produced the SV40 poly (A) tail fragment with the addition of a XhoI recognition domain at the 5' terminal. The product from first PCR reaction was used in the second. Here the primers 'XhoI SV40 Poly (A) Long Forw' and 'I-SceI SV40 Poly (A) Rev' (Table 3.1) were used for the addition of an I-SceI recognition domain at the 3' terminal of the fragment.

Similarly, an alternative, smaller SV40 Poly (A) tail was amplified in much the same way as the previously described SV40 Poly (A) tail. For the first PCR reaction the primers 'XhoI SV40 Poly (A) Forw' and 'SV40 Poly (A) Rev' were used (Table 3.2). This produced the SV40 poly (A) tail fragment with the addition of a XhoI recognition domain at the 5' terminal. The product from the first PCR reaction was used in the second. Here the primers 'XhoI SV40 Poly (A) Forw' and 'I-SceI SV40 Poly (A) Rev' (Table 3.2) were used for the addition of an I-SceI recognition domain at the 3' terminal of the fragment.

Table 3.1: List of primers used for PCR amplification of the primary constituent fragments used to synthesize pRSF-zTNFα-mCherry.

Primer	Sequence
zTNF Forw	5' CCCGCATGCTCCACGTCTCC 3'
zTNF Rev	5' AGCTTCATAATTGCTGTATGTCTTA 3'
I-SceI zTNF Forw	5' TAGGGATAACAGGGTAATCCCGCATGCTCCACGTCTCCACATCCT 3'
PstI zTNF Rev	5' CGCTGCAGACTCTCAAGCTTCATAATTGCTGTATG 3'
PstI mCherry Forw	5' GTCTGCAGGCAATCATCAAAGAATTTATGCGGT 3'
XhoI mCherry Rev	5' CTTACTCGAGTTATTTATATAATTCATCCATACCA 3'
XhoI SV40 Poly (A) Long Forw	5' TAACTCGAGCAGACATACAGCCACTTCCAACTAAA 3'
SV40 Poly (A) Rev	5' CCCTAACGCGTTAAGATACATTGATGAGTTTGG 3'
I-SceI SV40 Poly (A) Rev	5' ATTACCCTGTTATCCCTAACGCGTTAAGATACATTGATGAGTTTG 3'

Table 3.2: List of additional primers used for PCR amplification of alternative variants of the constituent fragments used to synthesize pRSF-zTNFα-mCherry.

Primer	Sequence
zTNF alt 1 Forw	5' GTTGTAAAAGCATAAAAAGAGACGC 3'
zTNF alt 2 Forw	5' GGGTAATCCCGCATGCTCCACGTCTCCACATCCTCTT 3'
zTNF Rev	5' AGCTTCATAATTGCTGTATGTCTTA 3'
PstI GFP Forw	5' GTCTGCAGCGGAGTAAAGGAGAAGAACTTTTCA 3'
XhoI GFP Rev	5' CTTACTCGAGTTATTTGTATAGTTCATCCATGCCA 3'
XhoI SV40 Poly (A) Forw	5' TAACTCGAGAAAAAACCTCCCACACCT CCCCCTG 3'
SV40 Poly (A) Rev	5' CCCTAACGCGTTAAGATACATTGATGAGTTTGG 3'
I-SceI SV40 Poly (A) Rev	5' ATTACCCTGTTATCCCTAACGCGTTAAGATACATTGATGAGTTTG 3'

3.1.1.5 Digestion and ligation of transgene fragments

Among the variants of isolated and amplified transgene fragments, those needed for assembly of the final transgene construct were chosen. These included the TNF-α1 promoter (+6 AA) fragment initially amplified with the primers 'zTNF Forw' and 'zTNF Rev' (Table 3.1), the mCherry fragment, and the elongated SV40 Poly (A) tail fragment initially amplified using the primers 'XhoI SV40 Poly (A) Long Forw' and 'SV40 Poly (A) Rev' (Table 3.1). Following PCR amplifications, these fragments were analyzed through gel electrophoresis and individually

purified from the agarose gel using Monarch® DNA Gel Extraction Kit (NEB, South Africa), according to the manufacturer's instructions. Purified fragments were then digested as follows: The TNF-α1 promoter was digested with PstI. mCherry was digested with PstI and XhoI. The SV40 Poly (A) tail was digested with XhoI. Reaction mixes for digestions were set up according to Table 3.3 and incubated at 37°C for 15 minutes.

Table 3.3: Reaction mixes for digestion of the constituent transgene fragments prior to ligation of said fragments.

Reagent	Final concentration	Volume per reaction
DNA	1000 ng	Variable
10x CutSmart® Buffer	1X	5 µl
Restriction enzyme	0.4 U/µl (each if doing double digest)	1 µl (each if doing double digest)
dH_2O	Variable	Variable
		50 µl

Following digestions, DNA fragments were individually purified using Monarch® PCR & DNA Cleanup Kit (NEB, South Africa), according to manufactures instructions. Purified fragments were then ligated for 10 minutes at room temperature with the ligation reaction set up according to Table 3.4.

Table 3.4: Reaction mix for ligation of the ~3700 bp TNF-α1 promoter, 696 bp mCherry, and 594 bp SV40 Poly (A) tail. 6:1:1 ratio of TNF-α1 promoter, mCherry, and SV40 Poly (A) tail respectively was used for ligations.

Reagent	Final concentration	Volume per reaction
TNF-α1 promoter DNA	3 ng/µl	Variable
mCherry DNA	0.5 ng/µl	Variable
SV40 Poly (A) tail DNA	0.5 ng/µl	Variable
T4 ligase	> 4U	2 µl
10x T4 buffer	1X	2 µl
dH_2O	Variable	Fill to 20 µl
		20 µl

Following ligation of the constituent transgene fragments, DNA was purified using Monarch® PCR & DNA Cleanup Kit (NEB, South Africa), according to manufactures instructions. Following DNA purification, the whole fragment was PCR amplified using the primers 'I-SceI zTNF Forw' and 'I-SceI SV40 Poly (A) Rev' (Table 3.1). The newly PCR amplified transgene construct was run through gel electrophoresis to confirm successful amplification of the full transgene construct, followed by purification of the transgene construct from the agarose gel using Monarch® DNA Gel Extraction Kit (NEB, South Africa), according to the manufacturer's instructions.

3.1.1.6 Cloning of transgene insert into pRSF Duet vector

The newly amplified and purified transgene insert was then blunt-end cloned into the pRSF Duet vector as illustrated in Figure 3.1. While the transgene insert was blunted as a result of PCR amplification, the pRSF Duet vector was blunted by digestion with the EcoRV restriction enzyme at 37°C for 15 minutes. The digestion reaction was set up according to Table 3.5.

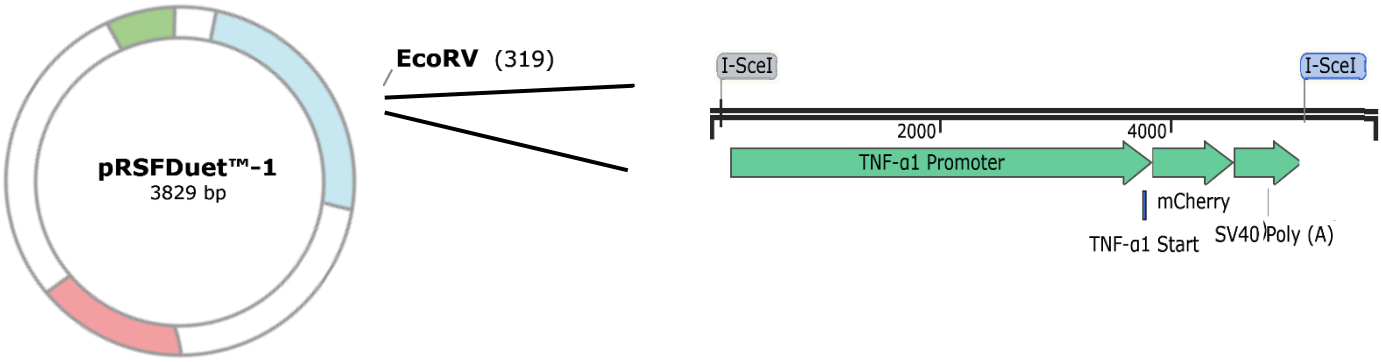

Figure 3.1: Illustration of pRSF Duet vector with EcoRV restriction enzyme recognition domain for blunting of the vector as well as the fully synthesized transgene construct to be ligated into the pRSF Duet vector. Create with SnapGene.com.

Table 3.5: Reaction mix for blunt-end digestion of the pRSF Duet vector prior to cloning of the transgene insert into the pRSF Duet vector.

Reagent	Final concentration	Volume per reaction
pRSF Duet vector DNA	1000 ng	Variable
10x CutSmart® Buffer	1X	5 µl
EcorRV restriction enzyme	0.4 U/µl	1 µl
dH_2O	Variable	Variable
		50 µl

Following blunting of the pRSF Duet vector, the plasmid was purified using Monarch® PCR & DNA Cleanup Kit (NEB, South Africa), according to manufactures instructions. The purified plasmid and transgene insert were then ligated for 10 minutes at room temperature with the ligation reaction set up according to Table 3.6.

Table 3.6: Reaction mix for ligation of the 3829 bp pRSF Duet vector and ~5000 bp transgene insert. 1:1 ratio of the PRSF Duet vector and transgene insert was used for ligation.

Reagent	Final concentration	Volume per reaction
pRSF Duet vector DNA	2.5 ng/µl	Variable
Transgene insert DNA	2.5 ng/µl	Variable
T4 ligase	> 4U	2 µl
10x T4 buffer	1X	2 µl
dH_2O	Variable	Fill to 20 µl
		20 µl

The newly cloned pRSF-zTNFα-mCherry vector was then transformed into chemical competent *E.coli* cells by heat shock transformation (90 µl competent *E.coli* cells, 10 µl cloned ligation mixture). Transformed cells were then plated (3.7 g/100 ml LB nutrient broth powder, 1.2% agar,

and 100 µg/ml kanamycin) and incubated at 37°C overnight. Plated colonies were picked and tested by colony PCR for the presence of the transgene insert using the primers 'I-SceI zTNF Forw' and 'I-SceI SV40 Poly (A) Rev' (Table 3.1). Positive colonies were repicked and inoculated in LB nutrient broth (3.7 g/100 ml LB nutrient broth powder and 100 µg/ml kanamycin) overnight at 37°C under constant aeration. The pRSF-zTNFα-mCherry plasmid was then isolated from inoculated colonies by miniprep, using Monarch® Plasmid Miniprep Kit (NEB, South Africa), according to the manufacturer's instructions. The isolated pRSF-zTNFα-mCherry plasmid was subjected to a number of digestions with PstI, NotI, I-SceI, and XhoI at 37°C for 1 hour and run through gel electrophoresis to confirm the presence of the constituent fragments of the transgene insert. Finally, the pRSF-zTNFα-mCherry vector was sent for Sanger sequencing at Central Analytical Facilities (CAF), University of Stellenbosch, South Africa, to confirm the success of synthesis of pRSF-zTNFα-mCherry. Each sequenced fragment of pRSF-zTNFα-mCherry was aligned to their theoretical counterpart using EMBOSS Needle Pairwise Sequence Alignment, to determine the percentage identity, and therefore, the extent of successful cloning of each fragment.

3.1.2 Results

3.1.2.1 TNF-α1 promotor isolation

Initial isolation and cloning of the TNF-α1 promoter fragment was confirmed by digestion of the fragment from its intermediate plasmid, pMiniT 2.0, followed by gel electrophoresis (Figure 3.2). Digestions were performed using XhoI, a restriction enzyme with recognition domains flanking the TNF-α1 promoter insert in the multiple cloning site of pMiniT 2.0. As seen in Figure 3.2 various sizes of the TNF-α1 promoter fragment were initially isolated and cloned into the pMiniT 2.0 vector. Lane 1 shows digestion of an ~3300 bp TNF-α1 promoter fragment as well as a ~2500 bp fragment of the remaining digested pMiniT 2.0 backbone. Likewise, lane 2 and 3 shows digestion of an ~3700 bp TNF-α1 promoter fragment and the remaining ~2500 bp pMiniT 2.0 backbone.

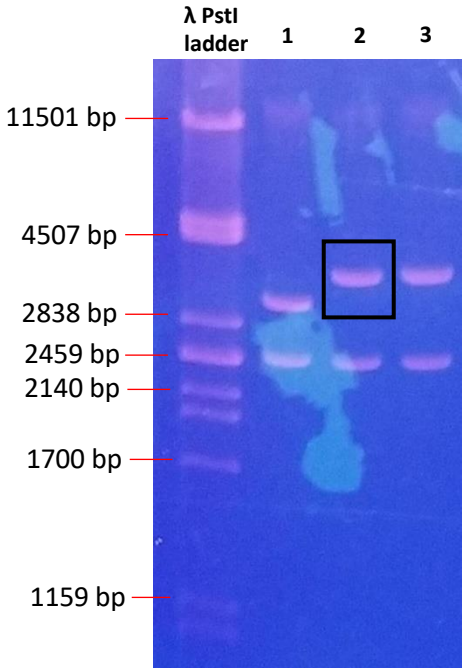

Figure 3.2: XhoI digestion of pMiniT 2.0 plasmids cloned with various TNF-α1 promoter fragment sizes. Lane 1: ~3300 bp TNF-α1 promoter fragment and ~2500 bp pMiniT 2.0 backbone. Lane 2-3: ~3700 bp TNF-α1 promoter fragment and ~2500 bp pMiniT 2.0 backbone. Band highlighted in black box: ~3700 bp TNF-α1 promoter fragment isolated for second PCR amplification for addition of an I-SceI and PstI recognition sequence at the 5' and 3' ends of the fragment respectively (see Figure 3.6).

Clones 1, 2, 3 (Figure 3.2, lanes 1, 2, 3 respectively) were sent for sequencing at the Central Analytical Facilities (CAF) to further confirm successful isolation and cloning of the TNF-α1 promoter fragments (Figures 3.3, 3.4, 3.5). Sequencing confirmed successful isolation and cloning of the TNF-α1 promoter fragments from clones 2 and 3. Clone 2 was chosen for further synthesis of the desired transgene construct, and as such, the alignment of sequence data from clone 2 and the *Danio rerio* reference genome, GRCz11, can be seen in Figures 3.4 and 3.5. As seen in Figures 3.4 and 3.5, sequence data was produced using the forward and reverse primers initially used to amplify said fragment (highlighted sequence) (illustration of sequencing layout shown in Figure 3.3). In Figure 3.4, an alignment of a 672 bp 5' to 3' sequence starting at the 5' distal region of the zebrafish TNF-α1 promoter can be seen. In Figure 3.5, an alignment of a 416 bp 5' to 3' sequence starting at the 3' coding region of zebrafish TNF-α1 can be seen. While both sequence alignments appear to have several gaps and point mutations, alignments seen in Figures 3.4 and 3.5 present with high levels of identity (90.9 and 93.9 respectively) and similarity (91.1 and 93.9 respectively).

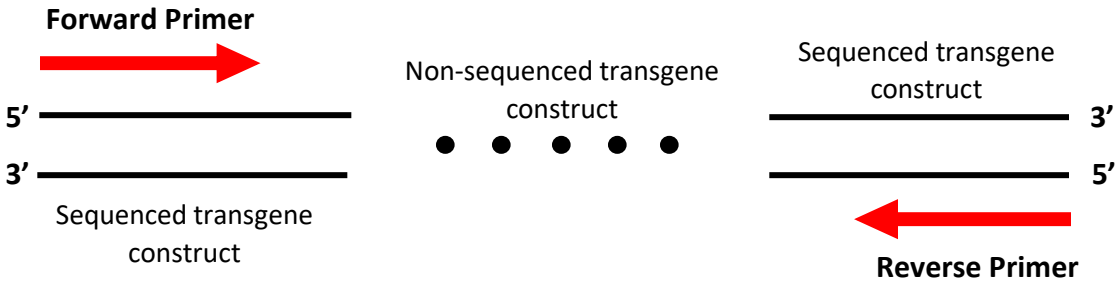

Figure 3.3: Illustrative diagram of layout of short fragment sequence data presented in Figures 3.4 and 3.5

```
########################################
# Program: needle
# Rundate: Thu 14 Jul 2022 12:39:44
# Commandline: needle
#    -auto
#    -stdout
#    -asequence emboss_needle-I20220714-123516-0283-34303395-p1m.asequence
#    -bsequence emboss_needle-I20220714-123516-0283-34303395-p1m.bsequence
#    -datafile EBLOSUM62
#    -gapopen 10.0
#    -gapextend 0.5
#    -endopen 10.0
#    -endextend 0.5
#    -aformat3 pair
#    -sprotein1
#    -sprotein2
# Align_format: pair
# Report_file: stdout
########################################

#=======================================
#
# Aligned_sequences: 2
# 1: Forward_primer
# 2: Danio_rerio_GRCz11_Primary_Assembly
# Matrix: EBLOSUM62
# Gap_penalty: 10.0
# Extend_penalty: 0.5
#
# Length: 673
# Identity:     612/673 (90.9%)
# Similarity:   613/673 (91.1%)
# Gaps:          19/673 ( 2.8%)
# Score: 3192.0
#
#
#=======================================

Forward_prime      1 CCCGCATGCTCCACGTCTCCACATCCTCTTGTGGTGTGCTGAAAACTTGT     50
                     |||||||| ||||||||||||||||||||||||||||||||||||||||||
Danio_rerio_G      1 CCCGCATG-TCCACGTCTCCACATCCTCTTGTGGTGTGCTGAAAACTTGT     49

Forward_prime     51 ATCATTTGGCTCATCAGTGTATGAACTGGAAATTATTTTTG-AAGTGTTT     99
                     ||||||||||||||||||||||||||||||||||||||| |||||
Danio_rerio_G     50 ATCATTTGGCTCATCAGTGTATGAACTGGAAATTATTTTTGAAAGTG---     96

Forward_prime    100 TTTTTTTTTGTTGGTACAGTGGCACACCACAATTTACCATTGTGACTAAA    149
                     ||||||||||||||||||||||||||||||||||.||||||||||||||||
Danio_rerio_G     97 TTTTTTTTTGTTGGTACAGTGGCACACCACAATTCACCATTGTGACTAAA    146

Forward_prime    150 CCACGTGCACCAACAAGTGTTTGAGTGGTAAATATGACATAGGTTTTCAG    199
                     ||||||||||||||||||||||||||||||||||||||||||||||||||||
Danio_rerio_G    147 CCACGTGCACCAACAAGTGTTTGAGTGGTAAATATGACATAGGTTTTCAG    196

Forward_prime    200 CACTCTGCGCAAGTCATAAGATGGTTTTTATTATTAATTTCCATGGACAT    249
                     ||||||||||||||||||||||||||||||||||||||||||||||||||||
Danio_rerio_G    197 CACTCTGCGCAAGTCATAAGATGGTTTTTATTATTAATTTCCATGGACAT    246

Forward_prime    250 ACAACTTGGAAACAAAAATGACAAAACCATGTTGTCATCGGTTCTCTAGA    299
                     ||||||||||||||||||||||||||||||||||||||||||||||||||||
Danio_rerio_G    247 ACAACTTGGAAACAAAAATGACAAAACCATGTTGTCATCGGTTCTCTAGA    296

Forward_prime    300 TTTTCACATGAAAAATATAGATAATAATGTATAGGCTAATTCACACAAAT    349
                     ||||||||||||||||||||||||||||||||||||||||||||||||||||
Danio_rerio_G    297 TTTTCACATGAAAAATATAGATAATAATGTATAGGCTAATTCACACAAAT    346

Forward_prime    350 AAATTATTTACTGCMAACAGCATCACAAAACATGCYCAGCTATAGTGTTA    399
                     ||||||||||||||.||||||||||||||||||||.||||||||||||.|
Danio_rerio_G    347 AAATTATTTACTGCAAACAGCATCACAAAACATGCTCAGCTATAGTGTAA    396

Forward_prime    400 GCTTGTCAGCCAATGATGAACTTCCAGTGACAGTTTTATGTAACTATTTT    449
                     ||||||||||||||||||||||||||||||||||||||||||||||||||||
Danio_rerio_G    397 GCTTGTCAGCCAATGATGAACTTCCAGTGACAGTTTTATGTAACTATTTT    446

Forward_prime    450 AATTTTCATAAGGTTCCTTTTATAGMAYCGATGTARTAATGTTAYTTAAA    499
                     .|||||||||||||||||||||||.|.|||||||.||||||||.|.|||
Danio_rerio_G    447 CATTTTCATAAGGTTCCTTTTATAGCATCGATGTAGTAATGTTATTCAAA    496

Forward_prime    500 TATAATCCGTTAAAAAGACTTAAGCATCCATTTTGGTTGTAAAGCCWMAA    549
                     |||||||.|||||||||||||||||||| ||||||||||..|..||
Danio_rerio_G    497 TATAATCAGTTAAAAAGACTTAAGCATCCA-TTTGGTTGTAAAAGCATAA    545

Forward_prime    550 AAAKAGACTCTAGAACAACRATACCGTWTTGAAAATACCTGGSARTTACA    599
                     |||.||||.|.||||||| .|.|.||..||||||||| ||||:.  ||.|
Danio_rerio_G    546 AAAGAGACGCAAGAACAA-TAAAACGCATTGAAAATA-CTGGAG--TAAA    591

Forward_prime    600 AGGCCTGCTATCTATATGGRTAAATTTCRTGYAATTCACTCGCCGCTTCC    649
                     ||| |||.||| |||||||| |||||||| ||.||||.|.|..|.|.|
Danio_rerio_G    592 AGG-CTGTTAT-TATATGG-TAAATTTC-TGTAATTTAATGTCTGTT---    634

Forward_prime    650 TTTYTTMGACAATCCTCCTGCAA    672
                     |||..|.|..|||  |.|||.|.
Danio_rerio_G    635 TTTTATAGTAAAT--TTCTGTAT    655


#---------------------------------------
#---------------------------------------
```

Figure 3.4: 5’ to 3’ alignment of sequenced TNF-α1 promoter fragment (from Figure 3.2, lane 2) and *Danio rerio* reference genome, GRCz11, using the forward primer ‘zTNF Forw’ (Table 3.1). The highlighted sequence represents the forward primer used for sequencing and begins at the 5’ distal end of the TNF-α1 promoter.

```
########################################
# Program: needle
# Rundate: Thu 14 Jul 2022 13:52:53
# Commandline: needle
#    -auto
#    -stdout
#    -asequence emboss_needle-I20220714-135252-0281-71232124-p2m.asequence
#    -bsequence emboss_needle-I20220714-135252-0281-71232124-p2m.bsequence
#    -datafile EBLOSUM62
#    -gapopen 10.0
#    -gapextend 0.5
#    -endopen 10.0
#    -endextend 0.5
#    -aformat3 pair
#    -sprotein1
#    -sprotein2
# Align_format: pair
# Report_file: stdout
########################################

#=======================================
#
# Aligned_sequences: 2
# 1: Danio_rerio_GRCz11_Primary_Assembly
# 2: Reverse_primer
# Matrix: EBLOSUM62
# Gap_penalty: 10.0
# Extend_penalty: 0.5
#
# Length: 427
# Identity:     401/427 (93.9%)
# Similarity:   401/427 (93.9%)
# Gaps:          11/427 ( 2.6%)
# Score: 2076.5
#
#
#=======================================

Danio rerio G      1 CCTGAATATACCTGAAAGTCTTTGTTGTATATAAATCATTATTACAATGA     50
                     |||.|||||| |.|||||||||.|||| |.||.||||||||||.|||| ||
Reverse prime      1 CCTAAATATA-CGGAAAGTCTTAGTTG-AGATTAATCATTATGACAA-GA     47

Danio rerio G     51 ATGATATTTAAGTGGGGGTCTTCTGGTGACACATTTTCCGTGGCACATTC    100
                     ||.|||.||||||||||  ||.||||||||||||||.|||||||||||
Reverse_prime     48 ATTATAGTTAAGTGGGGG--TTTTGGTGACACATTTTCCATGGCACATT-     94

Danio rerio G    101 CTATGAGTGGGAAAAATATAATTCAAGCACAATTTGTATATTAGATATTT    150
                     |||||||||||||||||||| ||.||||||||||.|||||||||||| ||
Reverse prime     95 CTATGAGTGGGAAAAATAT-ATACAAGCACAATTGGTATATTAGATA-TT    142

Danio rerio G    151 CATGGATCTATAAATATCACGACGAAAATGTCACCACCACAAACAAATAT    200
                     ||| |||||||||||||| ||. |||||||||||||||||||||||||||||
Reverse prime    143 CAT-GATCTATAAATATCA-GAT-AAAATGTCACCACCACAAACAAATAT    189

Danio_rerio_G    201 ACTTACAGGTTTGTTATTATCTGTATGTGTATGCATGTGGGTGTGTGTGT    250
                     ||||||||||||||||||||||||||||||||||||||||||||||||||||
Reverse_prime    190 ACTTACAGGTTTGTTATTATCTGTATGTGTATGCATGTGGGTGTGTGTGT    239

Danio_rerio_G    251 TATATGACATCACTGGAGTTTCCCCTTCCTCTTCAGATCTTTAAAAAGAA    300
                     ||||||||||||||||||||||||||||||||||||||||||||||||||||
Reverse_prime    240 TATATGACATCACTGGAGTTTCCCCTTCCTCTTCAGATCTTTAAAAAGAA    289

Danio_rerio_G    301 AGAAGAAGCAGTTATTCTGAACATTACACTGATAGAACAACCCAGCAAAC    350
                     ||||||||||||||||||||||||||||||||||||||||||||||||||||
Reverse_prime    290 AGAAGAAGCAGTTATTCTGAACATTACACTGATAGAACAACCCAGCAAAC    339

Danio_rerio_G    351 TCGATTTGACTTAACAAGACCTTATCAAAAGCATTTACACTTGTAGAATC    400
                     ||||||||||||||||.|||||||||||||||||||||.|||||||
Reverse_prime    340 TCGATTTGACTTAACAAAACCTTATCAAAAGCATTTACACTTCTAGAATC    389

Danio rerio G    401 TTTAAGACATACAGCAATTATGAAGCT    427
                     |||||||||||||||||||||||||||
Reverse_prime    390 TTTAAGACATACAGCAATTATGAAGCT    416

#---------------------------------------
#---------------------------------------
```

Figure 3.5: 5’ to 3’ alignment of sequenced TNF-α1 promoter fragment (from Figure 3.2, lane 2) and *Danio rerio* reference genome, GRCz11, using the reverse primer ‘zTNF Rev’ (Table 3.1). The highlighted sequence represents the reverse primer used for sequencing and starts at the 3’ coding region of the TNF-α1 promoter.

Following sequencing of the ~3700 bp TNF-α1 promoter fragment, clone 2 (see Figure 3.2, lane 2, highlighted in black box) was chosen and isolated for further PCR amplification using the primers 'I-SecI zTNF Forw' and 'PstI zTNF Rev' (Table 3.1). As a result of the second PCR amplification the resulting TNF-α1 promoter fragment of ~3700 bps (seen in Figure 3.4, lane 2) was extended with the addition of an I-SceI and PstI recognition sequence at the 5' and 3' ends of the fragment respectively.

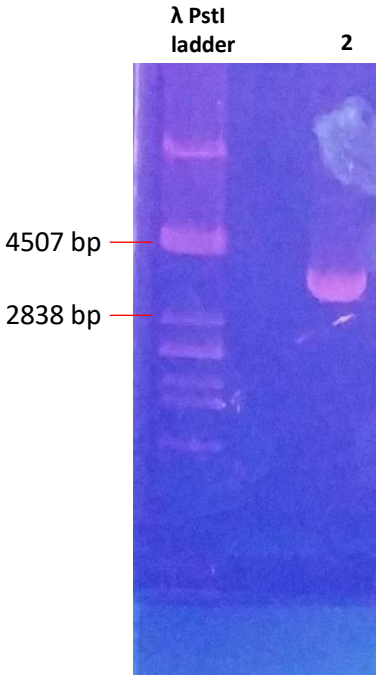

Figure 3.6: Lane 2: PCR amplification of the ~3700 bp TNF-α1 promoter fragment from clone 2 seen in Figure 3.2, lane 2. PCR amplifications were performed using the primers 'I-SceI zTNF Forw' and 'PstI zTNF Rev' (see table1).

3.1.2.2 mCherry, GFP, and SV40 Poly (A) tail isolation

Successful isolation and amplification of the two fluorescent reporter genes, GFP and mCherry, was confirmed by gel electrophoresis. As seen in Figure 3.7, lane 1, a 717 bp GFP fragment, with the addition of PstI and XhoI recognition domains on the 5' and 3' terminals respectively, was amplified. In lane 2, a 696 bp mCherry fragment with the addition of a PstI and XhoI recognition domain on the 5' and 3' terminals respectively, was amplified. Amplification of both the GFP and mCherry fragments resulted in bands of expected sizes at 717 bps and 696 bps respectively. The mCherry fragment (highlighted in black box) was chosen for further synthesis of the transgene construct. Similarly, successful PCR amplification of the SV40 Poly (A) tail was confirmed by gel electrophoresis. As seen Figure 3.8, three variations of the SV40 Poly (A) tail were amplified in a two-step PCR amplification. In lane 1 a 240 bp SV40 Poly (A) tail fragment

was amplified. In lane 2 a similarly sized SV40 Poly (A) tail fragment with the addition of XhoI and I-SceI recognition domains on the 5' and 3' terminals, respectively, was amplified. Finally, as seen in lane 3, a 594 bp elongated variant of the SV40 Poly (A) tail with the addition of XhoI and I-SceI recognition domains on the 5' and 3' terminals, respectively, was amplified. The SV40 Poly (A) tail fragment (highlighted in black box) was chosen for further synthesis of the transgene construct.

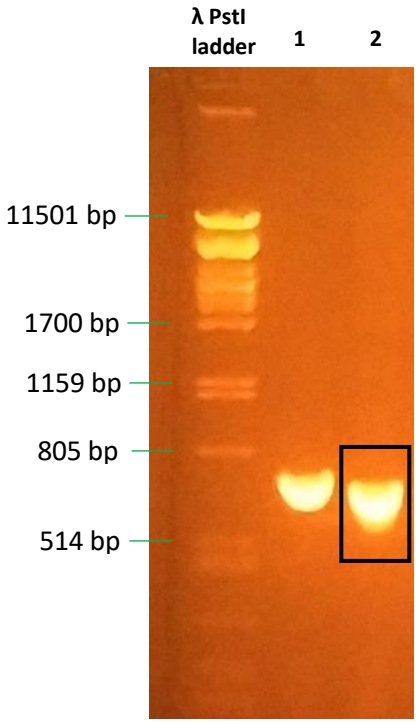

Figure 3.7: PCR amplification of the fragments to be used as reporter genes for pRSF-zTNFα-mCherry. Lane 1: GFP with the addition of a PstI and XhoI recognition domain on the 5' and 3' terminals respectively. Lane 2: mCherry with the addition of a PstI and XhoI recognition domain on the 5' and 3' terminals respectively. Band highlighted in black box: mCherry fragment chosen for further synthesis of the transgene construct.

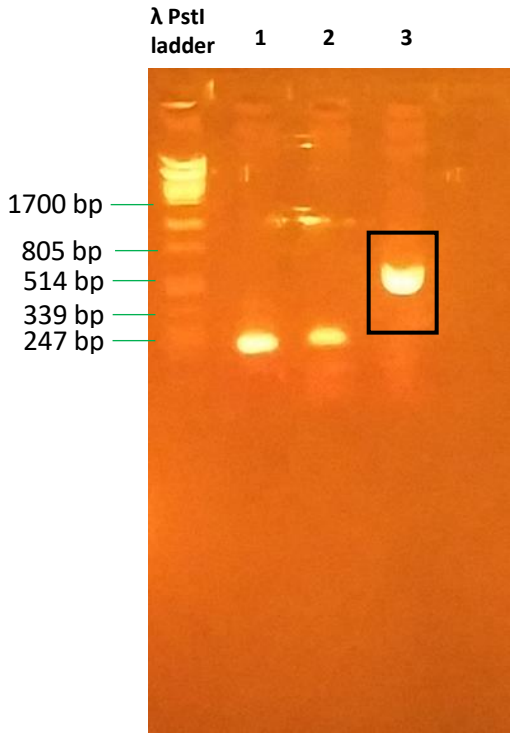

Figure 3.8: PCR amplification of three variations of the SV40 Poly (A) tail; the fragment to be used as a termination sequence in pRSF-zTNFα-mCherry. Lane 1: SV40 Poly (A) tail. Lane 2: SV40 Poly (A) tail with the addition of XhoI and I-SceI recognition domains on the 5' and 3' terminals respectively. Lane 3: An elongated SV40 Poly (A) with the addition of XhoI and I-SceI recognition domains on the 5' and 3' terminals respectively. Band highlighted in black box: SV40 Poly (A) tail fragment chosen for further synthesis of the transgene construct.

3.1.2.3 Cloning of transgene insert into pRSF Duet vector

Following isolation and ligation of the individual transgene fragments, the assembled transgene insert was cloned into a pRSF Duet plasmid vector, pRSF-zTNFα-mCherry (see Figure 3.10 for plasmid map with enzyme digestion sites). A number of *E.coli* colonies transformed with pRSF-zTNFα-mCherry were picked, and pRSF-zTNFα-mCherry clones were isolated by miniprep. The isolated pRSF-zTNFα-mCherry plasmid was subjected to several digestions to determine the presence of the constituent fragments of the transgene insert (See Figure 3.9). As seen in Figure 3.9, lane 1, digestion of the 2499 bp I-SceI control plasmid, NotI-linearized pGPS2, with the I-SceI enzyme resulted in the expected bands of 1518 bps and 981 bps respectively, confirming the successful enzymatic activity of I-SceI necessary for subsequent digestions of the pRSF-zTNFα-mCherry plasmid. It should be noted here that the 1518 bp and 981 bp dropout bands are considerably fainter than the 2499 bp undigested band. This suggests that most of the plasmid DNA remained undigested. This may be due to the expectedly slow rates of digestion from the I-SceI enzyme. As a result this will be seen again with digestion of the pRSF-zTNFα-mCherry plasmid with I-SceI. In lanes 2 and 3 we see bands of 4964 bps (red arrow) and 3722 bps (blue arrow) from digestion of pRSF-zTNFα-mCherry plasmid with the I-SceI enzyme. The 4964 bp band indicates the presence of the full transgene insert, while the 3722 bp band represents the remaining plasmid backbone. While these bands are faint, the brighter bands at 8686 bps and > 8686 bps, respectively, suggests most of the sample was linearized plasmid (partially digested), and circular plasmid (undigested). In lanes 4 and 5 we see an expected thick band from the digestion of the pRSF-zTNFα-mCherry plasmid with PstI and NotI. This consists of two bands which cannot be separated due to their similarity in size. However, from the plasmid map and bands on the agarose gel the larger band is predicted to be 3739 bps and is the result of digestion between two PstI sites. The smaller is predicted to be 3724 bps and is the results of digestion between a PstI and NotI site and confirms the presence of the TNF-α1 promoter fragment. Furthermore, in lanes 4 and 5, a 1004 bp band can be seen which confirms presences of the PstI restriction enzyme site on the 5’ end of the mCherry fragment. Further restriction enzyme mapping of the clones was performed with XhoI and are presented in lanes 6 and 7. As expected, three bands of 4400 bps, 3634 bps, and 652 bps can be seen. The 4400 bp band confirms the continuation of the TNF-α1 promoter through to the XhoI site where the mCherry and SV40 Poly (A) fragments meet. The 652 bp fragments confirms the presence of the SV40 Poly (A) fragment in its entirety.

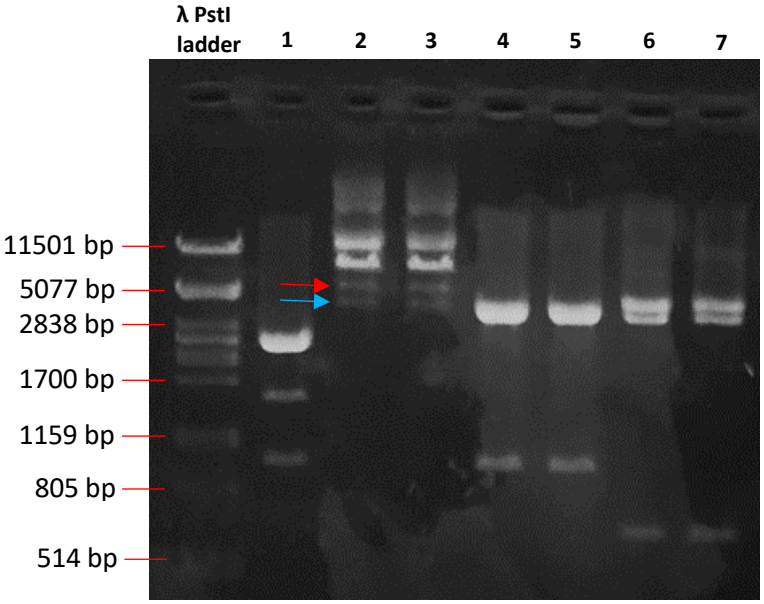

Figure 3.9: Digestions of pRSF-zTNFα-mCherry plasmid with various restriction enzymes to confirm the presence of the constituent transgene fragments of pRSF-zTNFα-mCherry. Lane 1: digestion of the 2499 bp I-SceI control plasmid, NotI-linearized pGPS2, digested with I-SceI. Lane 2: pRSF-zTNFα-mCherry plasmid from clone 2A digested with I-SceI (Red arrow: transgene insert; blue arrow: plasmid backbone). Lane 3: pRSF-zTNFα-mCherry plasmid from clone 2B digested with I-SceI. Lane 4: pRSF-zTNFα-mCherry plasmid from clone 2A digested with PstI and NotI. Lane 5: pRSF-zTNFα-mCherry plasmid from clone 2B digested with PstI and NotI. Lane 6: pRSF-zTNFα-mCherry plasmid from clone 2A digested with XhoI. Lane 7: pRSF-zTNFα-mCherry plasmid from clone 2B digested with XhoI.

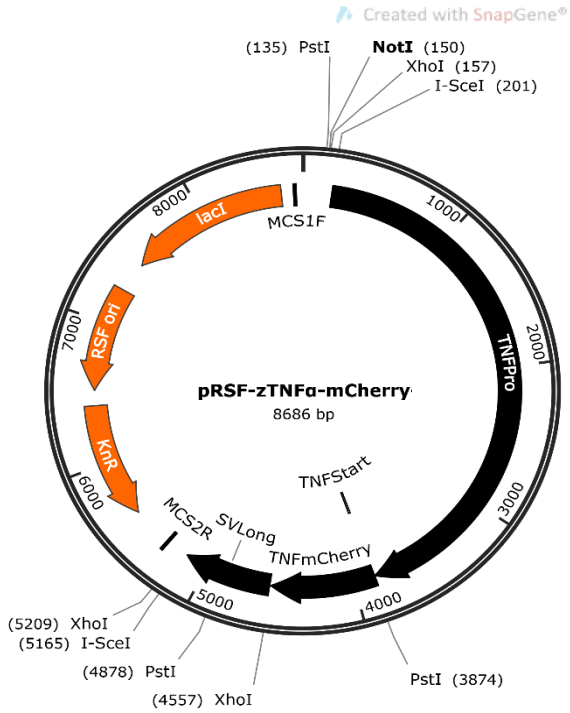

Figure 3.10: Map of the pRSF-zTNFα-mCherry plasmid annotated with the enzyme digestion sites, I-SceI, PstI, NotI, and XhoI, all of which were used to determine the presence of the constituent fragments of the transgene insert. Create with SnapGene.com.

3.1.2.4 pRSF-zTNFα-mCherry sequencing

To further confirm the presence and sequence homology of the constituent fragments of the full transgene insert, pRSF-zTNFα-mCherry from clone 2A, described in Figure 3.9, was sent for Sanger sequencing at the Central Analytical Facilities (CAF), University of Stellenbosch, South Africa. See Figure 3.11 for an illustration of the location of consensus sequence primers used for sequencing of the transgene insert. Sequence data for clone 2A is presented below. As seen in Table 3.7 the zebrafish TNF-α1 promoter fragment was present with 93.1% identity to the TNF-α1 promoter of the *Danio rerio* reference genome, GRCz11. Here it is worth noting that two large gaps of 174 bps and 48 bps were noticed within the pRSF-zTNFα-mCherry TNF-α1 promoter, 1354 bps and 2857 bps upstream of the transcription start site respectively. Given the unusually large nature of these gaps they were removed from the *Danio rerio* TNF-α1 promoter reference sequence. For this alternative analysis the reference sequence was realigned to the pRSF-zTNFα-mCherry TNF-α1 promoter sequence. Following this adjustment the zebrafish TNF-α1 promoter fragment presented with 98.9% identity to the TNF-α1 promoter of the *Danio rerio* reference genome, GRCz11. As seen in Table 3.7, both the mCherry and SV40 Poly (A) fragments were successfully cloned into pRSF-zTNFα-mCherry with 100% identity to their theoretical counterparts. Finally, the 3' ISce-I recognition domain of pRSF-zTNFα-mCherry was present with 94% identity (17/18 bps), with a thymine nucleotide missing from the far 3' end. Meanwhile, the 5' ISce-I recognition domain was successfully cloned with 100% identity.

Figure 3.11: Plasmid map of pRSF-zTNFα-mCherry including annotated final transgene construct, as well as the location of primers used to generate the consensus sequence for sequencing of the pRSF-zTNFα-mCherry transgene insert. Create with SnapGene.com.

Table 3.7: Sequence homology of each constituent fragment of pRSF-zTNFα-mCherry to their theoretical counterparts, as measured by percentage identity.

Sequenced fragment	Homology to theoretical fragment
TNF-α1 promoter	93.1% (98.9% - adjusted)
TNF-α1 first six amino acids	100%
mCherry	100%
SV40 Poly (A)	100%
5' ISce-I recognition domain	100%
3' ISce-I recognition domain	94%

3.1.3 Discussion

3.1.3.1 Initial zebrafish TNF-α1 promoter isolation

The decision to isolate a promoter fragment as large as 3700 bp was a conservative estimate made in the interest of including as many upstream transcriptional regulatory elements of the zebrafish TNF-α1 gene as possible. Previous studies have successfully used similarly sized zebrafish TNF-α1 promoters for transgenic reporter gene purposes [17,83]. Likewise, the addition of the first 6 amino acids of the zebrafish TNF-α1 gene was used to include the endogenous ATG codon of the TNF-α1 gene to help drive translation of the downstream reporter gene. Successful isolation and cloning of the zebrafish TNF-α1 promoter was confirmed by alignment of sequenced data to the *Danio rerio* reference genome, GRCz11. While the sequence alignments present with high levels of identity and similarity, a few gaps and point mutations can be seen. These misaligned nucleotides may be due to a number of factors: Firstly, minor differences in the promoter sequence of our WT zebrafish, from which the promoter was isolated, and the reference genome zebrafish may arise as a result of strain specificity. While this is plausible, significantly high levels of sequence conservation within the promoter of a major immunoregulatory gene should be expected between strains of the same species. Alternatively, misaligned sequences may be explained by sequencing data quality. Generally, short fragment sequence data is only reliable up to approximately 800 bp. As such, evaluation of the chromatogram data used to generate the data in Figures 3.4 and 3.5 appears to show undesirably low signal-to-noise ratios at the opposite ends of the sequenced fragment to the primers. This appears to be where most misaligned nucleotides are consternated and are as a result of an expected sequencing quality drop off.

3.1.3.2 Initial mCherry, GFP, and SV40 Poly (A) tail isolation

While both mCherry and GFP reporter genes were successfully isolated and cloned, numerous studies have displayed the capacity of whole zebrafish embryos to generate lower signal-to-noise ratios from background auto-fluorescence in GFP expressing transgenic fish than those expressing red fluorescent proteins, such as DsRed – the fluorescent protein from which mCherry was derived [84]. As such mCherry was chosen as the reporter gene for development of the transgene construct moving forward. Furthermore, green fluorescent tags are commonly

used to study inflammatory related processes within our research group. By employing mCherry as the reporter gene of choice, studies utilising green fluorescent tags may be simultaneously performed in the same zebrafish embryo.

Finally, the addition of a SV40 Poly (A) tail was included to aid in transgene transcription termination, as well as stability of the resulting mRNA. SV40 Poly (A) tails include the ~122 bp core element featuring copies of the AATAAA motif. Upstream of this core element (in between the SV40 Poly (A) core element and stop codon of the preceding protein) are the SV40 Poly (A) Upstream Efficiency Elements, also known as Upstream Sequence Elements (USEs). It has been shown that inclusion of these upstream elements enhances the ability of SV40 Poly (A) to stabilize and process mRNA [85]. While variably sized SV40 Poly (A) upstream sequences, containing USEs, have been utilized for transgene expression, there is no consensus on the optimal length as the full extent of elements that aid in mRNA stabilization and processing are unknown. Therefore, the conservative choice was made to include an ~472 bp SV40 Poly (A) upstream sequence, isolated from the SV40 Poly (A) of the functional LC3-GFP expression vector, resulting in the elongated, 594 bp, SV40 Poly (A) described throughout the synthesis of pRSF-zTNFα-mCherry. This elongated SV40 Poly (A) tail was favored to the shorter SV40 Poly (A) tail (isolated with a truncated SV40 Poly (A) upstream sequence) in the interest of including as many USEs as possible.

3.1.3.3 Cloning of the assembled transgene insert into the pRSF Duet vector

As seen in Figure 3.9, as well as the sequencing data of the pRSF-zTNFα-mCherry plasmid, all constituent fragments of the pRSF-zTNFα-mCherry transgene insert were successfully isolated and correctly assembled, after which, they were successfully cloned into the pRSF Duet vector creating the final pRSF-zTNFα-mCherry plasmid. It is worth noting two points when accessing the final sequence data of pRSF-zTNFα-mCherry.

Firstly, upon initial alignment of the TNF-α1 promoter sequence from pRSF-zTNFα-mCherry and the TNF-α1 promoter of the *Danio rerio* reference genome, two unusually large sequence gaps were missing from pRSF-zTNFα-mCherry TNF-α1 promoter sequence. This could have arisen from a number of factors. Minor sequence differences between the WT strain from which the TNF-α1 promoter was isolated and the strain of the *Danio rerio* reference genome can be expected. However, with gaps as large as 174 bps and 48 bps, as well as high levels of sequence homology both upstream and downstream of these gaps, differences in sequences

between strains is likely not the cause. Alternatively, an error during sequencing could explain these large gaps. Here the large gaps would present as false positives. In the case of a sequencing error, it is likely that the pRSF-zTNFα-mCherry TNF-α1 promoter and the TNF-α1 promoter of the *Danio rerio* reference genome would present with higher levels of homology than that seen form initial alignments. As such, the sequence of both gaps was removed from reference genome sequence before being realigned. This resulted in considerably higher homology between both sequences. While these gaps are likely false positives, in the unlikely case that they are not, it is worth pointing out that they are located 1354 bps and 2857 bps upstream of the transcription start site. This is likely outside of the proximal promoter in which most primary transcription factor binding sites would be located.

Finally, it can be seen that within the pRSF-zTNFα-mCherry plasmid a thymine nucleotide is missing from the far 3' end of the 3' I-SceI recognition domain. This mutation may have occurred as the result of repetitive cloning procedures. While this is not ideal, the ability of I-SceI to cleave domains similar to the 18 bp I-SceI recognition domain has been observed. In some cases, the I-SceI enzyme has been reported to cleave domains with as little as 14/18 bps found in the classically defined recognition domain, a number of which were missing the same thymine nucleotide on the 3' end [86]. As such, similar rates of digestion with I-SceI were observed in the NotI-linearized pGPS2 control plasmid and pRSF-zTNFα-mCherry plasmid, as seen in Figure 3.9. A point worth noting from the digestions seen in Figure 3.9 is the incomplete digestion of plasmid DNA using the I-SceI enzyme. While the mutation in the I-SceI domain may have resulted in some cleavage inefficiencies, resulting in low digestion turnover from I-SceI, this can be expected and is also noted in the control plasmid provided from the manufacturer. Additionally, previous studies have also noted a low turnover of digested DNA product following digestion with the I-SceI enzyme [87]. It has been suggested that this may be due to the biphasic nature of I-SceI DNA cleavage in which the I-SceI enzyme remains tightly bound to DNA following cleavage, resulting in slower release of cleaved DNA product. It has also been observed that I-SceI is enzymatically optimal at pH 9.5 [88] (a variable that was not controlled during these digestions). While I-SceI appears to have a low rate of enzymatic turnover, the increased capacity for transgene integration following plasmid digestion I-SceI has been well documented [77].

Given the successful synthesis of the pRSF-zTNFα-mCherry construct, as well as confirmation of I-SceI enzymatic activity, purified stocks of pRSF-zTNFα-mCherry plasmid DNA were prepared for transfection of zebrafish embryos by microinjection.

3.2 Part II: Survivability of zebrafish embryos microinjected with various dyes

Microinjection was utilized for transfection of zebrafish embryos. Prior to transfection of zebrafish by microinjection, a pilot study was conducted to determine the feasibility using dyes, a common addition to injection mixes [77,79], for visual assistance during the microinjection process. Notably, this pilot aimed to access the impact of dyes only on developing embryos. To investigate this, the survivability of zebrafish embryos injected with various dyes at the single-cell stage was accessed.

3.2.1 Methods

3.2.1.1 Ethical considerations

All animal experiments were performed in accordance with the ethical guidelines of Stellenbosch University. Ethical clearance for protocols were obtained from the Animal Research Committee of Stellenbosch University (reference # ACU-2020-18750). Approval for the handling of genetically modified and biohazardous material was obtained from the Biosafety and Environmental Ethics committee at Stellenbosch University (reference # BEE-2021-19235). All handling of adult zebrafish, as well as euthanasia procedures were conducted by registered SAVC personnel.

3.2.1.2 Zebrafish housing and husbandry

All adult zebrafish were maintained, bred, and experimentally handled in the Stellenbosch University zebrafish unit, by SAVC registered staff members. Zebrafish were kept in regulated tank water at 28.5°C, pH 6.8-7.5, conductivity of 500 - 800 µs/cm^3, and a day/night cycle of 14 hours light/10 hours dark. Breeding of adult zebrafish was performed according to standard husbandry procedures. Eggs were collected for use at single-cell stage.

3.2.1.3 Maintenance of zebrafish larvae

Zebrafish larvae were maintained in 90mm diameter petri dishes in E3 water (5 mM NaCl, 0.17 mM KCl, 0.33 mM $CaCl_2$, 0.33 mM, $MgSO_4$, 10^{-5} % Methylene Blue) at a maximum density of 50 larvae of petri dish. Petri dishes were incubated at 28.5°C with a day/night cycle of 14 hours light/10 hours dark. At the endpoint of all experiments, where indicated, zebrafish larvae were euthanized by tricaine (tricaine methanesulfonate) administration (0.016%), followed by freezing at -80°C.

3.2.1.4 Zebrafish microinjection

Single-cell eggs were placed in the grooves of a 1% low melting point agarose mould set with Z-MOULDS Microinjection and Transplantation Moulds (WPI, South Africa) with 10 - 15 eggs lined in each groove. All liquid was removed from the grooves and replaced with 0.3% methyl cellulose to hold the eggs in place during microinjection. Eggs were then staged and orientated for microinjection (see Figure 3.12). For microinjection, 1 mm borosilicate glass capillary pipette tips were pulled using WPI's PUL-1000 Micropipette Puller using the following parameters: Step = 1; Heat Index = 650; Force = 250 G; Distance = 8 mm; Delay = 0 s. 1 nl of dye solution was microinjected into the cytoplasm of single-cell stage zebrafish eggs using the PV820 Pneumatic PicoPump microinjector and WPI PZMIII-MI stereomicroscope. For calibration of the microinjector a drop of hydrophilic injection solution was injected into an oil droplet on a micrometre slide, adjusting the pressure and injection period until the suspended droplet had a radius of 124 µm – 156 µm. Three groups of zebrafish embryos were injected as follows: one group of single-cell embryos were injected with 0.05% phenol red (n = 27), while a second group was injected with 0.0167% methylene blue (n = 47) – at both concentrations the dyes were at the threshold of visibility and therefore practicality during microinjection. To access the mechanical impact of the microinjection on developing zebrafish embryos, (n = 24) eggs were sham injected, where the microinjection tip was inserted into the eggs without injecting solution. Finally, two groups of groups of control eggs (one for each injection day, as the whole experiment could not be completed on one day) remained uninjected (n = 70 for control 1; n = 27 for control 2). Following microinjection, all eggs were maintained under conditions described above. To access the rate of zebrafish larvae mortality, two sets of criteria were observed. Between 0 and 2 days post injection death was confirmed by cellular senescence which resulted in coagulation of the embryo. Coagulating embryos are milky white to the eye and a

dark brown mass under the microscope. From 2 days post injection, following the development of a heartbeat, lack of heartbeat was used as confirmation of mortality.

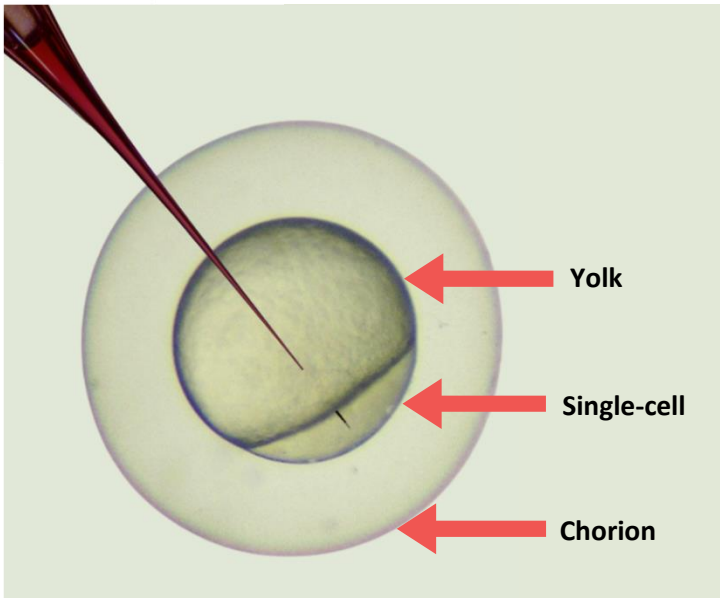

Figure 3.12: Single-cell zebrafish embryo at 0.2 hours post fertilization. At this stage the single cell may be difficult to see, and so correct orientation of the egg is critical prior to microinjection. Here the single cell can be seen at the bottom right pole of the yolk. The yolk and cell may be prone to rotating before the microinjection tip is able to penetrate either. For ease of microinjection, it is recommended that the cell is orientated on the opposite side of the yolk from where the microinjection tip penetrates the chorion. In a single, swift, and precise motion, the tip is pushed through the yolk, near the cell, and into the single cell.

3.2.2 Results

As seen in Figure 3.13, methylene blue (MB) injected zebrafish embryos and uninjected control 1 showed consistent and comparable rates of survival over the period of five days post injection (DPI). The initial survival rate for these two groups between 0 and 1 DPI was the same at 96%, while the final difference in survival rate after 5 DPI was only 5% (91% for MB vs. 96% for control 1). Given that both groups of eggs were obtained from the same adult stock and spawning event, this suggests that injection of 0.0167% methylene blue into zebrafish embryos at the single-cell stage has little to no effect on the rate of survival of zebrafish in the 5 days following microinjection.

While the initial survival rates drop relatively quickly between 0 and 1 DPI for the sham injected and control 2 groups (79% and 81% survival respectively), they appear to stabilize over the following 4 days. The phenol red group takes the largest initial drop in survival, between 0 and 1 DPI, with only 59% of injected fish surviving over this period. This is 22% lower than the control group 2. Comparatively, the sham injected fish only saw a 2% difference with control 2.

Likewise, the final survival rate of the phenol red group after 5 DPI is the lowest of all groups at only 52%. This is somewhat lower than the control group 2 at 81% and the sham injected group at 75% after 5 DPI.

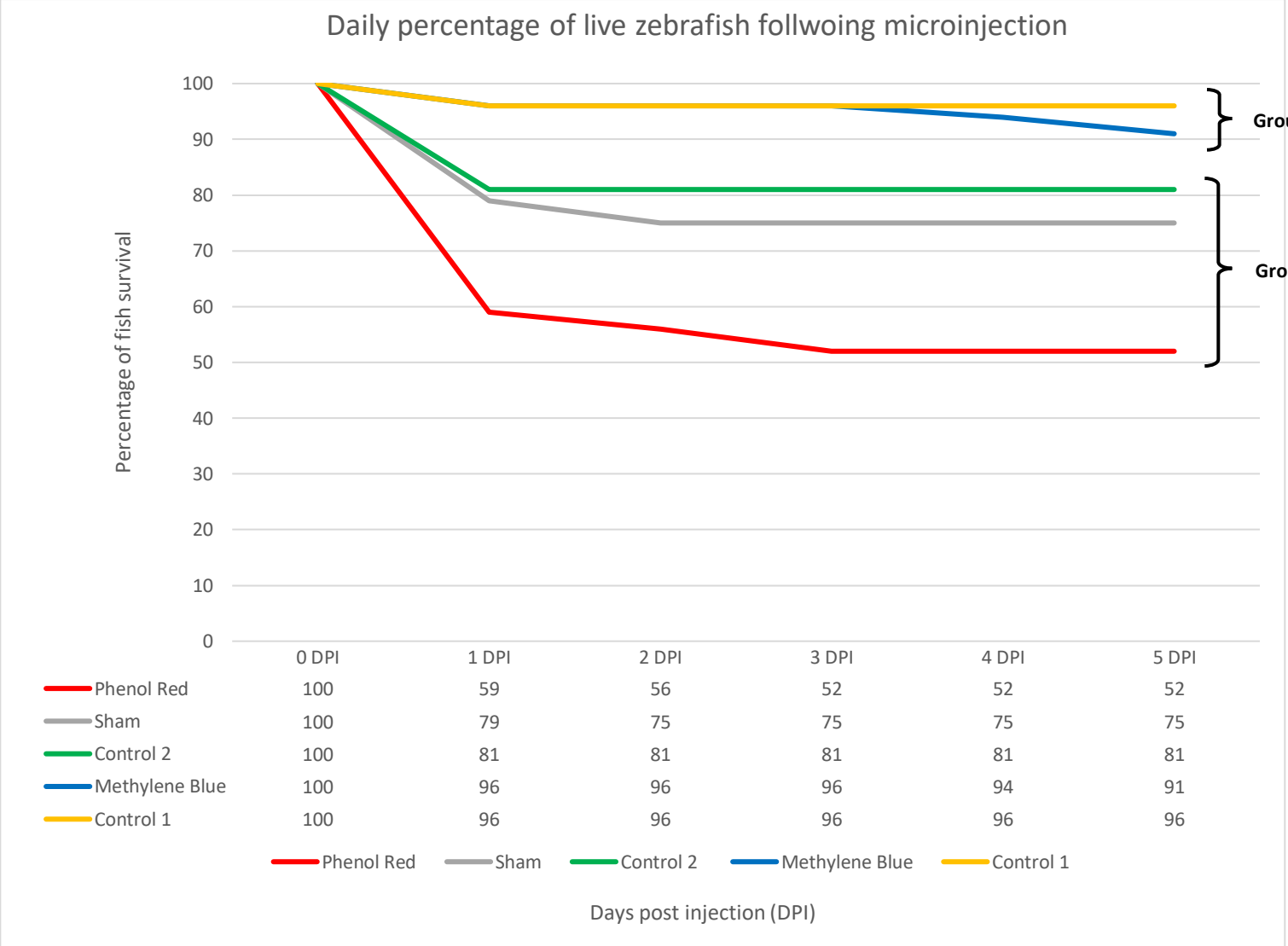

Figure 3.13: Graph representing the daily percentage of live zebrafish following microinjection at the single-cell stage with various dyes. Zebrafish microinjected with 0.0167% methylene blue were spawned from the same batch as those that were not injected in control group 1. Likewise, zebrafish that were microinjected with 0.05% phenol red were spawned from the same batch as those that were not injected in control group 2, as well as those that were sham injected by mechanical insertion of the microinjection tip with no solution injected.

3.2.3 Discussion

3.2.3.1 Introduction to microinjection set up

In the pilot presented above we see the first description of microinjection, a critical technique used throughout this study. While microinjection of zebrafish embryos at the single-cell stage is a well-documented technique [78,89], several observations and subtle deviations from the classical technique, as a result of troubleshooting, are worth noting.

Initially, two surface types were explored for placement of the eggs during microinjection. Initial attempts involved lining the eggs along the edge of a coverslip placed inside of a petri dish. While this method of embryo placement was viable, visibility as well as orientation of the eggs proved difficult. Alternatively, an agarose mold with shallow, parallel grooves, set inside of a petri dish was employed. This proved to be somewhat more efficient. Furthermore, once the eggs were lined in the grooves of the mold, it was found that fully submerging the eggs in a liquid resulted in easier visualization of the cells within the chorion. While E3 water can be used for this, the eggs tend to move more than desired during injections in this liquid. Use of the more viscous 0.3% methyl cellulose fixed this problem. Interestingly, at a concentration of 0.3%, the methyl cellulose appeared to slightly soften the egg chorion, making for easier penetration with the microinjection tip. Concentrations higher than 0.3%, however, softened the chorion too much, leaving the chorion with too much elasticity, making penetration more difficult. Likewise, it was found that a single, swift, and precise movement of the microinjection tip was optimal for penetration of the egg chorion. This makes for more precise injections and leaves the egg less damaged. For injection of embryos at the single-cell stage, a narrow window of 0.2 hours to 0.75 hours is available. As such the technique is time sensitive. For maximum output, injection of eggs must be quick and precise while still maintaining the integrity of the embryos. For this, approximately 20 eggs (no more than 30) were lined in the grooves of the mold while those waiting to be injected were kept at 28.5°C in the incubator. This allowed for maximum injection turnover without exposing the eggs to room temperature for too long.

3.2.3.2 Choice of microinjection dye

Large differences can be seen between the survival rate of phenol red injected embryos and uninjected control 2 embryos when compared to the considerably lower differences between sham injected embryos and uninjected control 2 (all of which were spawned from the same breeding event). In contrast, considerably lower differences were observed in the survival rate of methylene blue injected embryos and uninjected control 1 (spawned from same breeding event). As such it appears that phenol red may have a negative effect on the survival of embryos when injected at the single-cell stage. Comparatively, methylene blue appears to have little to no effect on the outcome of zebrafish survival rate following injection at the single-cell stage. While phenol red is commonly used as a dye in the microinjection process, the mechanisms behind the decreased survival rate of phenol red injected embryos is not completely understood. Studies in human cell cultures have suggested that phenol red may possess cytotoxic properties as a redox-active compound, while others have refuted this claim [90,91]. Meanwhile, zebrafish are routinely maintained in media containing the antifungal methylene blue, a compound that has been shown to decrease levels of reactive oxygen species in zebrafish embryos [92]. Given this data methylene blue was selected as the microinjection dye of choice moving forward.

3.3 Part III: Methylene blue and I-SceI enzyme interaction

Methylene blue was selected as the microinjection dye of choice. While the use of methylene blue as a dye results in better visualization of the injection mix, making the microinjection processes considerably easier, further investigation was needed to determine the viability of the dye in the presence of transfection reagents, notably the I-SceI enzyme. A second pilot study was conducted to determine the effect of methylene blue on the activity of the I-SceI enzyme.

3.3.1 Methods

Three separate reactions (control, 0.0167% MB, and 0.025% MB) were set up (Table 3.8). In each reaction pRSF-zTNFα-mCherry plasmid DNA was digested with the I-SceI enzyme in the presence of varying methylene blue concentrations. Each reaction was incubated at 37°C for 1 hour. Following incubation, each reaction was analysed by gel electrophoresis for the presence of digested DNA.

Table 3.8: Reaction mixes for the digestion pRSF-zTNFα-mCherry plasmid DNA with the I-SceI enzyme in the presence of varying methylene blue concentrations: Control (0% methylene blue); 0.0167% methylene blue; and 0.025% methylene blue.

	Control	Methylene blue (0.0167%)	Methylene blue (0.025%)
pRSF-zTNFα-mCherry plasmid DNA	2 µl	2 µl	2 µl
10x CutSmart® Buffer	3 µl	3 µl	3 µl
Methylene blue (0.05%)	0 µl	10 µl	15 µl
I-SceI (5 U/µl)	2 µl	2 µl	2 µl
dH_20	23 µl	13 µl	8 µl
Total	**30 µl**	**30 µl**	**30 µl**

3.3.2 Results

As seen in Figure 3.14, across lanes 1-3 the dominant band present is the 8686 bp band expected with undigested pRSF-zTNFα-mCherry (indicated by red arrow). While the ability of I-SceI to digest the pRSF-zTNFα-mCherry plasmid at 37°C for 1 hour appears to be low, given the excess of undigested pRSF-zTNFα-mCherry, faint bands are visible in lane 1 (as highlighted by the red box). These bands, at 4964 bps and 3722 bps, are the expected sizes of the plasmid backbone and transgene insert dropout, respectively, following successful digestion of pRSF-zTNFα-mCherry with I-SceI. Lanes 2 and 3, however, show no signs of bands at 4964 bps and 3722 bps, only the expected 8686 bp band for undigested pRSF-zTNFα-mCherry. Given the lack of digestion in the presence of methylene blue, and success of digestion in the absence of methylene blue, these results suggests that the interaction between the I-SceI enzyme and methylene blue (at both 0.0167% and 0.025%) inhibits the ability of the I-SceI enzyme to digest pRSF-zTNFα-mCherry at the I-SceI recognition domains.

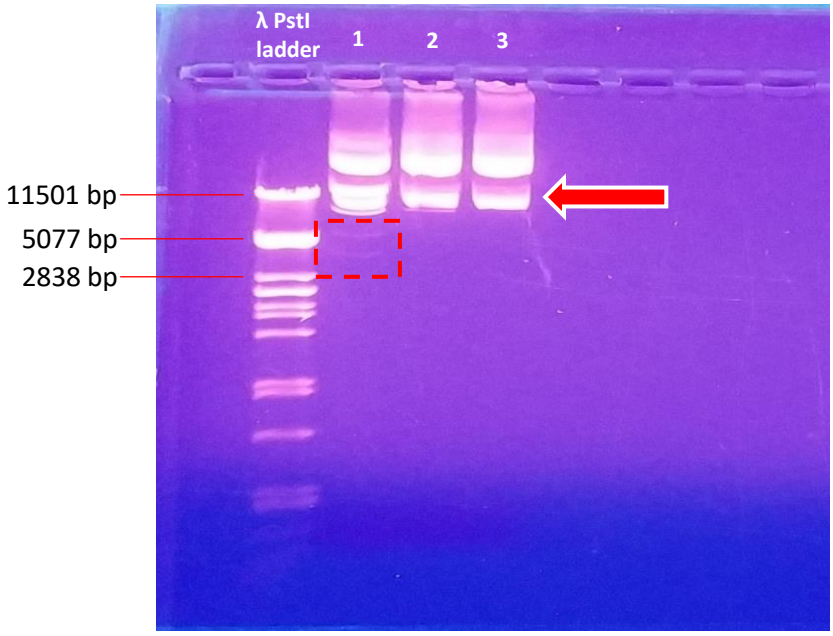

Figure 3.14: Digestion of pRSF-zTNFα-mCherry plasmid DNA with I-SceI enzyme for 1 hour at 37°C. Ladder: λ PstI; lane 1: Control digestion in the presence of 0% methylene blue; Lane 2: Digestion in the presence of 0.0167% methylene blue; Lane 3: Digestion in the presence of 0.025% methylene blue. Highlighted red box: plasmid backbone and transgene insert dropout from successful digestion of pRSF-zTNFα-mCherry with I-SceI. Red arrow: Undigested pRSF-zTNFα-mCherry plasmid.

3.3.3 Discussion

While the only observed DNA digestion was in the absence of methylene blue (highlighted by red box in Figure 3.14), the amount of fully digested DNA here is low compared to the amount of partially digested DNA. As previously discussed in section 3.1.3.3 (Cloning of the assembled transgene insert into the pRSF Duet vector), a low turnover of digested DNA product following digestion with the I-SceI enzyme can be expected [87]. It has been suggested that this may be due to the biphasic nature of I-SceI DNA cleavage in which the I-SceI enzyme remains tightly bound to DNA following cleavage, resulting in slower release of cleaved DNA product. Likewise, it has been observed that I-SceI is enzymatically optimal at pH 9.5 [88] (a variable that was not controlled during these digestions). Despite this expected low turnover of digested DNA product following digestion with the I-SceI enzyme, addition of methylene to the digestion mix appears to entirely inhibit the ability of I-SceI to digest the pRSF-zTNFα-mCherry plasmid.

Although the reason for the lack of I-SceI enzymatic activity in the presence of methylene blue is unclear, a few speculative factors may be contributing to this phenomenon. Firstly, a number of unknown contaminants such SDS, EDTA, glycerol, phenol, chloroform, ethanol, or high salt concentration may affect enzyme digestion activity (it is worth noting that methylene blue itself is a salt) (93,94). Another factor to consider is that methylene blue - as a basic hydrogen acceptor - may increase the pH of the reaction mix (95). While the pH of these reactions were not assessed due to the small volume, I-SceI activity appears to be optimal at a high pH (9.5), and so unless the addition of methylene blue increased the reaction mix pH above 9.5 (which is unlikely), it is reasonable to assume that methylene blue would not affect I-SceI activity through changes in pH. Finally, it is worth noting that methylene blue, as a dye, binds to DNA [96,97]. DNA bound with methylene blue may inhibit the ability of I-SceI to bind and cleave said DNA resulting in the lack of digestion seen in Figure 3.14.

While the exact cause of the apparent lack of enzymatic activity of I-SceI in the presence of methylene blue is unclear, as a result no dye was used for microinjection during transfection of zebrafish single-cell embryos. As an alternative, given the developed experience in using the microinjector, the skill to visualize the brief and slight volumetric expansion of the single cell as a result of microinjection was acquired. It was decided that the pRSF-zTNFα-mCherry plasmid would be microinjected without a dye, with successful microinjection confirmed by observation of transient expansion of the single cell.

3.4 Part IV: Zebrafish transfection

Microinjection of the pRSF-zTNFα-mCherry transgene vector and I-SceI enzyme was utilized for transfection of zebrafish embryos. Due to the lack of enzymatic activity of I-SceI in the presence of methylene blue, as seen in section 3.3.2, no dye was used for microinjection during transfection of zebrafish. Zebrafish transfection was performed as follows.

3.4.1 Methods

Immediately prior to microinjection, 30 µl of DNA solution was prepared as follows: 1 µg pRSF-zTNFα-mCherry, 10 units I-SceI enzyme (NEB, South Africa), 1X CutSmart® Buffer (NEB, South Africa) [78]. Single-cell eggs were injected with 1 nl of DNA solution as per procedure already described in section 3.2.1.4.

Following microinjection, sorting of fluorescence-positive zebrafish larvae was performed daily using the WPI PZMIII-MI stereomicroscope and the NIGHTSEA Model SFA Stereo Microscope Fluorescence Adapter with the green 510 – 540 nm (GR: excitation; 600 nm longpass emission) fluorescence filter set. Final sorting was performed at 9 days post fertilization (dpf). Throughout the period of 4 to 9 days following microinjection, zebrafish morphology was closely monitored. Zebrafish that showed signs of severe morphological defects as well as those that showed convincing signs of near demise (i.e. lack of response to touch, weakened heartbeat, and/or minimal ocular movement) were euthanized, transferred to 2 ml microfuge tubes of PBS solution and preserved in liquid nitrogen for further analysis.

Although TNF-α1 is normally expressed under basal conditions in developing embryos and larvae, we employed caudal fin transections in order to amplify expression, to prevent missing a positive result, given the limitations of the fluorescence microscopy available in the zebrafish unit at the time of this study. To elicit an acute inflammatory response the caudal fins of transfected 9 dpf zebrafish larvae were amputated. Zebrafish larvae were individually separated into the wells of 24 well plates and anesthetized in 0.016% tricaine for 10 minutes prior to

amputations. The caudal fins of anesthetized fish were then amputated, just short of the notochord, using sterile micro scissors (Figure 3.15). Injured fish were incubated in tricaine for a period of 6 hours [18]. Fish were then visualized using the WPI PZMIII-MI stereomicroscope and the NIGHTSEA Model SFA Stereo Microscope Fluorescence Adapter with the green 510 – 540 nm (GR: excitation; 600 nm longpass emission) fluorescence set. Following final visualization of amputated zebrafish, those that did not show any signs of fluorescence (all fish analysed in this experiment), were euthanized (by SAVC registered personnel), and individually transferred to 2 ml microfuge tubes of PBS solution, and preserved in liquid nitrogen for further analysis.

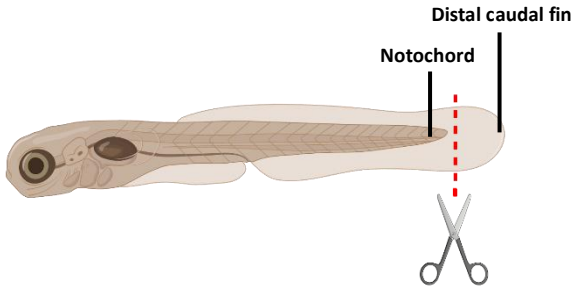

Figure 3.15: Illustration of caudal fin amputation of 9 dpf transfected zebrafish. For amputations, a transverse cut was made across the caudal fin, just short of the notochord, entirely removing the distal section of the caudal fin. Created with BioRender.com.

3.4.2 Results

A total of 126 zebrafish eggs were microinjected over multiple breeding sessions. 80 zebrafish survived to 9 dpf and were subjected to caudal fin amputation, 22 were euthanized and preserved prior to 9 dpf caudal fin amputations, and 24 neither survived nor were persevered for further analysis due to post-mortem tissue decomposition. Over the period of 9 days no transfected zebrafish showed any signs fluorescent signal. Likewise, of the 80 zebrafish subjected to caudal fin amputations at 9 dpf, none showed any signs of fluorescent signal. In total 102 transfected zebrafish, between 3 dpf and 9 dpf, were euthanized, transferred to 2 ml microfuge tubes of PBS solution, and preserved in liquid nitrogen for further analysis.

3.4.3 Discussion

Lack of detectable transgene expression may have been caused by a number of factors including: insufficient instrument sensitivity; insufficient transgene stimulation; integration of a dysfunctional transgene; lack of transgene integration. The mechanisms underlying each of these potential causes as well as the necessary means of accessing each will be discussed below.

Lack of equipment sensitivity (insufficient magnification) may explain the lack of observable transgene expression. While the NIGHTSEA Model SFA Stereo Microscope Fluorescence Adapter is a versatile fluorescent imaging tool, its small, modular nature and attachment to a simple stereo microscope makes the instrument less powerful than one that may be used through a service such as CAF. Fortunately, a new confocal fluorescence microscopy unit has been acquired within the research group, during the period of this study. While this study was unable to utilise this substantially more sensitive instrument due to time limitations, future fluorescence microscopy within the group will greatly benefit from this new equipment.

It is worth recalling that although basal levels of TNF-α1 expression are localized and low in zebrafish embryos, previous studies have managed to detect basal expression from similar TNF-α1 transgene constructs [24], and even more so following induction of an inflammatory response such as that elicited from caudal fin transections [17,24,54]. While caudal fin transections induce a strong inflammatory response [98], alternative methods of inducing inflammation may be explored, such as LPS administration, a practice used within our research

group. Concurrently, mRNA levels of endogenous zebrafish TNF-α1 expression as well as levels of pRSF-zTNFα-mCherry transgene expression may be measured using qPCR following induction of an inflammatory response. This may help determine whether or not the means of inducing inflammation is sufficient or not. It is also worth remembering that transgene integration, and therefore expression, is expected to be mosaic in injected embryos. As such, levels of transgene expression may be less than endogenous levels of TNF-α1 expression. By extensive breeding and transgene inheritance through the germline, non-mosaic transgenic zebrafish may be obtained in the following generation. Levels of transgene expression may be reassessed in this second generation. Although possible, this method is time consuming and labour intensive. Given the scope of this study, this was not attempted, although breeding of future transgenic lines within the research group is a possibility.

Alternatively, lack of detectable transgene expression may be caused by a dysfunctional transgene. While it is unlikely, as will be discussed below, given the extensive levels of sub-cloning procedures in the development of the pRSF-zTNFα-mCherry plasmid, it is possible that a mutation may have arisen leading to a dysfunctional transgene. Such a mutation could arise anywhere throughout the transgene insert. For example, a mutation within the TNF-α1 promoter could dysregulate transcription factor binding to the promoter and in turn downregulate transcription of the reporter gene. It is worth recalling that two large gaps of 174 bps and 48 bps were observed within the pRSF-zTNFα-mCherry TNF-α1 promoter. While these gaps were likely the result of a sequencing error, in the scenario that where they are not a false positive sequencing error, gaps of this size could lead to aberrant binding of transcription factors to the promoter. Again, it was observed that these gaps were 1354 bps and 2857 bps upstream of the transcription start site respectively, and therefore, likely outside of the region of primary transcription factor binding sites. Likewise, a mutation within the fluorescent reporter gene itself could lead to incorrect processing of the protein. Finally, a mutation in the SV40 poly (A) tail termination sequence could lead to aberrant transcription of the transgene construct, as well as instability of the transgene mRNA. While this is plausible, extensive sequencing confirmed that no discernable mutations were observed that could lead to dysregulation of the transgene. For future applications, transient expression of the transgene construct may be preliminarily assessed in zebrafish *in vitro* cell cultures, to determine whether or not the transgene is functional before being integrated into the genome of zebrafish embryos *in vivo*.

Likewise, integration of a fragmented transgene insert could lead to dysregulated expression or complete lack of expression of the transgene. Similarly, complete lack of integration of the entire

transgene could explain the lack of transgene expression observed. Although this may be explained by chance, it is worth recalling that while transgene integration using the I-SceI enzyme is not guaranteed, it is expected with approximately 30% [77,80] of embryos injected. Alternatively, lack of transgene integration could have arisen from a dysfunctional I-SceI enzyme. While this is possible, proper handling and storage of the enzyme was performed. Likewise, previous assays have displayed the successful enzymatic activity of our I-SceI enzyme stock (see Figure 3.9 and 3.14). In much the same way, lack of transgene integration may have arisen from the mutation seen in the I-SceI recognition domain flanking the transgene construct (described in section 3.1.2.4 pRSF-zTNFα-mCherry sequencing). Again, this can be ruled out due to the successful cleavage of this recognition domain of the pRSF-zTNFα-mCherry plasmid, as displayed in Figure 3.9 and 3.14. To access whether or not the transgene was successfully integrated into the genome of injected embryos, genotyping by PCR amplification of the fragments found within transgene insert may be performed. The details of such a genotyping method will be further explored in the following experiment.

While all of the assays described above could help elucidate the reasons for seeing no transgene expression, given the scope of this study, only genotyping was performed to access whether or not the transgene was successfully integrated in the genome of injected embryos.

3.5 Part V: Development of genotyping method for transfected zebrafish embryos

Given the lack of detectable fluorescent signal from any of the transfected zebrafish using the NIGHTSEA Model SFA Stereo Microscope Fluorescence Adapter, an alternative method was explored to assess the transgene integration rate achieved in the zebrafish larvae. For this, DNA was isolated from transfected zebrafish that were previously euthanized and preserved, from which samples were genotype for the presence of pRSF-zTNFα-mCherry transgene fragments.

3.5.1 Methods

3.5.1.1 DNA isolation

Genomic DNA (gDNA) was isolated from individual transfected fish, all between the ages of 3 dpf and 9 dpf. gDNA isolation was performed according to Meeker et al, 2007 [99]. Zebrafish larvae were fully submerged in 54 µl of 50 mM NaOH. The samples were then heated in a thermocycler at 95°C for 15 minutes, before being cooled for 10 minutes at 4°C. Following cooling, 1/10th volume (6 µl) of 1 M Tris-HCl, pH 8.0, was added to neutralize the solution. The samples were then briefly vortexed and centrifuged for 1 minute at 10 000 rpm to form a pellet of debris. 50 µl of supernatant, containing PCR ready gDNA, was carefully removed and transferred to a new 2 ml microfuge tube where it was stored at -80°C.

3.5.1.2 Genotyping

Genotyping was performed by PCR amplification of a 299 bp mCherry and 299 bp SV40 poly (A) fragment present on an integrated portion of the pRSF-zTNFα-mCherry transgene. A 412 bp amplicon of the endogenous VHL gene and 349 bp amplicon of the endogenous TNF-α1 gene were used as positive control genes [100] (See Table 3.9 for details of primers used and Figure 3.16 for pRSF-zTNFα-mCherry plasmid map with locations for primers described above).

Table 3.9: List of primers used for genotyping transfected zebrafish larvae. VHL primers were used to amplify a 412 bp fragment of the control gene VHL, an endogenous zebrafish gene. TNF-α1 plasmid primers were used to amplify a 349 bp fragment of the zebrafish TNF-α1 promoter, a gene both endogenous to zebrafish, as well as the pRSF-zTNFα-mCherry transgene. mCherry and SV40 Poly (A) primers were used to amplify a 299 bp fragments found only on the pRSF-zTNFα-mCherry transgene. All fragments, with sizes between 299 bps and 412 bps, were amplified on the same PCR run.

Primer	Sequence	Expected amplicon size
TNF-α1 plasmid primers forward	5´GTTTGTGGCTGGAAGGG 3’	349 bp
TNF-α1 plasmid primers reverse	5’ CAGTAATTAACAGGCAAAATGTCATT 3’	
mCherry forward	5’ GTCTGCAGGCAATCATCAAAGAATTTATGCGGT 3’	299 bp
mCherry reverse	5’ ACCATCTTCAAAATTCATAACCCGTTCCC 3’	
SV40 Poly (A) forward	5´ TAACTCGAGCAGACATACAGCCACTTCCAACTAAA 3’	299 bp
SV40 Poly (A) reverse	5´CCAGGGACATGACGACGTACACAACC 3´	
VHL forward	5’ TAAGGGCTTAGCGCATGTTC 3’	412 bp
VHL reverse	5’ CGAGTTAAACGCGTAGATAG 3’	

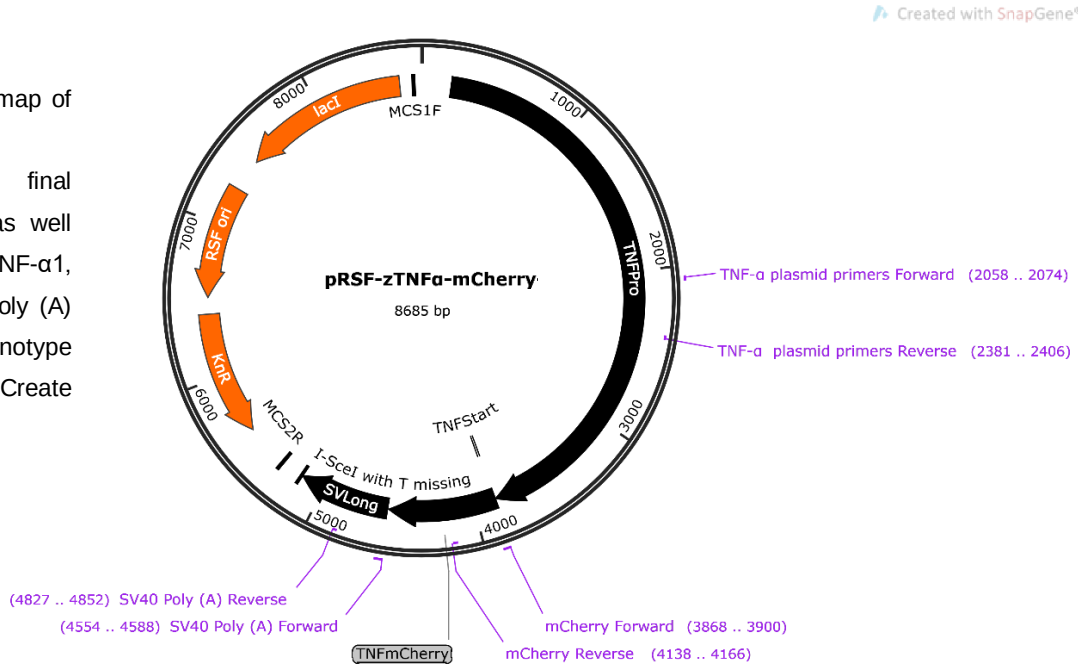

Figure 3.16: Plasmid map of pRSF-zTNFα-mCherry including annotated final transgene construct, as well as primers sets for TNF-α1, mCherry, and SV40 Poly (A) fragments, used to genotype transfected zebrafish. Create with SnapGene.com.

DNA samples were genotyped in batches of 10-15 samples per PCR run. For each primer set, all samples were tested in separate reactions, all amplified in the same thermocycler run. For each primer set tested within each batch, a PCR negative control was included, in which no DNA was added to the reaction. Similarly, a positive control with pRSF-zTNFα-mCherry plasmid DNA was included. The pRSF-zTNFα-mCherry positive control was included to identify amplicons of the mCherry, SV40 Poly (A), and TNF-α1 primer sets, all found within the

transgene construct. Finally, a non-transfected zebrafish control was included for each primer set within each batch.

Prior to PCR amplification, all zebrafish DNA samples were diluted to 1/10th of the concentration that they were isolated at using the HotSHOT method (6 µl DNA; 54 µl H_2O). Likewise, plasmid DNA stocks at an initial concentration of 465 ng/µl were diluted to 1/100th the stock concentration (1 µl DNA and 99 µl H_2O). Individual PCR reactions were set up as seen in Table 3.10, with thermocycler parameters set according to Table 3.11.

Table 3.10: List of reagents added to each PCR reaction: 5X Q5® Reaction Buffer, 5X Q5® High GC Enhancer, forward and reverse primers, dNTP mix (10 µM), and Q5® High-Fidelity Polymerase (2000 units/ml) were all supplied by New England Biolabs (NEB, South Africa).

Reagent	Volume
DNA	5 µl
Buffer	5 µl
Enhancer	5 µl
Forward primer	1.25 µl
Reverse primer	1.25 µl
dNTP mix	0.5 µl
Q5® polymerase	0.2 µl
dH_20	6.8 µl
Total	**25 µl**

Table 3.11: Thermocycler parameters used for simultaneous amplification of four primer sets: VHL; TNF-α1; SV40 Poly (A); and mCherry. See Table 3.9 for primer sequences.

PCR step	Temperature (°c)	Duration (seconds)
1) Initial denaturation	98	60
Step1: 1 cycle		
2) Denaturation	98	15
3) Annealing	60	30
4) Extension	72	30
Steps 2-4: 25 cycles		
5) Final extension	72	120
6) Cooling	4	∞
Steps 5-6: 2 cycles		

3.5.2 Results

3.5.2.1 Genotyping method development

Of the 102 transfected embryo samples, from which gDNA was isolated, 36 were used in the preliminary troubleshooting stages of the genotyping method development. Initial attempts at amplifying TNF-α1, mCherry, SV40 Poly (A), and VHL fragments appeared to yield inconsistent results. Through a number of troubleshooting attempts it was realized that the concentration of template DNA obtained from the HotSHOT method may be too high to yield consistent PCR amplification results. As such, comparisons were made between the outcome of TNF-α1, mCherry, SV40 Poly (A), and VHL PCR amplifications from transfected zebrafish with template DNA at the concentration it was initially isolated at, as well as 1/10th dilutions of template DNA (see Figure 3.17).

For all zebrafish samples, across all primer sets, undiluted template DNA resulted in smears down the lanes, while 1/10th dilutions of template DNA resulted in clear, non-smeared lanes. For mCherry and VHL amplifications, the concentration of template DNA appeared to have no effect on the outcome of the desired amplicon. For SV40 Poly (A) PCR amplifications, 1/10th diluted template DNA appeared to result in a brighter amplicon, although an amplicon is still present in the undiluted template DNA samples. For TNF-α1 PCR amplifications, undiluted template DNA fails to yield an amplicon, while 1/10th dilutions of template DNA results in the presence of a clear amplicon (Figure 3.17). As such all of the following genotyping procedures were carried out by diluting the concentration of templated DNA to 1/10th of that initially obtained from the HotSHOT DNA isolation method.

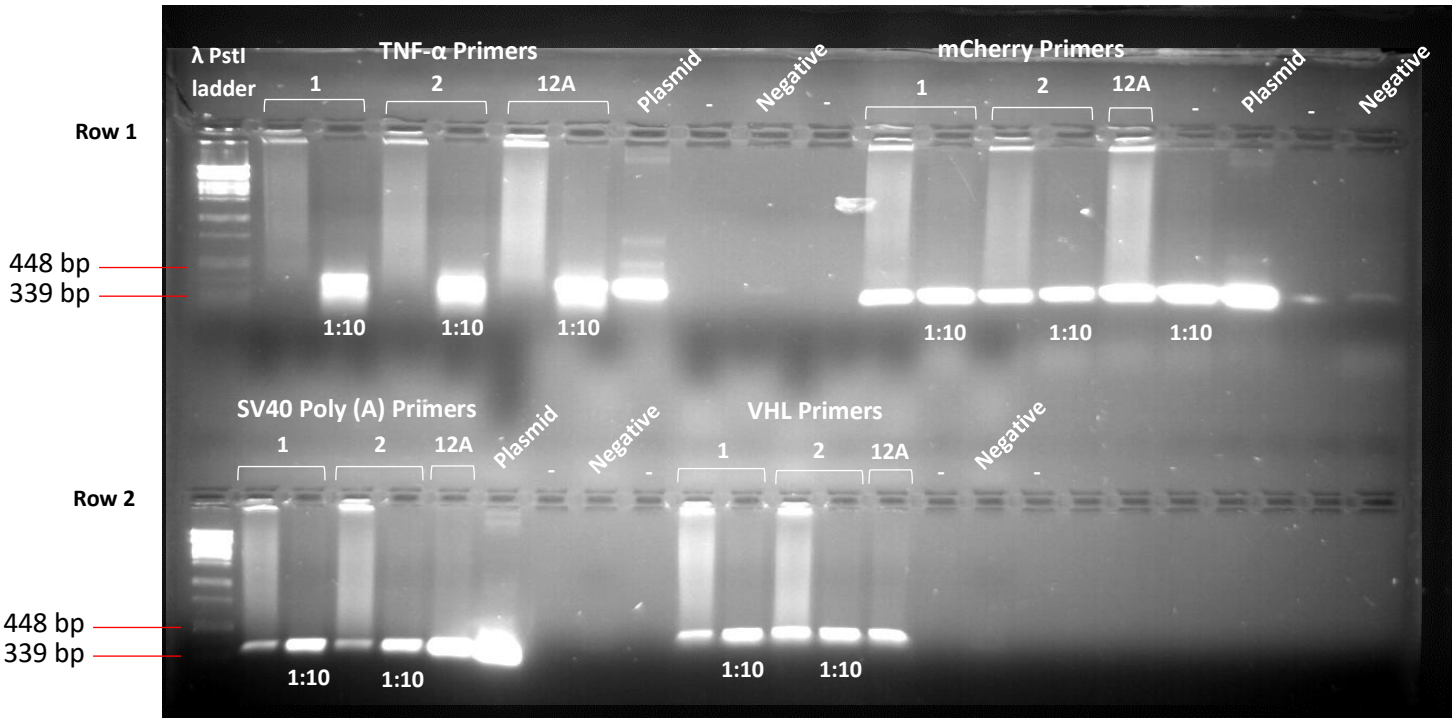

Figure 3.17: PCR amplification of TNF-α1, mCherry, SV40 Poly (A), and VHL from transfected zebrafish DNA. DNA isolated from each fish (1, 2, and 12A), using the HotSHOT method, was PCR amplified using undiluted and 1/10th dilutions of the DNA respectively. A plasmid control (pRSF-zTNFα-mCherry) was PCR amplified for 3 primer sets (TNF-α, mCherry, and SV40 Poly (A)), while on the far right of each primer set (TNF-α, mCherry, and SV40 Poly (A), and VHL) a negative control was amplified.

Figure 3.18 shows a representative gel illustrating the outcome of PCR amplifications with fully optimized parameters. For every batch of samples tested, a non-injected zebrafish control was included, as well as a PCR negative control, and a positive pRSF-zTNFα-mCherry plasmid control; the only exception being the lack of a plasmid control for the VHL primer sets. For all batches of samples tested the outcomes of the control samples were as expected: no amplicon was present for the non-injected zebrafish control with the SV40 Poly (A) and mCherry primer sets, while a 299 bp amplicon was present for the TNF-α1 primer set, and a 412 bp amplicon was present for the VHL primer set. As such, any observed artifacts were likely not the result of the PCR procedure. An interesting result worth noting was the presence of mCherry contamination across a number of samples. This can be seen in Figure 3.17 by the presence of a 299 bp amplicon in the negative control of the mCherry primer set. While this issue was resolved, the outcome of mCherry genotyping was not considered for the first 23 samples tested (see Figure 3.20). For these samples only SV40 Poly (A), TNF-α1, and VHL genotyping results were considered. Likewise, a number of artifacts worth noting were observed. As seen in

samples 7 and 8 (Figure 3.18), the VHL control amplicon was unable to amplify. Given the presence of a VHL amplicon in the non-injected zebrafish control lane, the lack of amplification in samples 7 and 8 was likely not due the PCR procedure but rather the HotSHOT DNA isolation of those particular samples. As seen in sample 6 a faint SV40 Poly (A) amplicon can be seen. Cases like these were considered negative for the presence of an amplicon due to the possibility of false positive results.

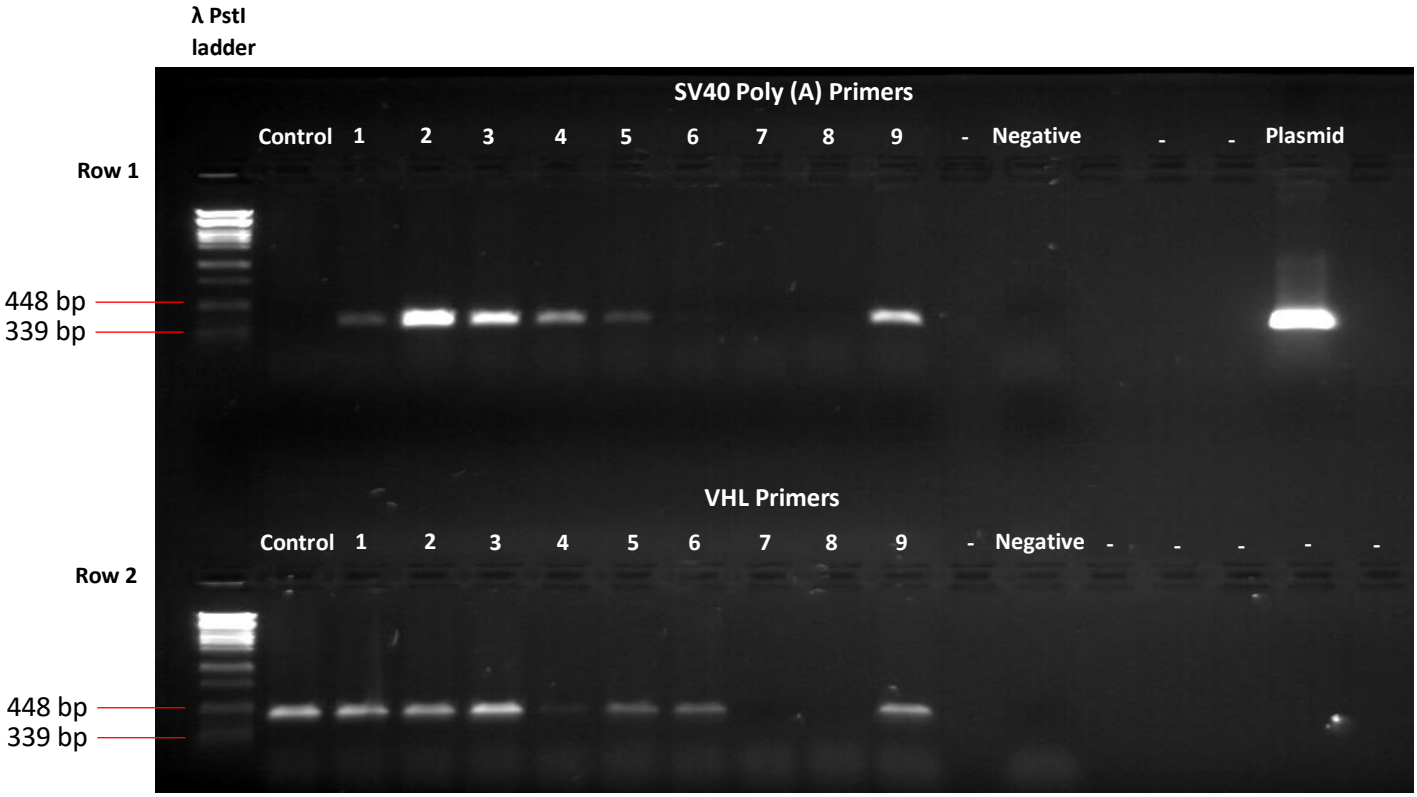

Figure 3.18: Representation of optimized PCR amplification of SV40 Poly (A) (row 1) and VHL (row 2) for genotyping of transfected zebrafish. Row 1: SV40 Poly (A) PCR amplification from non-transfected control fish; transfected fish (1-9) with 1/10th dilutions of DNA obtained from the HotSHOT method; negative PCR control; pRSF-zTNFα-mCherry as a positive plasmid control. Row 2: PCR amplification of VHL from non-transfected control fish; transfected fish (1-9) with 1/10th dilutions of DNA obtained from the HotSHOT method; negative PCR control; pRSF-zTNFα-mCherry as a positive plasmid control.

3.5.2.2 Transgene integration rate

DNA was extracted from the total 66 remaining injected zebrafish, all of which were genotyped for the presence of transgene fragments integrated from pRSF-zTNFα-mCherry. As seen in Figure 3.20, only 43 of the 66 samples were tested for the mCherry transgene fragment, while all 66 were tested for the SV40 Poly (A) transgene fragment. During the early stages of genotyping the first 23 samples tested showed signs of mCherry contamination and were not considered for analysis of mCherry integration (see Figure 3.17, mCherry negative control). For conservation of sample size these 23 samples were still analyzed for SV40 Poly (A) integration. As such, SV40 poly (A) and mCherry genotyping results were individually categorized and graphed in Figure 3.19 and Figure 3.20 respectively.

Among the samples tested for the presence of the SV40 poly (A) transgene fragment, 39.4% (26 of 66) showed no sign of amplification across any of the control primer sets, VHL and TNF-α1, as seen in Figure 3.19. These samples were removed from consideration for analysis of transgene integration, as the lack of amplification of control genes suggests unsuccessful DNA isolation. Of the remaining 40 samples, seen in Figure 3.19, 33 samples tested positive for both control primers sets, VHL and TNF-α1, of which 26 tested positive for the presence of the SV40 Poly (A) transgene fragment. This represents a successful transgene integration rate of 78.8% (26 of 33) among the samples that tested positive for both control genes (see Figure 3.21 for clarity on how the integration rates were determined). A less conservative analysis shows that of the 40 samples that tested positive for at least one of the two control primers sets, VHL and TNF-α1, 30 tested positive for the presence of the SV40 Poly (A) transgene fragment. This represents a successful transgene integration rate of 75% (30 of 40).

Much like the results seen from testing for the presence of the SV40 Poly (A) transgene fragment, the mCherry transgene fragment appeared to be present in a large proportion of zebrafish tested. Among the samples tested for the presence of the mCherry transgene fragment, 48.8% (21 of 43) showed no sign of amplification across any of the control primer sets, VHL and TNF-α1, as seen in Figure 3.20. These samples were removed from consideration for analysis of transgene integration, as the lack of amplification of control genes suggests unsuccessful DNA isolation. Of the remaining 22 samples, seen in Figure 3.20, 16 samples tested positive for both control primers sets, VHL and TNF-α1, of which 13 tested positive for the presence of the mCherry transgene fragment. This represents a successful transgene integration rate of 81.3% (13 of 16) among the samples that tested positive for both control genes (see Figure 3.21 for clarity on how the integration rates were determined). A less

conservative analysis shows that of the remaining 22 samples, all of which tested positive for at least one of the two control primers sets, VHL and TNF-α1, 18 tested positive for the presence of the mCherry transgene fragment. This represents a successful transgene integration rate of 81.8% (18 of 22)

These results indicate that genotyping of zebrafish for either the SV40 Poly (A) or mCherry transgene fragments yield comparable positive transfection rates: 78.8% vs 81.3% (conservative approach) and 75% vs 81.8% (less conservative approach).

Interestingly, of the samples that tested positive for mCherry and both control primers, 92% (12 of 13) were positive for SV40 Poly (A). Likewise, of the samples that tested positive for mCherry and at least one control primer, 83% (15 of 18) were positive for SV40 Poly (A).

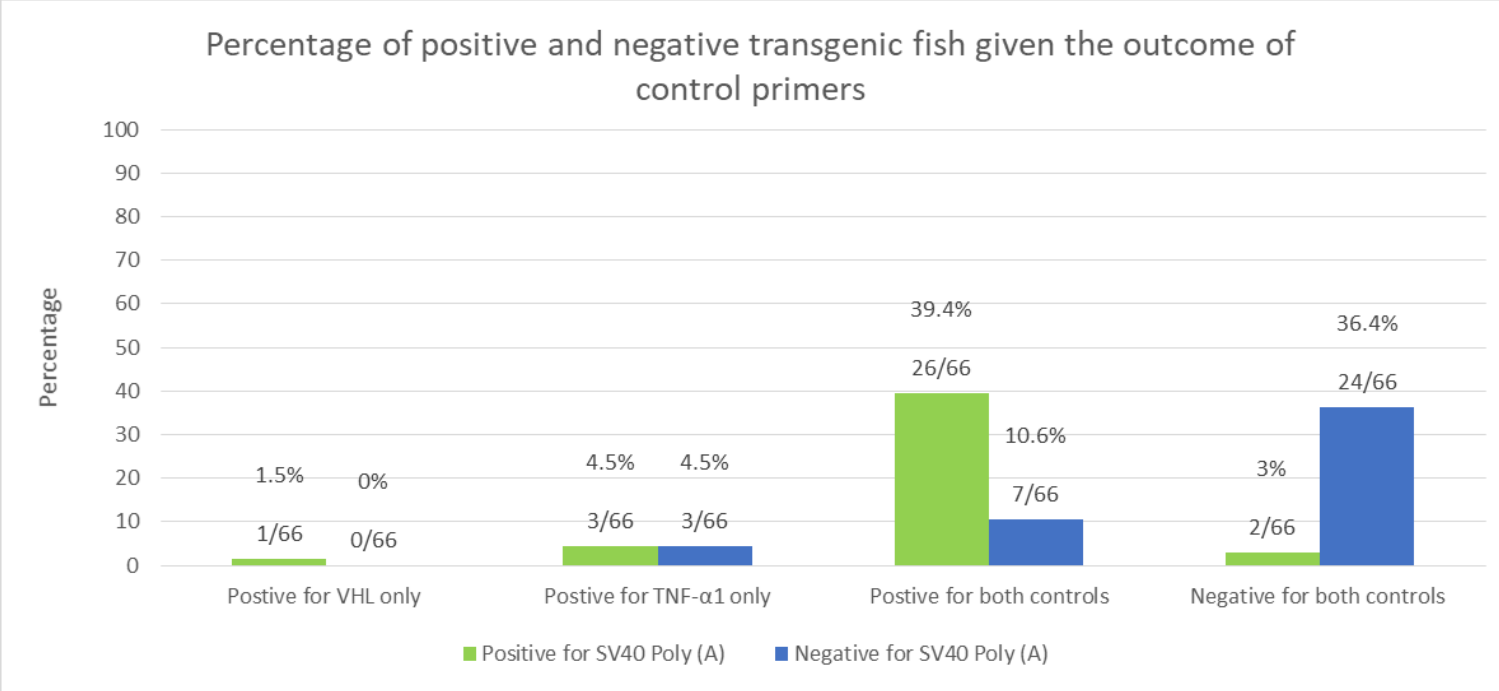

Figure 3.19: PCR analysis of the percentage of positive and negative transgenic zebrafish for SV40 Poly (A) given the outcome of control primers. Presence of the SV40 Poly (A) fragment from the pRSF-zTNFα-mCherry transgene was used to confirm whether or not the pRSF-zTNFα-mCherry transgene was successfully integrated into the genome of transfected zebrafish. For each sample tested, the presence of both control genes, VHL and TNF-α1 was considered, and the outcomes grouped accordingly. Total samples = 66 of 66

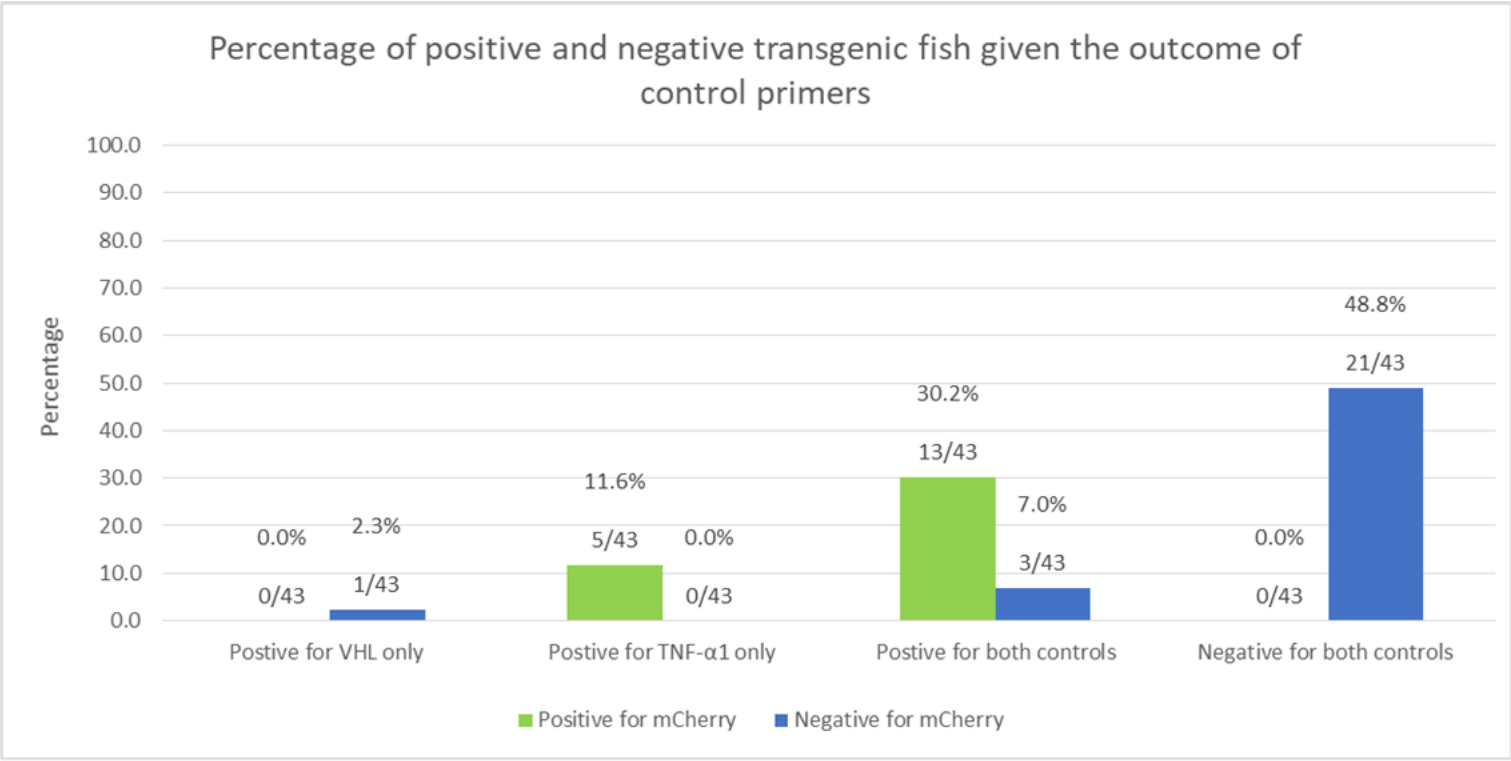

Figure 3.20: PCR analysis of the percentage of positive and negative transgenic zebrafish for mCherry given the outcome of control primers. Presence of the mCherry fragment from the pRSF-zTNFα-mCherry transgene was used to confirm whether or not the pRSF-zTNFα-mCherry transgene was successfully integrated into the genome of transfected zebrafish. For each sample tested, the presence of both control genes, VHL and TNF-α1 was considered, and the outcomes grouped accordingly. Total samples = 43 of 66

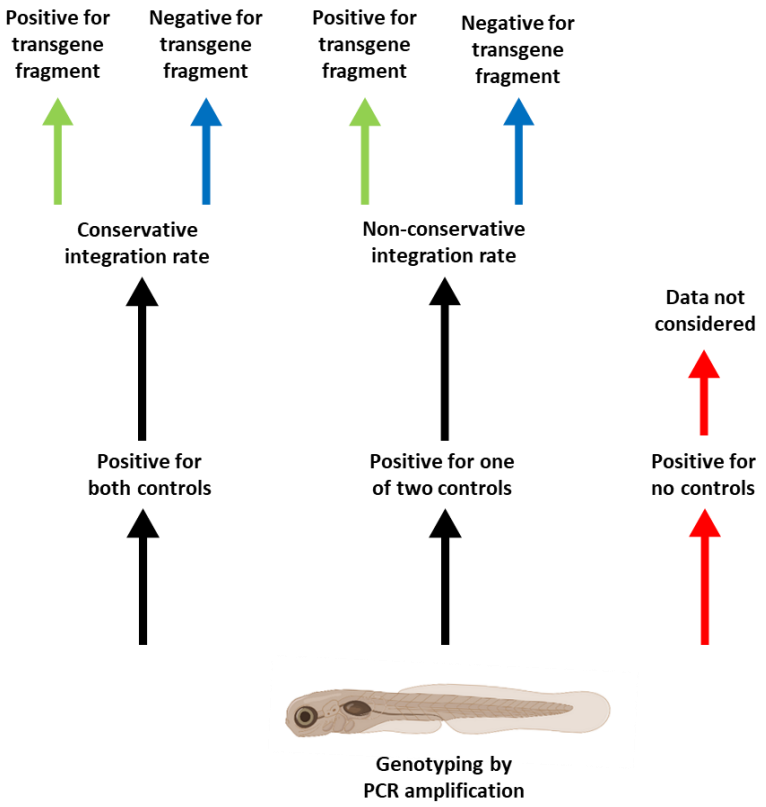

Figure 3.21: Simple flow diagram for clarity on how the transgene integration rates were determined from the data seen in Figure 3.19 and Figure 3.20

3.5.3 Discussion

3.5.3.1 Genotyping method development

All primer sets tested were run in separate reaction mixes, all in the same thermocycler run. For this to be possible all primers were designed with a similar primer melting temperature (Tm) and length in mind, such that all primer sets tested could simultaneously run on the same thermocycler run. The universal thermocycler parameters needed to simultaneously amplify all primer sets (as seen in Table 3.11) were optimized until parameters were found that could consistently amplify all primer sets. This helped save large amounts of time and effort when genotyping sizable batches of zebrafish.

Likewise, the processing of large batches was considered when deciding on a suitable method of gDNA extraction. Initially, when extracting DNA from zebrafish for the synthesis of pRSF-zTNFα-mCherry, DNA extraction kits were used for high molecular weight DNA. While this produced high quality DNA isolations, these types of kits would prove to be too time consuming and cost ineffective for genotyping large batches of zebrafish samples. The simple and quick method of gDNA extraction by Meeker et al, (2007), described above, proved more than efficient enough for genotyping by PCR. While this DNA was low molecular weight, the fragments amplified were relatively small (between 299 bps and 412 bps) and therefor easy to amplify with low molecular weight DNA. Similarly, this method of gDNA extraction was quick, simple and used few regents. Interestingly, it was found that the DNA isolated from this method was at a concentration that was too high resulting in smears in the lanes of the gel electrophoresis following PCR amplification, as seen in Figure 3.17. Through troubleshooting it was discovered that diluting the template DNA to $1/10^{th}$ the concentration of what it was isolated at before PCR amplification yielded consistent amplifications with no smears in the lanes of subsequent gel electrophoresis runs. It is worth noting that, as seen in Figure 3.19 and Figure 3.20, a number of samples failed to amplify either one or both control gene fragments, VHL and TNF-α1. While the data for these samples was recorded, they were excluded when determining the transgene integration rate. Given that all primer sets worked for all DNA controls (pRSF-zTNFα-mCherry plasmid DNA and non-injected zebrafish DNA) in all batches tested, it is reasonable to assume that the lack of amplification here was not as a result of PCR reaction mix preparation or thermocycler error. Rather the lack of amplification may have arisen due to the low molecular weight DNA isolation method or PCR inhibitors carried over from the extraction

process. This method of DNA isolation may have resulted in fragmented DNA, however, given the small size of fragments amplified for each primer set, most samples yielded positive control bands despite potential fragmentation of template DNA. To access the level of DNA fragmentation, template DNA may be run through gel electrophoresis prior to PCR amplifications.

With the genotyping method described above, all samples were genotyped and analysed for integration of the transgene.

3.5.3.2 Transgene integration rate

As briefly described in the results, the first 23 zebrafish samples tested showed signs of mCherry contamination. At this point the reagents used for PCR amplifications were thoroughly assessed and the issue was resolved for all remaining samples tested. While these 23 samples were not considered for mCherry transgene integration, for conservation of sample size, they were still considered for SV40 Poly (A) transgene integration. Following resolution of this issue, the remaining 43 samples tested were all considered for mCherry transgene integration. Meanwhile, all 66 samples tested were considered for SV40 Poly (A) transgene integration, bar those in which no control primers were amplified (as described previously).

When considering which fragment to use as a metric for positive transgene integration, SV40 Poly (A) or mCherry, it can be seen that both yielded similar results for integration rate: 78.8% vs 81.3% (conservative approach) and 75% vs 81.8% (less conservative approach). Therefore, analyzing either SV40 Poly (A) or mCherry should be a reasonable metric to access transgene integration rate.

Interestingly, of the samples that tested positive for mCherry and both control primers, 92% (12 of 13) were positive for SV40 Poly (A). Likewise, of the samples that tested positive for mCherry and at least one control primer, 83% (15 of 18) were positive for SV40 Poly (A). This shows that most samples that were positive for one transgene fragment were positive for both. This indicates that the transgene is likely integrating in its entirety and not in fragments. Any deviation from this i.e. one transgene fragment present but not the other is likely the results of DNA fragmentation during DNA isolation. This can also be seen in the large number of samples that failed to amplify endogenous control genes.

In total, the transgene integration rates appeared high (between 75% and 81.8%). This is considerably higher than transgene integration rates previously described at ~30% [77,80]. It is tempting to speculate that PCR amplifications may be amplifying residual transient pRSF-zTNFα-mCherry plasmid DNA from microinjections. In most cases, in the absence of a selectable marker, transient DNA is expelled from the host several hours to several days after transfection. Given that the majority of samples were analyzed at 9 dpf, well after transient DNA would remain in the host, PCRs are likely not amplifying transient DNA. As such, lack of detectable reporter gene expression is likely not due to lack on transgene integration.

As previously discussed in section 3.4.3, moving forward, a number of alternative assays may need to be employed to determine the reasons for lack of detectable transgene expression.

Chapter 4

Conclusion

It is clear from the literature reviewed throughout this study that the use of transgenic zebrafish lines has greatly contributed to our understanding of protein dynamics in zebrafish, notably in innate immunity related processes. As such, this study aimed to not only develop a line of stable transgenic zebrafish, expressing mCherry under the transcriptional control of the zebrafish TNF-α1 promoter, but also a methodology by which to develop future stable transgenic zebrafish lines. The necessary methodologies needed for development of a stable transgenic zebrafish line, as well as the potential shortcomings of said methodologies, were outlined throughout this study.

Firstly, the design and assembly of the transgene vector, pRSF-zTNFα-mCherry, was accomplished. For this, literature was extensively reviewed and careful consideration was given to each constituent fragment needed for assembly of the final construct. Crucially, the choice of inducible promoter, downstream reporter gene, and integration method were thoroughly accessed, resulting in the final design of the transgene construct pRSF-zTNFα-mCherry – characterized by a mCherry fluorescent protein downstream of the inducible zebrafish TNF-α1 promoter, all flanked by I-SceI recognition domains for integration of the transgene into the genome of transfected zebrafish. Standard cloning techniques were used to successfully assemble the final transgene construct, as confirmed by sequencing. While services are available for synthesis of DNA constructs, the in-house approach used throughout this study greatly contributed to the research group's understanding of transgenic construct synthesis.

For transfection of zebrafish embryos with pRSF-zTNFα-mCherry, microinjection was utilized. While microinjection of embryos at the single-cell stage proved to be a meticulous technique, extensive optimization of the technique was undertaken for ease and accuracy of future microinjections. It was noted and recommended that no dye be used to aid in microinjection. Despite their regular use throughout microinjection protocols, dyes such as phenol red appeared to induce mortality in injected single-cell embryos, while methylene blue appeared to severely hinder the enzymatic properties of I-SceI within the injection mix. For confirmation of successful injection it was recommended that visible expansion if the injected cell be used as an alternative to injection dyes.

Following transfection of embryos and subsequent induction of an inflammatory response, fluorescence microscopy was used to visualize expression of the transgene construct *in vivo*. The data presented in this study showed that no transfected zebrafish displayed any signs of detectable mCherry expression. A number of potential factors contributing to the lack of detectable mCherry fluorescence were hypothesized, including: insufficient instrument sensitivity; insufficient transgene stimulation; integration of a dysfunctional transgene; lack of transgene integration. While individual assays were suggested to clarify the impact of each of these factors, in this study, only the potential lack of transgene integration was experimentally assessed.

For this, a cost-effective genotyping method, by PCR of genomic DNA, was successfully developed to access the rates of genomic transgene integration among transfected zebrafish. While this method requires euthanasia of the fish, it is a useful means of accessing the validity of the chosen transgene integration method. For genotyping, the endogenous zebrafish VHL and TNF-α1 genes were used as controls, while the mCherry and SV40 Poly (A) genes, found on pRSF-zTNFα-mCherry, were used to confirm transgene integration. Interestingly, transfected zebrafish presented with considerably high levels of transgene integration at 78.8% and 81.3% for SV40 Poly (A) and mCherry respectively, using a conservative approach, and 75% and 81.8% for SV40 Poly (A) and mCherry respectively, using a less conservative approach. Given that the rate of transgene integration was likely not the cause of the lack of detectable fluorescence in transfected fish, it may be worthwhile experimentally accessing alternative factors.

Two major limitations, faced throughout this study, should be highlighted. Firstly, limitations imposed by the COVID-19 pandemic severely impacted laboratory availability. Due to time limitations, many intended methodologies, such as those assessing the reasons for lack of detectable transgene expression, could not be performed. The scope of this study was adjusted accordingly.

Finally, a number of limitations were imposed on this study as the result of scarcity of necessary literature. While many descriptions of transgenic zebrafish models can be found throughout literature, protocols describing the means by which these transgenic zebrafish were developed are scarce. This could likely be the result of authors choosing to withhold this intellectual property. Likewise, many aspects of zebrafish research are relatively novel, and so many gaps in literature were encountered. For example, annotations describing the location of transcription factor binding sites on the promoter of zebrafish TNF-α1 do not exist. Information such as this

would have greatly contributed to the development of the transgenic zebrafish in this study. It is also worth noting that the zebrafish genome was only fully sequenced in 2013, and so many aspects of zebrafish research are in their infancy. It is reasonable to assume that future information will become available on genomic annotations, and transgenic methodologies, including transgene construct libraries. This information would greatly improve the utility of transgenic zebrafish as a research tool. Databases such as ZFIN have already begun compiling data related to zebrafish research and is a highly beneficial tool in zebrafish research.

In conclusion, while development of the intended transgenic line was partially unsuccessful, this study introduced a number of techniques to the research group, necessary for future transgenic zebrafish development. Likewise, the data presented in this study elucidated factors that need to be closely assessed when developing transgenic zebrafish. In all, given the research group's intentions of developing and maintaining transgenic zebrafish, this study lays the foundation for any transgenic zebrafish work undertaken in the future.

Chapter 5

Bibliography

1. Sullivan C, Kim CH. Zebrafish as a model for infectious disease and immune function. Fish Shellfish Immunol. 2008;25(4):341–50.
2. Meeker ND, Trede NS. Immunology and zebrafish: Spawning new models of human disease. Dev Comp Immunol. 2008;32(7):745–57.
3. Renshaw SA, Trede NS. A model 450 million years in the making: Zebrafish and vertebrate immunity. DMM Dis Model Mech. 2012;5(1):38–47.
4. Trede NS, Langenau DM, Traver D, Look AT, Zon LI. The use of zebrafish to understand immunity. Immunity. 2004;20(4):367–79.
5. Briggs JP. The zebrafish: A new model organism for integrative physiology [Internet]. Vol. 282, American Journal of Physiology - Regulatory Integrative and Comparative Physiology. American Physiological Society; 2002 [cited 2021 Jun 6]. Available from: http://zfin.org/
6. Rahman Khan F, Sulaiman Alhewairini S. Zebrafish (Danio rerio) as a Model Organism . In: Current Trends in Cancer Management [Internet]. IntechOpen; 2019 [cited 2021 Jun 6]. Available from: www.intechopen.com
7. Novoa B, Figueras A. Zebrafish: Model for the Study of Inflammation and the Innate Immune Response to Infectious Diseases. Adv Exp Med Biol [Internet]. 2012;946:253–75. Available from: http://www.ncbi.nlm.nih.gov/pubmed/21948373
8. Oehlers SHB, Flores MV, Hall CJ, O'Toole R, Swift S, Crosier KE, et al. Expression of zebrafish cxcl8 (interleukin-8) and its receptors during development and in response to immune stimulation. Dev Comp Immunol. 2010;34(3):352–9.
9. Fleming A, Jankowski J, Goldsmith P. In Vivo Analysis of Gut Function and Disease Changes in a Zebrafish Larvae Model of Inflammatory Bowel Disease : A. 2010;16(7):1162–72.

10. Oehlers SH, Flores MV, Okuda KS, Hall CJ, Crosier KE, Crosier PS. A chemical enterocolitis model in zebrafish larvae that is dependent on microbiota and responsive to pharmacological agents. Dev Dyn. 2011 Jan;240(1):288–98.

11. Amsterdam A, Burgess S, Golling G, Chen W, Sun Z, Townsend K, et al. A large-scale insertional mutagenesis screen in zebrafish. Genes Dev [Internet]. 1999 Oct 15 [cited 2022 May 3];13(20):2713. Available from: /pmc/articles/PMC317115/

12. Thakur PC, Stuckenholz C, Rivera MR, Davison JM, Yao JK, Amsterdam A, et al. Lack of de novo Phosphatidylinositol Synthesis Leads to Endoplasmic Reticulum Stress and Hepatic Steatosis in cdipt-Deficient Zebrafish. Hepatology [Internet]. 2011 Aug [cited 2022 May 4];54(2):452. Available from: /pmc/articles/PMC3140628/

13. Thakur PC, Davison JM, Stuckenholz C, Lu L, Bahary N. Dysregulated phosphatidylinositol signaling promotes endoplasmic-reticulum- stress-mediated intestinal mucosal injury and inflammation in zebrafish. DMM Dis Model Mech [Internet]. 2014 Jan [cited 2022 May 4];7(1):93–106. Available from: /pmc/articles/PMC3882052/

14. Watzke Joerg, Schirmer Kristin SS. Bacterial lipopolysaccharides induce genes involved in the innate immune response in embryos of the zebrafish (Danio rerio) [Internet]. Fish & Shellfish Immunology. 2007 [cited 2022 Apr 28]. p. 901–5. Available from: https://www.sciencedirect.com/science/article/abs/pii/S1050464807000514

15. Philip AM, Wang Y, Mauro A, El-Rass S, Marshall JC, Lee WL, et al. Development of a zebrafish sepsis model for high-throughput drug discovery. Mol Med [Internet]. 2017 Jun 7 [cited 2022 Apr 28];23(1):134–48. Available from: https://molmed.biomedcentral.com/articles/10.2119/molmed.2016.00188

16. Kinoshita S, Biswas G, Kono T, Hikima J, Sakai M. Presence of two tumor necrosis factor (tnf)-α homologs on different chromosomes of zebrafish (Danio rerio) and medaka (Oryzias latipes). Mar Genomics [Internet]. 2014;13:1–9. Available from: http://dx.doi.org/10.1016/j.margen.2013.10.004

17. Nguyen-Chi M, Laplace-Builhe B, Travnickova J, Luz-Crawford P, Tejedor G, Phan QT, et al. Identification of polarized macrophage subsets in zebrafish. Elife. 2015 Jul 8;4(JULY 2015).

18. Nguyen-Chi M, Laplace-Builhé B, Travnickova J, Luz-Crawford P, Tejedor G, Lutfalla G, et al. TNF signaling and macrophages govern fin regeneration in zebrafish larvae. Cell

Death Dis. 2017 Aug 10;8(8):e2979.

19. Yan B, Han P, Pan L, Lu W, Xiong J, Zhang M, et al. Il-1β and Reactive Oxygen Species Differentially Regulate Neutrophil Directional Migration and Basal Random Motility in a Zebrafish Injury–Induced Inflammation Model. J Immunol [Internet]. 2014 Jun 15 [cited 2022 Apr 26];192(12):5998–6008. Available from: https://www.jimmunol.org/content/early/2014/05/16/jimmunol.1301645

20. Renshaw SA, Loynes CA, Trushell DMI, Elworthy S, Ingham PW, Whyte MKB. A transgenic zebrafish model of neutrophilic inflammation. Blood [Internet]. 2006 Dec 15 [cited 2022 May 17];108(13):3976–8. Available from: https://ashpublications.org/blood/article/108/13/3976/6567/A-transgenic-zebrafish-model-of-neutrophilic

21. Mathias JR, Perrin BJ, Liu T-X, Kanki J, Look AT, Huttenlocher A. Resolution of inflammation by retrograde chemotaxis of neutrophils in transgenic zebrafish. J Leukoc Biol [Internet]. 2006 Dec 1 [cited 2022 Apr 28];80(6):1281–8. Available from: https://onlinelibrary.wiley.com/doi/full/10.1189/jlb.0506346

22. Howe K, Clark MD, Torroja CF, Torrance J, Berthelot C, Muffato M, et al. The zebrafish reference genome sequence and its relationship to the human genome. Nat 2013 4967446 [Internet]. 2013 Apr 17 [cited 2022 Aug 26];496(7446):498–503. Available from: https://www.nature.com/articles/nature12111

23. Ellett F, Pase L, Hayman JW, Andrianopoulos A, Lieschke GJ. mpeg1 promoter transgenes direct macrophage-lineage expression in zebrafish. Blood [Internet]. 2011 Jan 27 [cited 2022 May 18];117(4):e49–56. Available from: https://ashpublications.org/blood/article/117/4/e49/28611/mpeg1-promoter-transgenes-direct-macrophage

24. Marjoram L, Alvers A, Deerhake ME, Bagwell J, Mankiewicz J, Cocchiaro JL, et al. Epigenetic control of intestinal barrier function and inflammation in zebrafish. Proc Natl Acad Sci U S A. 2015;112(9):2770–5.

25. Ogryzko N V., Lewis A, Wilson HL, Meijer AH, Renshaw SA, Elks PM. Hif-1 alpha induced Expression of Il-1β Protects against Mycobacterial Infection in Zebrafish. J Immunol [Internet]. 2018 Jul 30 [cited 2022 May 19];202(2):494–502. Available from: https://www.biorxiv.org/content/10.1101/306506v3

26. Kanther M, Sun X, Mhlbauer M, MacKey LC, Flynn EJ, Bagnat M, et al. Microbial colonization induces dynamic temporal and spatial patterns of NF-κB activation in the zebrafish digestive tract. Gastroenterology [Internet]. 2011 [cited 2022 May 18];141(1):197. Available from: /pmc/articles/PMC3164861/

27. Bradford, Y.M., Van Slyke, C.E., Ruzicka, L., Singer, A., Eagle, A., Fashena, D., Howe, D.G., Frazer, K., Martin, R., Paddock, H., Pich, C., Ramachandran, S., Westerfield M. Zebrafish Information Network, the knowledgebase for Danio rerio research. [Internet]. Genetics. 220(4). 2022. Available from: https://zfin.org/

28. Ravi V, Venkatesh B. Rapidly evolving fish genomes and teleost diversity. Curr Opin Genet Dev. 2008;18(6):544–50.

29. Duan Y, Wang Y, Li Z, Ma L, Wei X, Yang J, et al. The unique structure of the zebrafish TNF-α homotrimer. Dev Comp Immunol. 2021 Sep 1;122:104129.

30. Hong S, Li R, Xu Q, Secombes CJ, Wang T. Two Types of TNF-α Exist in Teleost Fish: Phylogeny, Expression, and Bioactivity Analysis of Type-II TNF-α3 in Rainbow Trout Oncorhynchus mykiss . J Immunol. 2013;191(12):5959–72.

31. Glenney GW, Wiens GD. Early Diversification of the TNF Superfamily in Teleosts: Genomic Characterization and Expression Analysis. J Immunol. 2007;178(12):7955–73.

32. Sepulcre MP, Alcaraz-Pérez F, López-Muñoz A, Roca FJ, Meseguer J, Cayuela ML, et al. Evolution of Lipopolysaccharide (LPS) Recognition and Signaling: Fish TLR4 Does Not Recognize LPS and Negatively Regulates NF-κB Activation. J Immunol. 2009;182(4):1836–45.

33. Li Y, Li Y, Cao X, Jin X, Jin T. Pattern recognition receptors in zebrafish provide functional and evolutionary insight into innate immune signaling pathways. Vol. 14, Cellular and Molecular Immunology. Chinese Soc Immunology; 2017. p. 80–9.

34. Zhao C, Meng A. Sp1-like transcription factors are regulators of embryonic development in vertebrates. Dev Growth Differ. 2005;47(4):201–11.

35. Lin CJ, Hsiao TH, Chung YS, Chang WN, Yeh TM, Chen BH, et al. Zebrafish Sp1-like protein is structurally and functionally comparable to human Sp1. Protein Expr Purif [Internet]. 2011;76(1):36–43. Available from: http://dx.doi.org/10.1016/j.pep.2010.10.010

36. Ellett F, Kile BT, Lieschke GJ. The role of the ETS factor erg in zebrafish vasculogenesis.

Mech Dev [Internet]. 2009;126(3–4):220–9. Available from: http://dx.doi.org/10.1016/j.mod.2008.11.001

37. Chang CP, Neilson JR, Bayle JH, Gestwicki JE, Kuo A, Stankunas K, et al. A field of myocardial-endocardial NFAT signaling underlies heart valve morphogenesis. Cell. 2004;118(5):649–63.

38. Marjoram L, Alvers A, Deerhake ME, Bagwell J, Mankiewicz J, Cocchiaro JL, et al. Epigenetic control of intestinal barrier function and inflammation in zebrafish. Proc Natl Acad Sci U S A. 2015 Mar 3;112(9):2770–5.

39. Kochanek S, Radbruch A, Tescht H, Renz D, Doerfler W. methylation profiles in the human genes for tumor necrosis factors a and 18 in subpopulations of leukocytes and in leukemias (genomic sequencing/magnetic ceil sorting-mediated ceU separation/5-methyl-2'-deoxycytidine in human DNA/methylation patterns). Vol. 88, Medical Sciences DNA. 1991.

40. Kim TK, Eberwine JH. Mammalian cell transfection: The present and the future. Anal Bioanal Chem [Internet]. 2010 Aug [cited 2021 Jun 7];397(8):3173–8. Available from: /pmc/articles/PMC2911531/

41. Smith C. Stable vs. Transient Transfection of Eukaryotic Cells | Biocompare Editorial Article [Internet]. 2013 [cited 2021 Jun 8]. Available from: https://www.biocompare.com/Editorial-Articles/126324-Transfection/

42. Vallone D, Santoriello C, Gondi SB, Foulkes NS. Basic Protocols for Zebrafish Cell Lines. In 2007. p. 429–41.

43. Sassen WA, Lehne F, Russo G, Wargenau S, Dübel S, Köster RW. Embryonic zebrafish primary cell culture for transfection and live cellular and subcellular imaging. Dev Biol. 2017 Oct 1;430(1):18–31.

44. Rafferty SA, Quinn TA. A beginner's guide to understanding and implementing the genetic modification of zebrafish. Vol. 138, Progress in Biophysics and Molecular Biology. Elsevier Ltd; 2018. p. 3–19.

45. Pfeiffer BD, Truman JW, Rubin GM. Using translational enhancers to increase transgene expression in Drosophila. Proc Natl Acad Sci U S A [Internet]. 2012 Apr 24 [cited 2021 Jun 8];109(17):6626–31. Available from:

www.pnas.org/cgi/doi/10.1073/pnas.1204520109

46. Udalova IA, Knight JC, Vidal V, Nedospasov SA, Kwiatkowski D. Complex NF-κB interactions at the distal tumor necrosis factor promoter region in human monocytes. J Biol Chem. 1998 Aug 14;273(33):21178–86.

47. Falvo J V., Tsytsykova A V., Goldfeld AE. Transcriptional control of the TNF Gene. Vol. 11, Current Directions in Autoimmunity. NIH Public Access; 2010. p. 27–60.

48. Addgene. Promoters [Internet]. Plasmid Reference / Molecular Biology Reference / Promoters. [cited 2021 Jun 4]. Available from: https://www.addgene.org/mol-bio-reference/promoters/

49. Neefjes M, Housmans BAC, Van Den Akker GGH, Van Rhijn LW, Welting TJM, Van Der Kraan PM. Reporter gene comparison demonstrates interference of complex body fluids with secreted luciferase activity. Sci Reports | [Internet]. 123AD [cited 2021 Jun 6];11:1359. Available from: https://doi.org/10.1038/s41598-020-80451-6

50. Kuri P, Ellwanger K, Kufer TA, Leptin M, Bajoghli B. A high-sensitivity bi-directional reporter to monitor NF-κB activity in cell culture and zebrafish in real time. 2017;

51. The Bioluminescence Advantage [Internet]. [cited 2021 Jun 6]. Available from: https://worldwide.promega.com/resources/pubhub/enotes/the-bioluminescence-advantage/

52. Fluorescence or Chemiluminescence: Which Reporter Is Right For You? | Biocompare: The Buyer's Guide for Life Scientists [Internet]. [cited 2021 Jun 6]. Available from: https://www.biocompare.com/Editorial-Articles/170764-Selecting-Fluorescent-vs-Chemiluminescent-Reporters/

53. Alcaraz-Pérez F, Mulero V, Cayuela ML. Application of the dual-luciferase reporter assay to the analysis of promoter activity in Zebrafish embryos. BMC Biotechnol [Internet]. 2008 Oct 27 [cited 2021 Jun 6];8(1):1–8. Available from: http://www.biomedcentral.com/1472-6750/8/81

54. Lewis A, Elks PM. Hypoxia induces macrophage tnfa expression via cyclooxygenase and prostaglandin E2 in vivo. Front Immunol. 2019;10(SEP):1–14.

55. Shi X, Teo LS, Pan X, Chong S-W, Kraut R, Korzh V, et al. Probing Events with Single Molecule Sensitivity in Zebrafish and Drosophila Embryos by Fluorescence Correlation

Spectroscopy. Dev Dyn [Internet]. 2009 Dec 1 [cited 2021 Jun 6];238(12):3156–67. Available from: www.interscience.wiley.com

56. Fink D, Wohrer S, Pfeffer M, Tombe T, Ong CJ, Sorensen PHB. Ubiquitous expression of the monomeric red fluorescent protein mcherry in transgenic mice. Genesis. 2010 Dec;48(12):723–9.

57. Kleeman B, Olsson A, Newkold T, Kofron M, DeLay M, Hildeman D, et al. A guide to choosing fluorescent protein combinations for flow cytometric analysis based on spectral overlap. Cytom Part A [Internet]. 2018 May 1 [cited 2021 Jun 6];93(5):556–62. Available from: https://onlinelibrary.wiley.com/doi/full/10.1002/cyto.a.23360

58. Yeh CD, Richardson CD, Corn JE. Advances in genome editing through control of DNA repair pathways. Vol. 21, Nature Cell Biology. Nature Research; 2019. p. 1468–78.

59. Woods IG, Schier AF. Targeted mutagenesis in zebrafish. Vol. 26, Nature Biotechnology. 2008. p. 650–1.

60. Sertori R, Trengove M, Basheer F, Ward AC, Liongue C. Genome editing in zebrafish: A practical overview. Brief Funct Genomics [Internet]. 2016 Jul 1 [cited 2021 Jun 9];15(4):322–30. Available from: http://bfg.oxfordjournals.org

61. Li M, Zhao L, Page-McCaw PS, Chen W. Zebrafish Genome Engineering Using the CRISPR–Cas9 System [Internet]. Vol. 32, Trends in Genetics. Elsevier Ltd; 2016 [cited 2021 Jun 9]. p. 815–27. Available from: /pmc/articles/PMC5127170/

62. Morita H, Taimatsu K, Yanagi K, Kawahara A. Exogenous gene integration mediated by genome editing technologies in zebrafish [Internet]. Vol. 8, Bioengineered. Taylor and Francis Inc.; 2017 [cited 2021 Jun 9]. p. 287–95. Available from: https://www.tandfonline.com/action/journalInformation?journalCode=kbie20

63. Kirchhoff J, Schiermeyer A, Schneider K, Fischer R, Ainley WM, Webb SR, et al. Gene expression variability between randomly and targeted transgene integration events in tobacco suspension cell lines. Plant Biotechnol Rep [Internet]. 2020 Aug 1 [cited 2021 Jun 6];14(4):451–8. Available from: https://link.springer.com/article/10.1007/s11816-020-00624-7

64. Munoz-Lopez M, Garcia-Perez J. DNA Transposons: Nature and Applications in Genomics. Curr Genomics [Internet]. 2010 Mar 6 [cited 2021 Feb 3];11(2):115–28.

Available from: /pmc/articles/PMC2874221/?report=abstract

65. Clark KJ, Urban MD, Skuster KJ, Ekker SC. Transgenic zebrafish using transposable elements. In: Methods in Cell Biology [Internet]. Academic Press Inc.; 2011 [cited 2021 Jan 31]. p. 137–49. Available from: /pmc/articles/PMC3454445/?report=abstract

66. Ni J, Wangensteen KJ, Nelsen D, Balciunas D, Skuster KJ, Urban MD, et al. Active recombinant Tol2 transposase for gene transfer and gene discovery applications. Mob DNA [Internet]. 2016 Dec 31 [cited 2021 Feb 2];7(1):6. Available from: https://mobilednajournal.biomedcentral.com/articles/10.1186/s13100-016-0062-z

67. Koga A, Suzuki M, Inagaki H, Bessho Y, Hori H. Transposable element in fish [Internet]. Vol. 383, Nature. Nature Publishing Group; 1996 [cited 2021 Feb 2]. p. 30. Available from: http://www.nature.com/articles/383030a0

68. Kawakami K. Tol2: A versatile gene transfer vector in vertebrates [Internet]. Vol. 8, Genome Biology. BioMed Central; 2007 [cited 2021 Feb 4]. p. S7. Available from: http://genomebiology.biomedcentral.com/articles/10.1186/gb-2007-8-s1-s7

69. Kawakami K, Shima A, Kawakami N. Identification of a functional transposase of the Tol2 element, an Ac-like element from the Japanese medaka fish, and its transposition in the zebrafish germ lineage. Proc Natl Acad Sci U S A [Internet]. 2000 Oct 10 [cited 2021 Feb 5];97(21):11403–8. Available from: www.pnas.org

70. Urasaki A, Morvan G, Kawakami K. Functional dissection of the Tol2 transposable element identified the minimal cis-sequence and a highly repetitive sequence in the subterminal region essential for transposition. Genetics [Internet]. 2006 [cited 2021 Feb 4];174(2):639–49. Available from: /pmc/articles/PMC1602067/?report=abstract

71. Kawakami K, Takeda H, Kawakami N, Kobayashi M, Matsuda N, Mishina M. A transposon-mediated gene trap approach identifies developmentally regulated genes in zebrafish. Dev Cell [Internet]. 2004 Jul [cited 2021 Feb 4];7(1):133–44. Available from: https://pubmed.ncbi.nlm.nih.gov/15239961/

72. Kondrychyn I, Garcia-Lecea M, Emelyanov A, Parinov S, Korzh V. Genome-wide analysis of Tol2 transposon reintegration in zebrafish. BMC Genomics [Internet]. 2009 Sep 8 [cited 2021 Feb 2];10:418. Available from: /pmc/articles/PMC2753552/?report=abstract

73. Belfort M, Roberts RJ. Homing endonucleases: Keeping the house in order [Internet]. Vol.

25, Nucleic Acids Research. Oxford University Press; 1997 [cited 2021 Feb 17]. p. 3379–88. Available from: https://academic.oup.com/nar/article/25/17/3379/1061169

74. Chevalier BS, Stoddard BL. Homing endonucleases: Structural and functional insight into the catalysts of intron/intein mobility. Nucleic Acids Res [Internet]. 2001 Sep 15 [cited 2021 Feb 5];29(18):3757–74. Available from: /pmc/articles/PMC55915/?report=abstract

75. Haugen P, Simon DM, Bhattacharya D. The natural history of group I introns [Internet]. Vol. 21, Trends in Genetics. 2005 [cited 2021 Feb 18]. p. 111–9. Available from: https://linkinghub.elsevier.com/retrieve/pii/S016895250400335X

76. Burt A, Koufopanou V. Homing endonuclease genes: The rise and fall and rise again of a selfish element. Curr Opin Genet Dev. 2004;14(6):609–15.

77. Thermes V, Grabher C, Ristoratore F, Bourrat F, Choulika A, Wittbrodt J, et al. I-SceI meganuclease mediates highly efficient transgenesis in fish. Mech Dev. 2002;118(1–2):91–8.

78. Grabher C, Joly JS, Wittbrodt J. Highly efficient zebrafish transgenesis mediated by the meganuclease I-SceI. Methods Cell Biol. 2004;2004(77):381–401.

79. Soroldoni D, Hogan BM, Oates AC. Simple and efficient transgenesis with meganuclease constructs in zebrafish. Methods Mol Biol [Internet]. 2009 [cited 2021 Mar 3];546:117–30. Available from: http://link.springer.com/10.1007/978-1-60327-977-2_8

80. Harrold I, Carbonneau S, Moore BM, Nguyen G, Anderson NM, Saini AS, et al. Efficient transgenesis mediated by pigmentation rescue in zebrafish. Biotechniques [Internet]. 2016 Jan 1 [cited 2021 Feb 24];60(1):13–20. Available from: /pmc/articles/PMC4768720/

81. Teh C, Parinov S, Korzh V. New ways to admire zebrafish: Progress in functional genomics research methodology [Internet]. Vol. 38, BioTechniques. Eaton Publishing Company; 2005 [cited 2021 Jun 8]. p. 897–906. Available from: https://www.future-science.com/doi/abs/10.2144/05386RV01

82. Kurita K, Burgess SM, Sakai N. Transgenic zebrafish produced by retroviral infection of in vitro-cultured sperm. Proc Natl Acad Sci U S A [Internet]. 2004 Feb 3 [cited 2021 Jun 9];101(5):1263–7. Available from: /pmc/articles/PMC337041/

83. Roh-Johnson M, Shah AN, Stonick JA, Poudel KR, Kargl J, Yang GH, et al. Macrophage-dependent cytoplasmic transfer during melanoma invasion in vivo. Dev Cell [Internet].

2017 Dec 12 [cited 2022 Aug 13];43(5):549. Available from: /pmc/articles/PMC5728704/

84. Finley KR, Davidson AE, Ekker SC. Three-Color Imaging Using Fluorescent Proteins in Living Zebrafish Embryos. https://doi.org/102144/01311st02 [Internet]. 2018 Sep 5 [cited 2022 Aug 13];31(1):66–72. Available from: https://www.future-science.com/doi/10.2144/01311st02

85. Carswell S, Alwine JC. Efficiency of Utilization of the Simian Virus 40 Late Polyadenylation Site: Effects of Upstream Sequences. Mol Cell Biol. 1989;9(10):4248–58.

86. Petek LM, Russell DW, Miller DG. Frequent Endonuclease Cleavage at Off-target Locations In Vivo. Mol Ther [Internet]. 2010 May 5 [cited 2022 Aug 13];18(5):983. Available from: /pmc/articles/PMC2890094/

87. Perrin2 A, Buckle1 M, Dujon B. Asymmetrical recognition and activity of the I-SceI endonuclease on its site and on intron-exon junctions. Vol. 12, The EMBO Journal. 1993.

88. Monteilhet C, Perrin A, Thierry A, Colleaux L, Dujon B. Purification and characterization of the in vitro activity of I-Sce I, a novel and highly specific endonuclease encoded by a group I intron [Internet]. Vol. 18, Nucleic Acids Research. Available from: https://academic.oup.com/nar/article/18/6/1407/1325016

89. Rosen JN, Sweeney MF, Mably JD. Microinjection of Zebrafish Embryos to Analyze Gene Function. JoVE (Journal Vis Exp [Internet]. 2009 Mar 9 [cited 2022 Aug 14];(25):e1115. Available from: https://www.jove.com/v/1115/microinjection-of-zebrafish-embryos-to-analyze-gene-function

90. Morgan A, Babu D, Reiz B, Whittal R, Suh LYK, Siraki AG. Caution for the routine use of phenol red – It is more than just a pH indicator. Chem Biol Interact [Internet]. 2019;310:108739. Available from: https://doi.org/10.1016/j.cbi.2019.108739

91. Zhu Y, Zhang X, Zhu J, Zhao Q, Li Y, Li W, et al. Cytotoxicity of Phenol Red in Toxicity Assays for Carbon Nanoparticles. Int J Mol Sci [Internet]. 2012 [cited 2022 Aug 22];13(10):12336. Available from: /pmc/articles/PMC3497275/

92. Vaccaro A, Patten SA, Ciura S, Maios C, Therrien M, Drapeau P, et al. Methylene Blue Protects against TDP-43 and FUS Neuronal Toxicity in C. elegans and D. rerio. PLoS One [Internet]. 2012 Jul 27 [cited 2022 Aug 14];7(7). Available from: /pmc/articles/PMC3407135/

93. Lohman TM, Von Hippel PH. Kinetics of protein-nucleic acid interactions: Use of salt effects to probe mechanisms of interactio. Crit Rev Biochem Mol Biol. 1986;19(3):191–245.

94. Methylene blue | C16H18ClN3S - PubChem [Internet]. [cited 2022 Jul 26]. Available from: https://pubchem.ncbi.nlm.nih.gov/compound/Methylene-blue

95. Cusimano VJ. Enzyme kinetics: The use of methylene blue. J Biol Educ. 1976;10(5):258–64.

96. Li WY, Xu JG, He XW. Characterization of the binding of methylene blue to DNA by spectroscopic methods. Anal Lett. 2000;33(12):2453–64.

97. Rohs R, Sklenar H. Methylene blue binding to dna with alternating at base sequence: Minor groove binding is favored over intercalation. J Biomol Struct Dyn. 2004;21(5):699–711.

98. Xie Y, Meijer AH, Schaaf MJM. Modeling Inflammation in Zebrafish for the Development of Anti-inflammatory Drugs [Internet]. Vol. 8, Frontiers in Cell and Developmental Biology. Frontiers Media S.A.; 2021 [cited 2021 May 4]. p. 620984. Available from: www.frontiersin.org

99. Meeker ND, Hutchinson SA, Ho L, Trede NS. Method for isolation of PCR-ready genomic DNA from zebrafish tissues. Biotechniques. 2007;43(5):610–4.

100. Wilkinson RN, Elworthy S, Ingham PW, van Eeden FJM. A method for high-throughput PCR-based genotyping of larval zebrafish tail biopsies. Biotechniques [Internet]. 2013 [cited 2022 Feb 19];55(6):314–6. Available from: www.BioTechniques.com

Appendices

Ethical approval letters

A) ACU approval letter (ACU-2020-18750)

UNIVERSITEIT
STELLENBOSCH
UNIVERSITY

Protocol Approval

Date: 17 March 2021

PI Name: Mr Wade Ambrose

Protocol #: ACU-2020-18750

Title: Generation of zebrafish with fluorescent TNF-a

Dear Wade Ambrose ,

Your application (response to modifications) , was reviewed by the Research Ethics Committee: Animal Care and Use via committee review procedures and was approved. Please note that this clearance is only **valid for a period of twelve months**. Ethics clearance of protocols spanning more than one year must be renewed annually through submission of a progress report **(due one moth prior to the expiry date of this approval)**, up to a maximum of three years.

Approval Date: 17 March 2021 - 16 March 2022

Animal Species: *Danio rerio (Zebrafish)*

Animal Numbers: 460

Applicants are reminded that they are expected to comply with accepted standards for the use of animals in research and teaching as reflected in the South African National Standards 10386: 2008. The SANS 10386: 2008 document is available on the Division for Research Developments website www.sun.ac.za/research.

As provided for in the Veterinary and Para-Veterinary Professions Act, 1982. It is the principal investigator's responsibility to ensure that all study participants are registered with or have been authorised by the South African Veterinary Council (SAVC) to perform the procedures on animals, or will be performing the procedures under the direct and continuous supervision of a SAVC-registered veterinary professional or SAVC-registered para-veterinary professional, who are acting within the scope of practice for their profession.

Please remember to use your protocol number 18750 on any documents or correspondence with the REC: ACU concerning your research protocol.

Please note that the REC: ACU has the prerogative and authority to ask further questions, seek additional information, require further modifications or monitor the conduct of your research.

Any event not consistent with routine expected outcomes that results in any unexpected animal welfare issue (death, disease, or prolonged distress) or human health risks (zoonotic disease or exposure, injuries) must be reported to the committee, by creating an Adverse Event submission within the system.

We wish you the best as you conduct your research.

If you have any questions or need further help, please contact the REC: ACU Secretariat at wabeukes@sun.ac.za or 021 808 9003.

Sincerely,

Winston Beukes

REC: ACU Secretariat

Research Ethics Committee: Animal Care and Use

B) BEE approval letter (BEE-2021-19235)

UNIVERSITEIT
STELLENBOSCH
UNIVERSITY

Approval with Stipulations

15 March 2021

PI: Mr Wade Ambrose

REC: BEE Reference #: BEE-2021-19235

Title: Generation of Zebrafish with fluorescent TNF-a reporter gene

Dear Mr Wade Ambrose

Your response to modifications, with reference number #BEE-2021-19235 was reviewed by the Research Ethics Committee: Biosafety and Environmental Ethics via committee review procedures and was approved on condition that the following stipulations are adhered to:

1. All containment procedures must be adhered to and there must be no return of potential GMO fishes to stock.

Approval period: 13 March 2021 - 12 March 2022

Note: Please note that your annual progress report is due one month prior to the expiry date of this approval.

Please note that the application for approval and registration of this project will be cancelled automatically if no feedback is received from you within 6 (six) months of the date of this letter.

Please remember to use your REC: BEE reference number: # BEE-2021-19235 on any documents or correspondence with the REC: BEE concerning your research protocol.

If you have any questions or need further help, please contact the REC: BEE office at 021 808 9003.

Visit the Division for Research Developments website www.sun.ac.za/research for documentation on REC: BEE policy and procedures.

Sincerely,

Mr Winston Beukes

Coordinator: Research Ethics (Biosafety)